Stockholm University

Master Thesis

Degree Project in Geochemistry 60 hp

Weathering in the Torneträsk Region - The Importance of Sulfide Weathering seen through Catchment-scaled Isotope Studies

Johannes West

Stockholm 2017

Department of Geological Sciences
Stockholm University
SE-106 91 Stockholm

ABSTRACT 3

SAMMANFATTNING 4

1. INTRODUCTION 5

1.1 AIMS 8

2. STUDY AREAS 9

2.1 KÄRKEVAGGE 9
2.2 MIELLAJOKKA 13

3. METHODS 15

3.1 FIELDWORK 15
3.2 LABORATORY PROCEDURES 17
3.2.1 INITIAL ANALYSIS AND SUBSAMPLING 17
3.2.2 DOC 18
3.2.3 ICP-OES 20
3.2.4 IC 20
3.2.5 ALKALINITY 20
3.2.6 ISOTOPE ANALYSIS 21
3.2.7 DATA PROCESSING 25

4. RESULTS 26

4.1 METEORIC WATER 26
4.2 SOLID SAMPLES 27
4.3 STREAM WATER 28
4.3.1 WATER CHEMISTRY 28
4.3.2 ISOTOPES 35

5. DISCUSSION 39

5.1 DATA EVALUATION 39
5.1.1 POTENTIAL ERROR EVALUATION 39
5.1.2 RAIN WATER $\delta^{18}O_{SO4}$ 40
5.1.3 RAIN WATER δD & $\delta^{18}O_{H2O}$ 41
5.2 LOCAL VARIATIONS WITHIN STUDY AREAS 41
5.3 COMPARISON BETWEEN STUDY AREAS 43
5.3 SULFIDE WEATHERING IN THE TORNETRÄSK REGION 45
5.3.1 RELATIVE IMPORTANCE OF CARBONATE AND SILICATE ROCK WEATHERING 45
5.3.2 δ34S END MEMBERS 47
5.3.3 MASS BALANCES 52
5.3.4 FLUX ESTIMATIONS 54
5.3.5 RELATIVE IMPORTANCE OF SULFURIC ACID WEATHERING 56

6. CONCLUSIONS 59

ACKNOWLEDGEMENTS 61

REFERENCES 62

APPENDIX 67

APPENDIX 1: POTENTIAL CONTAMINATION AND OTHER POTENTIAL ERRORS DURING SULFUR ISOTOPE PREPARATION 68
APPENDIX 2: DATA TABLES 71
2.1 MAIN WATER CHARACTERISTICS 71
2.2 MAIN ELEMENTS (ICP-OES) 73
2.3 MAIN ANIONS (IC) 76
2.4 TRACE ELEMENTS (ICP-OES) 78
2.5 ISOTOPE DATA 84
2.6 DIC, ALKALINITY AND DOC 87
APPENDIX 3: LINEAR ALGEBRA PROJECTION METHOD 89
APPENDIX 4: KEELING PLOTS 90

Front page: weathered boulder in Kärkevagge a late evening in July

Abstract

Two catchments in the Torneträsk region were the subject of a multi-parameter study with the purpose of evaluating the relative importance of sulfide weathering within study areas. The mountain valley of Kärkevagge is a well-studied area known for high weathering rates and an exposed sulfide mineralization, but has never been the subject of thorough sulfate isotope mapping. The catchment of Miellajokka is less studied, but is interpreted to better represent the weathering regime of the larger area. Additional samples from the broader Torneträsk area were also analyzed for the isotopic composition of sulfate. Results from the study corroborates local variations as implied by previous studies in Kärkevagge and reveals the presence of local sulfide enrichments in Miellajokka. It is shown that sulfide weathering is the vastly dominating source of sulfate in Kärkevagge, but also contributes to roughly half of the sulfate in Miellajokka. Samples from the broader Torneträsk region show that approximately 60% of stream water sulfate in the region is derived from sulfide weathering. Primitive flux estimations reveal that the sulfide weathering rates of Kärkevagge is approximately 30-60 times faster than old estimated global rates, while Miellajokka fall in line with these estimations despite low annual temperature and precipitation and generally low saturation indices. For Kärkevagge, weathering by sulfuric acid produced by sulfide weathering is shown to have a visible impact over dissolved inorganic carbon isotope compositions. Even if general weathering rates in the study areas are low, the relative importance of sulfuric acid weathering therefore seems to be significant. These results are along the line of several modern studies displaying the need for a new global estimation of sulfide weathering rates. Since weathering mediated by sulfuric acid does not lead to the net carbon drawdown associated with carbonic acid-mediated weathering, this will potentially lead to a reevaluation of the influence on weathering on atmospheric CO_2 drawdown and subsequent climate control on geologic time scales.

Sammanfattning

Två avrinningsområden i området kring Torneträsk har studerats i en multi-parameter-studie i syfte att undersöka den relativa betydelsen av sulfidvittring. Den alpina dalen Kärkevagge är sedan tidigare noggrant studerad, känd för att vittra snabbt och för att inneha en stor sulfidminieralisering. Trots detta har svavelisotopvärden aldrig tidigare kartlagts i dalen. Avrinningsområdet för jokken Miellajokka är ett mindre studerat område, men är tolkat som ett område mer likt den större regionen i avseende på berggrund och dominerande vittringsprocesser. Ytterligare prover från det större området kring Torneträsk har även analyserats för svavelisotopsammansättning. Resultaten från studien bekräftar lokala variationer som antytts eller dokumenterats genom tidigare studier i Kärkevagge, samt avslöjar närvaron av lokala sulfidberikningar i Miellajokka. Det är påvisat att sulfidvittring är den avlägset största källan av sulfat i Kärkevagge, men att denna källa även utgör ungefär hälften av sulfatet i Miellajokka. Prover från det större området kring Torneträsk visar att ungefär 60% av sulfatet i området härstammar från sulfidvittring. Primitiva uppskattningar av massförflyttningar visar att sulfidvittringen i Kärkevagge per yta motsvarar ungefär 30–60 gånger hastigheten jämfört med gamla globala uppskattningar. Samtidigt faller Miellajokka ungefär i linje med dessa äldre beräkningar. Isotopsammansättningen av inorganiskt kol visar att vittring med svavelsyra som protondonator är en betydelsefull källa till inorganiskt kol i Kärkevagge. Medan kemisk vittring verkar ske ganska långsamt i de studerade områdena visar denna studie på en stor relativ betydelse av vittring med svavelsyra. Resultaten i denna studie sällar sig till ett antal moderna studier som tillsammans påvisar behovet av en ny global uppskattning av global sulfidvittring. Vittring med svavelsyra som protondonator leder inte till den konsumtion av atmosfärisk koldioxid som annars förknippas med vittring, och möjligen kan en omvärdering av sulfidvittring därför även påverka synen på vittringens kontroll över atmosfäriska CO_2-koncentrationer och klimatet över geologiska tidsskalor.

1. Introduction

The formulation of the faint young sun paradox by Carl Sagan and George Mullen in 1972 demanded for a previously unknown mechanism for climate control, active in prehistoric times, capable of sustaining heat for the oceans to remain unfrozen in times when the sun was considerably weaker than today. This mechanism was provided by Owen *et al* (1979) who suggested that the young atmosphere on Earth contained elevated CO_2 levels and thereby experienced a much stronger greenhouse effect, and by Walker *et al* (1981) who suggested a negative feedback mechanism between climate and atmospheric CO_2 levels responsible for lowering these levels simultaneous to a successive increase in incoming solar radiation. The basis for the mechanism is the consumption of CO_2 through carbonic acid-mediated weathering of Ca and Mg –silicate and carbonate minerals, producing secondary carbonate minerals and thereby effectively acting as a CO_2 sink after equilibration with the atmosphere. This process can be conceptually summarized by equations 1-3:

$$CO_2 + H_2O \rightarrow H_2CO_3 \qquad (1)$$

$$H_2CO_3 + CaCO_3 \rightarrow 2HCO_3^- + Ca^{2+} \qquad (2)$$

$$2H_2CO_3 + CaSiO_3 + H_2O \rightarrow 2HCO_3^- + Ca^{2+} + H_4SiO_4 \qquad (3)$$

Chemical weathering rates would therefore have a control over CO_2 levels. These rates would in turn be effected by temperature and humidity, since these factors accelerate weathering. With a residence time of sedimentary calcium carbonate of about $3{,}5*10^8$ years (Garrels and Perry, 1974, cited in Spence and Telmer, 2005), silicate weathering could in theory have a long-term climate effect. Large-scale mountain building events would also consume CO_2 and give colder surface temperatures while tectonic activity in the form of increased volcanism and metamorphism would have opposite effects (Berner *et al.,* 1983, and references therein). To further test the validity of this concept, two questions must be evaluated: 1) evaluating the factors controlling chemical weathering and estimating the global rate of silicate weathering 2) investigate the importance of a negative feedback mechanism as initially proposed by Walker *et al* (1981).

To explore these aspects, the study of river chemistry has been adapted, a work complicated by variations in weathering products (congruent vs incongruent weathering)

produced by varying lithologies, as well as the influence of runoff on weathering rates (*e.g.* Garrels and Mackenzie, 1971, Gaillardet *et al.*, 1999). Additionally, it has been shown that the assumed relationship between temperature and chemical weathering rates not always holds true, since cold environments can still have high weathering rates. This was early observed by Rapp (1960) in the mountain valley of Kärkevagge, Swedish Lapland. Despite the problems associated with large-scale extrapolations, Gaillardet *et al.*, (1999) estimated CO_2 consumption from silicate weathering to 0,058 GT yr^{-1}.

As for processes potentially counteracting the positive feedback between weathering and climate control, the most apparent is probably sulfide weathering, conceptualized here by the weathering of pyrite (FeS_2):

$$4FeS_2 + 15O_2 + 8H_2O \rightarrow 2Fe_2O_3 + 8H_2SO_4 \qquad (4)$$

Sulfide weathering could be assumed to follow patterns similar to those of silicate weathering, given that they would both be controlled by climate, tectonic uplift and tectonic weathering. However, it does not contribute to atmospheric CO_2 drawdown. On the contrary, the formation of sulfuric acid would require neutralization such as through the subsequent weathering of carbonate or silicate minerals.:

$$8H_2SO_4 + 16CaCO_3 \rightarrow 8SO_4^{2-} + 16HCO_3^- + 16Ca^{2+} \quad (5)$$
$$8H_2CO_3 + 8CaSiO_3 + 8H_2O \rightarrow 8SO_4^{2-} + 8Ca^{2+} + 8H_4SiO_4 \quad (6)$$

Equation 5 incorporates the production of free bicarbonate species, eventually adding to the carbon budget of the ocean-atmosphere system. In the longer perspective, sulfide weathering would be counteracted by sulfide deposition, but with the long residence time for sulfate in the oceans of about 10^7 years (Holland, 1978), this opens for very long time scales for which there is a net gain or net drawdown of atmospheric CO_2. This imbalance is confirmed by the varying isotopic composition of buried evaporites. As short mixing time of the oceans (~1000 years, Rees, 1991, and references therein) leads to a homogenous isotopic composition of marine sulfate. Since no significant fraction occurs during precipitation of evaporites, these formations record the changes in sea-water sulfate over time (e.g. Claypool *et al.*, 1980, Thode *et al.*, 1991). The sedimentary evaporite sequences display a span of $\delta^{34}S_{SO4}$ signatures from ~+10-30‰. The geological evaporite record thereby indicates massive shifts in the global

sedimentary sulfur cycle over geologic times, sometimes with relatively quick shifts and excursions (e.g. Claypool *et al.*, 1980).

To understand the importance of sulfide weathering to the global weathering budget, an estimation for global sulfide weathering rates is necessary. A complicating factor is that riverine sulfate can have multiple origins, with possible end members including evaporites, sulfides, deposition and anthropogenic sources. François and Walker (1992) estimated sulfate derived from chemical weathering to be around $0{,}65*10^{12}$ mol/yr globally, based on a steady-state assumption between weathering and volcanic emission rates and deposition, but without support by direct measurements. Berner and Berner (1996) Presented a similar estimation of global fluxes of $0{,}48*10^{12}$ mol/yr. However, by the increased use of stable isotope ratios for understanding river chemistry and source quantification, methods for direct measurement of sulfide weathering rates have become accessible.

While minor isotope fractionations do occur, the process thought to mostly affect the isotopic composition of S on earth is biologically mediated anaerobic sulfate reduction (SR), which returns a sulfide product depleted in ^{34}S of between 2-47‰ (Thode, 1991 and references therein, Kaplan and Rittenberg, 1964, Brüchert, 2004). As mentioned above, seawater sulfate is homogenous in composition, presently at +21‰ (Rees *et al.*, 1978). These attributes make sulfur isotopes suitable for source apportionment because the end members are often easily distinguishable (*e.g.* Calmels *et al.,* 2007, Berner et al., 2002**,** Ingri *et al.,* 1997, Dold & Spangenberg, 2005, Dold *et al.,* 2011). The additional use of oxygen isotopes in sulfate benefits from extremely low exchange rates between sulfate and water under normal conditions, extremely high exchange rates between SO_2 and H_2O, and a big mass difference between the stable ^{16}O and ^{18}O isotopes of water yielding large isotope fractionation effects (Holt and Kumar, 1991; Lloyd, 1967; Kusakabe and Robinson, 1977). Thus, while sulfur isotopes contain information about the source of the sulfur, the oxygen isotopes in sulfate inherits the information of the environment where the molecule formed. When combined, these tools gives a stronger picture for the source apportionment of sulfur (*e.g.* Calmels *et al.*, 2007, Dogramaci *et al* 2001, Dold & Spangenberg, 2005, Dold *et al.*, 2011, Berner *et al.*, 2002).

The use of $\delta^{34}S_{SO4}$ and $\delta^{18}O_{SO4}$ for source apportionment have indicated that sulfide weathering and sulfuric acid-based weathering may be largely underestimated processes (*e.g.* Calmels *et al.,* 2007**,** Li et al., 2008, Das et al., 2012). More studies are needed, however,

to construct a new estimate of these fluxes and to draw more advanced conclusions on the implication of sulfide weathering on climate.

In this work, the nature of sulfide weathering in subarctic environments is investigated, a climate region where weathering rates traditionally have been considered low. The study is conducted mainly within two closely located but geochemically distinct headwater catchments: the well-studied Kärkevagge where extensive sulfide weathering and high chemical denudation rates have been noted (*e.g.* Thorn *et al.,* 2001, Campbell *et al.,* 2002), and the Miellajokka catchment, which is indicated to more accurately represent the wider geographic area. The study relies on multiple analyses and data types, including pH and conductivity measurements, pCO_2, Dissolved organic carbon (DOC) and alkalinity measurements, major ions and elements and trace element concentrations, as well as isotopic data ($\delta^{34}S_{SO4}$, $\delta^{18}O_{SO4,}$ $\delta^{13}C_{DIC}$, $\delta^{18}O_{H2O}$ and δD_{H2O}).

1.1 Aims

This study is aimed at:

1. Modelling the relative contribution of sulfide oxidation to stream water SO_4 in the two catchments
2. Improving the knowledge of carbon fluxes due to weathering in the two catchments
3. Comparing the two catchments in terms of general geochemistry and relative importance of weathering pathways, and extrapolate implications of the finds for the wider geographical region.

The working hypotheses is that sulfide weathering will be much more important in Kärkevagge, but that both areas will exceed the classical estimations of sulfide weathering as estimated by Berner and Berner (1996) and Francois and Walker (1992), with subsequent consequences for sulfuric acid weathering and CO_2 drawdown by weathering.

2. Study Areas

The region around Abisko (figure 1) is a transition zone between the Atlantic coast and inland northern Scandinavia, exhibiting a precipitation gradient from east to west. Because of the foundation of the Abisko Scientific Research Station, this is now a well-studied area. The effects of global warming have been well documented in a region experiencing thawing permafrost and associated changes in ecology and geochemistry (*e.g.* Giesler *et al.*, 2014, Callaghan *et al.*, 2010, 2013). The regional bedrock is dominated by metamorphosed rock units belonging to the Caledonian orogeny, divided into layered nappes which extend across the length of the Scandinavian mountain range. Sulfide mineralizations occurs locally across the whole mountain chain (Thelander 2009, Bergman *et al.*, 2012).

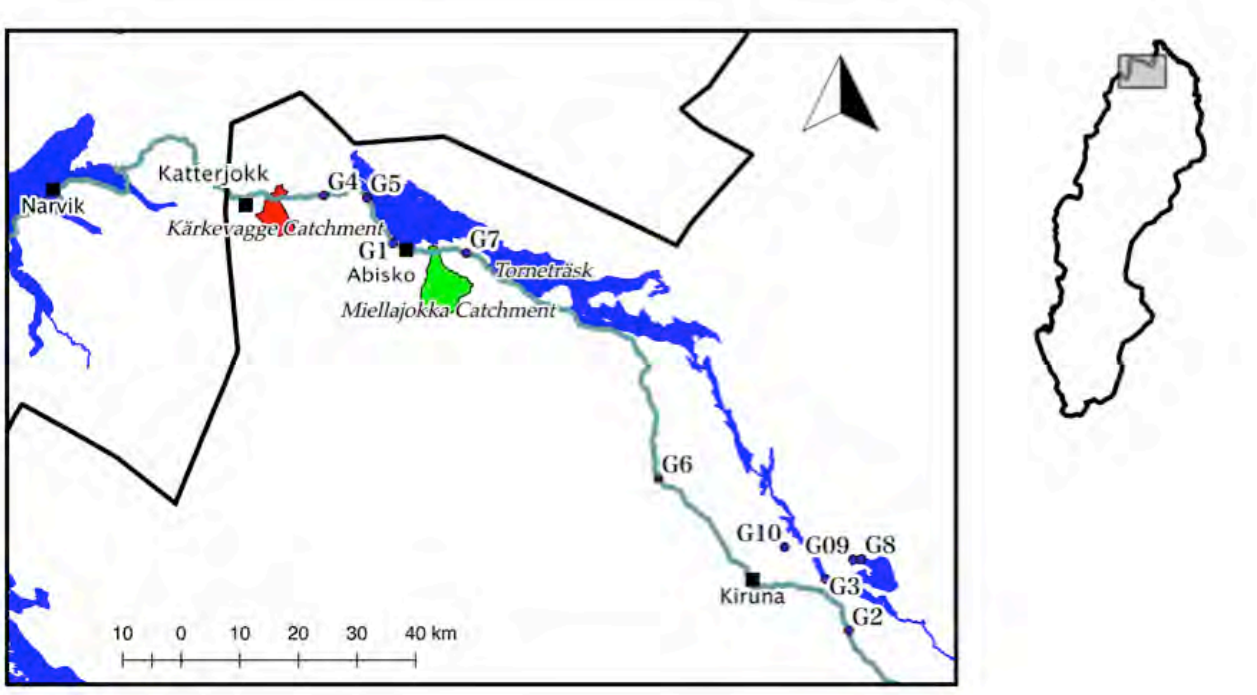

Figure 1. The geographical siting of Kärkevagge and Miellajokka in relation to road E10, auxiliary sites G1-10, lake Torneträsk and the Torneälv river.

2.1 Kärkevagge

The valley Kärkevagge is located about 30 km west of Abisko, accessible from road E10 between Abisko and Narvik. The name translates to "Valley of the Boulders" in sami language, a name derived from the great boulder field dominating the valleys central parts. Kärkevagge is a U-

shaped glacial valley, about 5 km long with its opening towards the north, and is bordered on three sides by steep cliff faces. Elevation level from the mouth of Kärkevagge to the surrounding mountaintops are between approximately 1500-500 m.a.s.l. Heath and meadows dominates the valley floor, while the birch forest only reaches the lowermost end of the catchment. Many small streams emerge from the steep slopes in the valley and on the western slope two cirques are found at higher elevations. In the southern end, the valley ends in a cirque-like formation occupied by Lake Rissajaure, dammed by an ancient rock fall constituting a second boulder field. The lake, known for its extreme water clarity, does not have a subaerial outlet. Instead it is believed to be connected to the Kärkejokk stream system through an underground outlet below the boulder dam (e.g. Malmsten and Boström, 2002). The total drainage area of the Kärkejokk is about 26,3 km^2 (SMHI, 2017).The nearby weather station of Katterjokk, a few km west of the valley mouth (figure 1), has a mean annual precipitation of 918 mm/year and an air temperature of -0,4° C for the period 2009-2015. For the period 1973-2015, the mean annual temperature is about -1° C (SMHI, 2017). The valley walls reveal a series of roughly horizontally bedded metamorphic rocks, overlain at the top by hard garnet mica schist which acts as a caprock for the lower formations. This rock type is also dominating among the boulders found on the valley floor. Below this unit, grey or black mica schists, phyllitic mica schists, as well as marble are found. Dolomitic marble is also found in the north-western end of the valley (Kulling et al., 1964**,** Dixon *et al.*, 1995). The valley has an intriguing appearance with white efflorescent crusts decorating streambeds along the eastern valley side, and with colorful stains of secondary minerals found along the sides of many great boulders in the valley (figure 2).

Kärkevagge has been the subject for geochemical and geomorphological research at numerous occasions. It was first investigated by Rapp (1960) who studied mountain slope development in the valley. Based on precipitation and water conductivity data and following the assumption that Rissajaure is a representative water mass for the valley, Rapp concluded that chemical denudation was the most important mass wasting process in the valley, occurring at rates of 26 tons/km^2/yr. This was unexpectedly high for a site at this latitude at the time. The geochemistry of the valley was most thoroughly studied through a series of campaigns around the millennium. These studies included calculation of chemical denudation rates, analysis of water chemistry, determination of weathering rinds and efflorescent crust compositions, measurements of potential weathering rates, soil classification and others (*e.g.*

Darmody *et al.,* 2000a, 2002, 2000b, 2005, 2008, Dixon *et al.*, 1995, 2001, 2002, 2006, Thorn *et al.,* 2001, 2002a, 2002b, 2006, Campbell *et al.*, 2001, 2002, Allen *et al.*, 2001, Allen 2002). Although all articles contribute to an understanding of the larger picture, the work is partially summarized in Thorn *et al.,* 2001.

For the stream water chemistry, calcium and magnesium were found to be the dominating cations throughout the valley, while dominating anion species were sulfate (generally in the southern end of the valley), bicarbonate (in a few streams in the north-western end of the catchment) or a mixture of the two (generally in the northern end of the valley). Stream water pH is generally high, but lower in some streams mainly on the eastern valley slope. Total Dissolved Solids (TDS) tend to be higher along the central eastern slope. However, the latter trend did not hold with TDS normalized against discharge (Campbell *et al.,* 2001). A revision of Rapp's chemical denudation rate raised estimations up to 46 tons/km^2 over 82 days of summer. This rate is comparable to that of large equatorial rivers draining sedimentary rocks, such as the Amazon (Campbell *et al.*, 2002) . A handful of sulfur isotope measurements has been performed for Kärkejokk and the neighboring streams Vassijokk, Låktajokk and Katterjokk. Light isotopic sulfur compositions for the first three streams indicate a stronger lithospheric influence in these streams, whereas a heavier signature for Katterjokk indicate a larger proportion of sulfate derived from deposition (Malmsten and Boström, 2002).

Soil types varies throughout the valley, generally with a pH between 3,5-5,5. Calcium is the dominant base cation, and muscovite the dominating mineral. Valley soils are most often developed on alluvium or colluvium, and often contains buried soil horizons, indicating instability of the valley slopes (Darmody 2000a, Allen *et al.,* 2001).

Mineralogical and chemical analyses of the of the great boulders in the lower boulder field as well as the rock fall damming up Lake Rissajaure revealed that the chemical composition of the mica-schist and garnet-mica-schist are very similar. Weathering seem to be primarily accelerated by vertical schistosity orientation as well as rock iron content, likely reflecting a higher concentration of weathering-accelerating pyrite in these rocks. Elevated sulfur concentrations in strongly weathered rocks when compared to neighboring fresh rocks further confirm these observations. Production of sulfuric acid from weathered boulders likely also lead to 'dead' soils observed downslope of some boulders (Allen, 2001., referenced in Allen, 2002, Allen, 2002, Darmody *et al.,* 2001, 2005, 2008). Other indications of chemical weathering have been studied, including rock coatings and weathering rinds (Dixon *et al.,* 1995, 2002).

Figure 2. Photo over Kärkevagge towards the valley opening in the north. The southern boulder field is visible to the left and the central boulder field extends towards the edges of the image. Many boulders in the foreground are coated with a white-brownish crust.

Weathering rinds are commonly depleted in soluble cations and have increasing iron concentration towards the edges. Several types of rock coatings were found, including iron films and coatings of silica and heavy metals. Iron films were found on both the stream channels and boulders. The films sometimes also contained high concentrations of Al and Si as well as S. Films were also associated with Fe-concentrating coccus-bacteria, suggesting a biological mediation of the Fe-precipitation. Silica glazes were mainly found along the eastern valley side, with varying abundance of Al and Fe. Introduction of fresh rocks to the valley demonstrated the influence of soil pH and drainage capability for dolomite weathering, while granite rocks formed weathering rinds in a relatively short period of time (Thorn *et al.,* 2002, 2006, Dixon *et al.*, 2001, 2006). The efflorescent crusts along the eastern valley walls were found to vary in composition in between locations, with some dominated by Ca and others by Al. The distinguishable mineralogy has been somewhat disputed between authors, due to dominating minerals being largely amorphous or poorly crystalline. Still, gypsum seem to be an important constituent in crusts in the valley (Malmsten and Bodström, 2002, Darmody *et al.*, 2001, 2002, Dixon *et al.*, 2002).

In recent years, the geochemical nature of Kärkevagge has been explained by a high pyrite content in the black schists in the valley (*e.g.* Thorn *et al.*, 2001, Darmody *et al.*,

2001). In accordance with equations 4-5, the sulfuric acid formed would be neutralized by reaction with local carbonate rocks, giving the stream water of Kärkevagge its special geochemistry. Reaction between sulfuric acid and the underlying material is thought to give rise to efflorescent crusts of varying composition (Darmody *et al.*, 2002). Unstable soil profiles indicate historically high rates of physical mass wasting, and the exposure of rock in the slopes after the late deglaciation in the valley has left the pyrite-rich rocks extra vulnerable to chemical weathering, similar to what occurs during acid mine drainage (Darmody *et al.*, 2000b, Allen *et al.*, 2001, Thorn *et al.*, 2001). This explanation does however fail to explain why discharge-normalized solute fluxes are distributed across the valley, instead of concentrated on the eastern side where the efflorescent crusts and rock coatings are abundant (Campbell *et al.*, 2001). Due to the special nature of Kärkevagge, while interesting, the catchment is unlikely to be typical for the region. For example, the nearby alpine valley of Latnjavagge show mean annual chemical denudation rates of 5,4 t km^{-2} yr^{-1} (Beylich *et al.*, 2005).

2.2 Miellajokka

The Miellajokka catchment covers an area of about 50,5 km^2 immediately south-west of Abisko. Visitors may recognize Miellajokka as the watershed draining the famous landmark of Lapporten, a spectacular U-shaped valley above the Abisko village. While not confined in a single valley, the catchment is dominantly restricted to steep mountain slopes ranging from the highest peaks of over 1700 m.a.s.l. to the stream outlet at Torneträsk at about 400 m.a.s.l. The catchment has a mean height of about 955 m.a.s.l. and only 11% of the watershed is covered by forest. Dwarf shrub heath dominates the mountain slopes in the area. The western Abisko Mountains provides a rain shadow from the Atlantic, resulting in low annual precipitation of about 340 mm yr^{-1} in the Abisko village for the period 2009-2015. Corresponding mean annual temperature is about +0,3° C, although the site has a long record of increasing temperature (Giesler *et al.*, 2013, 2014, Callaghan *et al.,* 2013, SMHI, 2017). Bedrock in the lower end of the catchment is dominated by metasedimentary rocks, while amphibolite rocks and quartz- and feldspar-rich gneisses are found at higher altitudes. The westernmost part of the catchment is dominated by older metasedimentary units (Thelander, 2009, Bergman *et al*, 2012). The bedrock and vegetation cover are representative for the northern Caledonides.

Only a few geochemical studies have been conducted in Miellajokka. However, these studies indicate that the catchment may not be fully representative to the larger geographical region in terms of carbon concentrations, phases and fluxes. When compared to 48 other regional streams, the dissolved CO_2 concentrations in Miellejokka both show a relatively strong temporal variation and seasonal dependence on total dissolved inorganic carbon (DIC). CO_2 contribution to DIC was also highest in this stream at 24%. In the same study, $\delta^{13}C_{DIC}$ values showed a large variation in Miellajokka, as well as a negative relationship with DIC and $\ln(pCO_2)$ for the ice-free season. A mixing model for weathering products of silicate and carbonate minerals and carbonic acid produced from soil CO_2 predicted $\delta^{13}C_{DIC}$ values lower than the observed, a trend that was also valid for other streams in the area (Giesler *et al.*, 2013). Over the course of a year 2008-2009, the DOC and DIC concentrations in the Miellajokka catchment varied between 1-8 and 2-10 mg L^{-1}, respectively (Giesler *et al.*, 2014). Presently, Miellajokka is subject to a study of investigating biological and geochemical controls on the carbon cycle across the whole catchment. (Gerard Rocher, pers. Comm.).

3. Methods

3.1 Fieldwork

Sampling was concentrated to the watersheds of Miellajokka and Kärkevagge, with a few samples collected early in the summer over a wider region of the Torneträsk area (figure 1). Seven sites were selected for the Kärkejokk and Miellajokka headwaters, respectively, and sampled twice over the course of the summer 2016. Miellajokka sites and names were chosen as to correspond with a contemporary sampling scheme in the catchment (Gerard Rocher, pers. Comm.). In addition, 25 low discharge sites, taken from springs or minor tributaries, were sampled once during the same period. The same was done in Miellajokka for 15 springs or minor tributaries. Additional samples were taken from site M1 and K7 in the spring/early summer and late autumn to capture spring and base flow conditions at the outflow of the respective catchments. In Kärkevagge, two solid samples of weathered sulfide, KR1-2, were also recovered, as well as soil samples representing different soil types within the valley. Rain water was collected twice in central parts of the two catchment areas. Sampling locations are marked out in figures 4-5.

Figure 3. Sampling at site MS2, a small runnel draining a snow patch in the Miellajokka catchment.

Sample location	Sampling dates 2016	Location	Type of sample	Analysis
K1-K7	9/7, 18/8	Kärkevagge	Main headwater	pH, cond, pCO_2, DOC, alk, ICP-OES, IC, $\delta^{34}S_{SO4}$, $\delta^{33}S_{SO4}$, $\delta^{18}O_{SO4}$, $\delta^{13}C_{DIC}$, $\delta^{18}O_{H2O}$, δD_{H2O}
KS1-KS25	22-26/7	Kärkevagge	Springs & minor tributaries	pH, cond, pCO_2*, DOC, alk, ICP-OES, IC, $\delta^{34}S_{SO4}$, $\delta^{33}S_{SO4}$, $\delta^{18}O_{SO4}$, $\delta^{13}C_{DIC}$, $\delta^{18}O_{H2O}$, δD_{H2O}
K7	22/6	Kärkevagge	Early season	$\delta^{34}S_{SO4}$, $\delta^{33}S_{SO4}$, $\delta^{18}O_{SO4}$
K7	25/10	Kärkevagge	Base flow	pH, cond, pCO_2, DOC, alk, ICP-OES, IC, $\delta^{34}S_{SO4}$, $\delta^{33}S_{SO4}$, $\delta^{18}O_{SO4}$, $\delta^{13}C_{DIC}$, $\delta^{18}O_{H2O}$, δD_{H2O}
KM1	1-23/7	Kärkevagge	Rain water	ICP-OES, IC, $\delta^{34}S_{SO4}$, $\delta^{33}S_{SO4,}$ $\delta^{18}O_{H2O,}$ δD_{H2O}
KM2	18/8-30/9	Kärkevagge	Rain Water	ICP-OES, IC, $\delta^{34}S_{SO4}$, $\delta^{33}S_{SO4,}$ $\delta^{18}O_{H2O,}$ δD_{H2O}
KR1-2	18/8	Kärkevagge	Solid rock samples	$\delta^{34}S_{SO4}$, $\delta^{33}S_{SO4}$
KSM	18/8	Kärkevagge	Soil sample, meadow	$\delta^{34}S_{SO4}$, $\delta^{33}S_{SO4}$, $\delta^{18}O_{SO4}$
KSB	18/8	Kärkevagge	Soil sample, boulder soil	$\delta^{34}S_{SO4}$, $\delta^{33}S_{SO4}$, $\delta^{18}O_{SO4}$
M1-M3, M6, M9-M11	6-8/7, 16-17/8	Miellajokka	Main headwater	pH, cond, pCO_2, DOC, alk, ICP-OES, IC, $\delta^{34}S_{SO4}$, $\delta^{33}S_{SO4}$, $\delta^{18}O_{SO4}$, $\delta^{13}C_{DIC}$, $\delta^{18}O_{H2O}$, δD_{H2O}
MS1-MS15	12-15/7	Miellajokka	Springs & minor tributaries	pH, cond, pCO_2, DOC, alk, ICP-OES, IC, $\delta^{34}S_{SO4}$, $\delta^{33}S_{SO4}$, $\delta^{18}O_{SO4}$, $\delta^{13}C_{DIC}$, $\delta^{18}O_{H2O}$, δD_{H2O}
M16	23/6	Miellajokka	Early Season	$\delta^{34}S_{SO4}$, $\delta^{33}S_{SO4}$, $\delta^{18}O_{SO4}$
M1	23/5	Miellajokka	Early Season	pH, cond, pCO_2, DOC, alk, IC, $\delta^{34}S_{SO4}$, $\delta^{33}S_{SO4}$, $\delta^{18}O_{SO4}$, $\delta^{13}C_{DIC}$, $\delta^{18}O_{H2O}$, δD_{H2O}
M1	26/10	Miellajokka	Base flow	pH, cond, pCO_2, DOC, alk, ICP-OES, IC, $\delta^{34}S_{SO4}$, $\delta^{33}S_{SO4}$, $\delta^{18}O_{SO4}$, $\delta^{13}C_{DIC}$, $\delta^{18}O_{H2O}$, δD_{H2O}
MM1	8/7-16/8	Miellajokka	Rain water	ICP-OES, IC, $\delta^{34}S_{SO4}$, $\delta^{33}S_{SO4,}$ $\delta^{18}O_{SO4,}$ $\delta^{18}O_{H2O,}$ δD_{H2O}
MM2	16/8-30/9	Miellajokka	Rain Water	ICP-OES, IC, $\delta^{34}S_{SO4}$, $\delta^{33}S_{SO4,}$ $\delta^{18}O_{H2O,}$ δD_{H2O}
G1-G10	23/5-1/7	Torneträsk region	Gradient Samples	$\delta^{34}S_{SO4}$, $\delta^{33}S_{SO4,}$ $\delta^{18}O_{SO4}$

Table 1. Total list of samples in this study, and performed analyses per sample groups. See maps in figures 1, 4 & 5 for sampling locations. Cond = conductivity, alk = alkalinity.

Water was collected in 2 L and 0,5 L bottles pre-rinsed with stream water for sulfur isotope analysis of sulfate and general water chemistry, respectively. For $\delta^{13}C_{DIC}$ analysis, 5 ml of water was inserted via syringe through the septa into 12 ml vials prepared with 80 μL of 99% H_3PO_4 and flushed with He gas. This procedure minimize air contamination, conserves the sample and transform bicarbonate to $CO_{2(g)}$ (Taipale and Sonninen, 2009). Temperature and conductivity measurements were analyzed with a Hanna multiparameter instrument, and pCO_2 was measured with a Vaisala CO_2 probe. pCO_2 measurements were calculated assuming a 10 cm water depth of the probe, an assumption yielding good results and overcoming difficulties of field measurements (Gerard Rocher, pers. Comm). Measured pCO_2 were corrected using pressure and temperature components deviating from calibration conditions according to the method described in Johnson *et al.*, (2009). Due to faulty equipment, reliable in-situ pH measurements were only available for the October sampling campaign.

3.2 Laboratory procedures

The large number of samples and analyses resulted in a complex matrix of combinations that is summarized in table 1. In total, 91 samples of various types were successfully analyzed for one or multiple parameters.

3.2.1 Initial analysis and subsampling

Subsamples for DOC and inductively coupled plasma – atomic emission spectroscopy (ICP-OES) analysis were filtrated through 0,45µm sterile Sarstedt filtropur S 0,45µm filters and syringes pre-rinsed with stream water. DOC subsamples were acidified with 250 µl 8 M HCl. ICP-OES subsamples were acidified with 500 µl concentrated HCl. All samples were stored in refrigerator awaiting further analysis. Initial laboratory treatment including pH and conductivity measurements as well as acidification and cold storage was performed in the laboratory the day of sampling, with exception of KS1-12 which were kept chilled in the field and then subsampled and stored in refrigerator within 2 days after sampling.

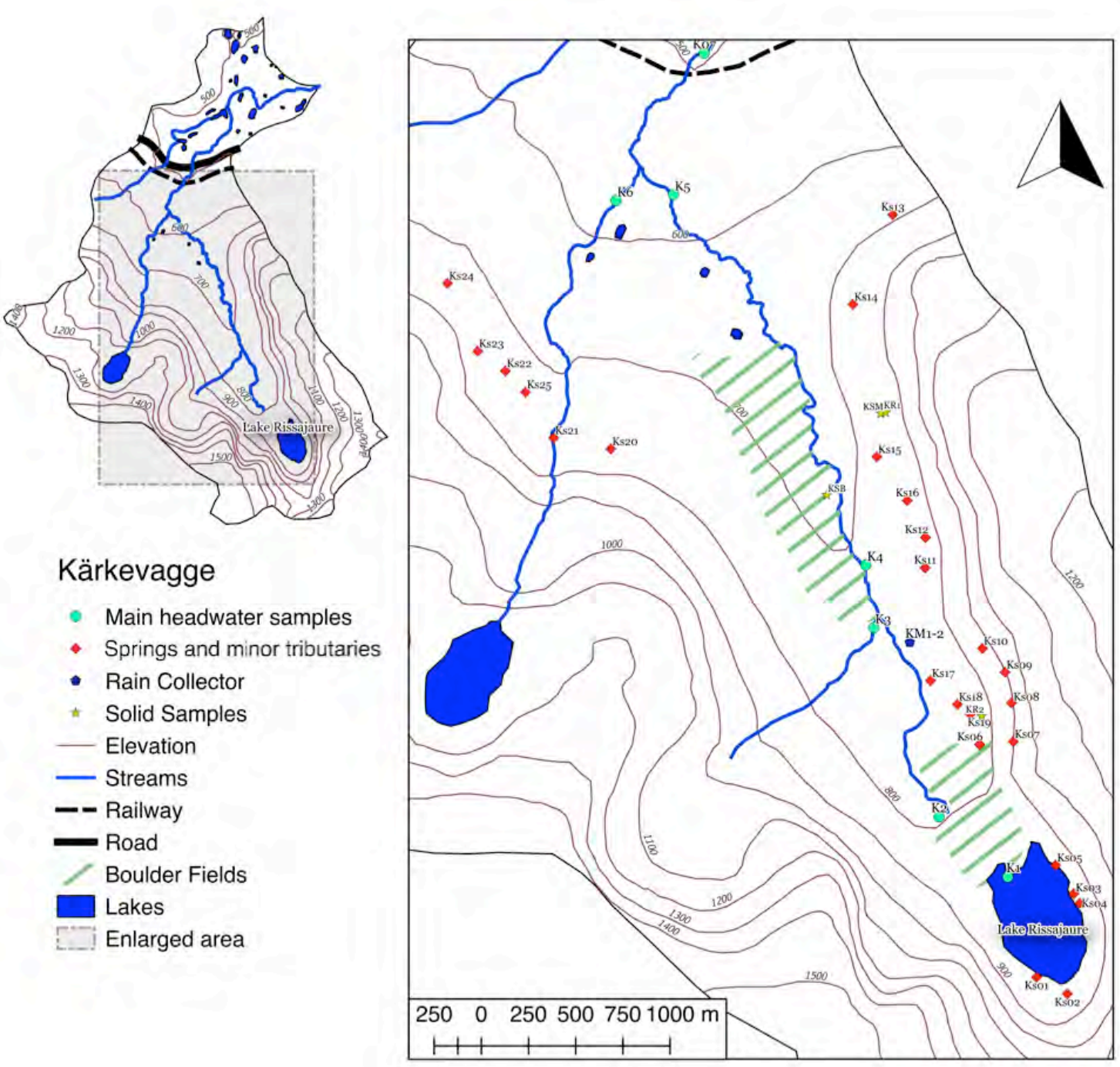

Figure 4. Map over Kärkevagge, with boulder fields and sampling sites marked out.

3.2.2 DOC

Samples were analyzed on a Shimadzu TOC-VcPH total organic carbon analyzer. The instrumental uncertainty for the machine is ±0,3 mg/L (Giesler *et al.*, 2014).

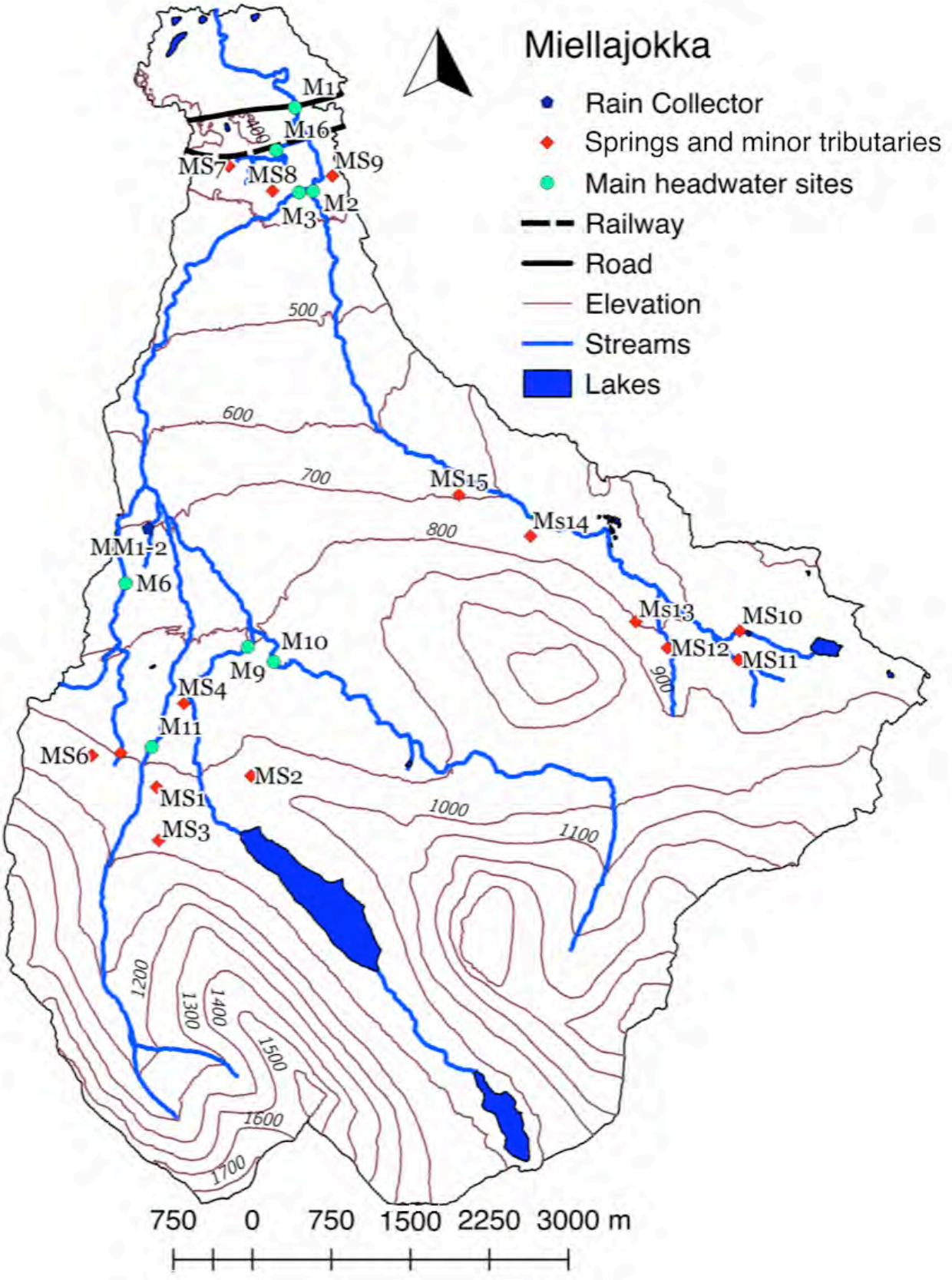

Figure 5. Map over Miellajokka, with sampling locations marked out.

3.2.3 ICP-OES

ICP-OES subsamples were analyzed on a Thermo ICAP 6500 Duo with a v-groove nebulizer and an Ultra Sonic Nebulizer Cetac 5000AT and a Cetac ASX-520 autosampler. Detection limits were calculated as three times the standard deviation of 10 blank samples. Samples were run in two different sets of main elements and trace elements analysis, resulting in a total of four sets of detection limits (DL) and error estimations. Error were estimated as the median error of elements when compared to a standard of known concentration. For main elements, error was estimated to 0,22% and 1,17% for the two runs. For trace elements, error was estimated to ±3,16% and ±1,29%. All errors and DL are added to data tables in appendix 2.1 and 2.3.

3.2.4 IC

Major anions were analyzed through ion chromatography (IC) on a Dionex IC20 ion chromatograph with an IonPac AS22 4x250 mm column and an AERS 500 4 mm suppressor. The eluent consisted of a 4,5 mM Na_2CO_3/1,4 mM $NaHCO_3$ solution, with a flow rate of 1,2 ml/minute. The limit of quantification (LOQ) for the different species was 0,25 mg/L for SO_4 and Cl, and 0,05 mg/L for F. This limit was not validated for NO_3. 95% confidence interval for the same species was 22% for F, 15% for Cl and 11% for SO_4.

3.2.5 Alkalinity

Alkalinity was measured with a Metrohm automated system using a Methrohm Aquatrode Plus (6,0257/000) pH electrode (Metrohm AG, Switzerland). Samples were acidified down to pH 4,0 with 0,1 M HCL and back-titrated to pH 5.6 using 0,1 M NaOH. Alkalinity was calculated from the difference in amount of acid and base used and the sample volume.

3.2.6 Isotope analysis

Measurement of several isotopic compositions were performed at Stockholm Isotope Laboratory (SIL), following the preparation and analysis steps explained below:

3.2.6.1 Sulfur Isotopes preparation

Sulfur isotope samples were allowed to drip through columns filled with about 9 ml wet Dowex 1x8 ion exchange resin, chloride form, pre-rinsed with 100 ml milli-Q high purity water and 0,2 L 0,5 M NaCl solution. Flow rate were around 5 ml/min and seldom faster. Columns were stored moist in refrigerator. In Stockholm, columns were rinsed with 0,2 L 0,5 M NaCl, and the eluate were collected in beakers. Since high purity NaCl were not always available, different samples experienced varying degrees of potential contamination during the ion exchange and eluation steps. Sulfur concentration were analyzed through ICP-OES for low purity grade salts. Appendix 1 gives complete information on Sulfur concentrations in salt used for the cleaning and rinsing of respective columns.

Eluates were acidified with HCl to a pH below pH 3. Eluates were then heated on a stove and boiled for a minimum of approximately one minute. These were then moved to a water bath of 90 where 5 ml 0,25 M BaCl solution were added in two turns, and $BaSO_4$ could precipitate out. Due to irregularities in the heating capacity of the stove, beaker designs, as well as the difficulty in consequent judgement of when a liquid starts to boil, it was not possible to keep a strict time restraint on the times during which the acidified solutions were heated. Lloyd (1968) demonstrated that the exchange of oxygen isotopes between sulfate species and water is strongly pH and temperature dependent. While not tested for pH below 3,8, the results by Lloyd (1968) indicate that the exchange rate at boiling temperatures and pH of about 2 would have a half-life on the scale of days. The exchange between HSO^-_4 and H_2O has shown to be faster (Hoering and Kennedy 1958), but under current pH conditions only a fraction of the sulfur would be in bisulfate form. It is therefore possible that samples would partly assimilate the $\delta^{18}O$ signature of laboratory water of about -8‰ (Heike Siegmund, pers. Comm), but it remains unlikely that this would occur to a larger degree. The exchange between $BaSO_4$ and H_2O is very low (Kusakabe and Robinson, 1977), meaning that this potential contamination would cease once the insoluble salt could precipitate out.

Samples were left on the water bath for the temperature to stabilize and then for two more hours. The temperature of bath and samples were continuously measured. After cooldown, samples were filtered and rinsed, and the precipitated $BaSO_4$ was collected on polycarbonate filters. Filters were oven dried at 60° C. When dry, filters were weighed and the samples scraped of and stored until analysis. Total recovery when compared with S concentrations as determined by IC and ICP-OES often equaled more than 100%, pointing towards an over-estimation through the analytical techniques despite a recalibration attempt of the ICP-OES. IC SO_4^{2-} concentrations were generally higher than ICP S concentrations and therefore deemed more reliable. The high recovery of the sulfur samples does however also indicate that virtually all SO_4 precipitated out as $BaSO_4$. Upon sulfur isotope analysis, approximately 0,5 mg of sample were weighed into tin capsules combined with a corresponding amount of V_2O_5. For oxygen isotope analysis, about 1 mg sample were weighed into a capsule.

Water content of soil samples was estimated through weight difference after oven drying at 60° C for 3 days. Sulfur content were measured through ICP-OES analysis of test extracts. Amounts representing 10 g dry soil was weighed up in 250 ml centrifuge bottles combined with 180 ml 0,04 M Na_2HCO_3 solution. Samples were left on a shaking table for 2 hours at 250 rpm and subsequently centrifuged at 4° C and 14 000 rpm for 15 minutes, maximum acceleration and deceleration. Supernatants were collected in bottles that subsequently was treated likewise to water samples, with two exceptions: 1) later treated eluates

Figure 6. Eluation of ion exchange colums with a NaCl solution at Stockholm University

were filtered before heating to enable efficient polycarbonate filtration without volume loss 2) the increased carbonate buffer in the eluates required about an order of magnitude larger HCl volume to push pH below pH 3. Although soil sample extraction was calculated to yield about 5 mg $BaSO_4$ per sample, the recovery was very unevenly distributed leading to only two samples being substantial enough for analysis (Table 1).

Solid samples were ground down to a powder and directly weighed up for sulfur isotope analysis in amounts of approximately 10 mg combined with with 2 mg V_2O_5.

Sulfur isotope ratios were measured on a En CarloErba NC2500 elemental analyzer connected through a Conflo open split interface to a Finnigan Delta Plus Isotopic rate mass spectrometer (IRMS). $\delta^{34}S_{SO4}$ and $\delta^{33}S_{SO4}$ were calculated in accordance with equations 7 and 8:

$$\delta^{34}S\ (‰) = \left[\frac{^{34}S/^{32}S_{Sample}}{^{34}S/^{32}S_{Standard}} - 1\right] * 1000 \quad (7)$$

$$\delta^{33}S\ (‰) = \left[\frac{^{33}S/^{32}S_{Sample}}{^{33}S/^{32}S_{Standard}} - 1\right] * 1000 \quad (8)$$

Standard for $\delta^{34}S_{SO4}$ and $\delta^{33}S_{SO4}$ was Vienna-Canyon Diablo Troilite (VCDT). 20 samples run in triplicates gave a standard deviation of 0,4‰ for $\delta^{34}S_{SO4}$ and 0,3‰ for $\delta^{33}S_{SO4}$. The instrumental setup was originally designed by Baublys *et al.*, 2004. Sulfate $^{18}O/^{16}O$ ratios were measured on a Temperature conversion elemental analyzer (TC/EA) connected through a ConfloIV open split interface to a Thermo Scientific DeltaV advantage Isotopic ratio mass spectrometer (IRMS).

Sulfur isotopes were analyzed for mass-independent fractionation (MIF) through the calculation of $\Delta^{33}S$ (equation 9):

$$\Delta^{33}S = \delta^{33}S - 0{,}515 * \delta^{34}S \quad (9)$$

A $\Delta^{33}S$ value outside of $\sim\pm$ 0,5‰, i.e. not placed on the mass-dependent fractionation line of $\delta\ ^{33}S \approx 0{,}515 * \delta\ ^{34}S$, indicates an origin of the rock from before the great oxygenation event (~2,3 Ga), before which the MIF-signal from photochemical reactions of sulfur-bearing gases in the atmosphere was not destroyed due to rapid oxidation (Pavlov & Kasting, 2002, Domagal-Goldman *et al.*, 2011).

$\delta^{18}O_{SO4}$ was calculated in accordance with equation 10:

$$\delta^{18}O\ (‰) = \left[\frac{^{18}O/^{16}O_{Sample}}{^{18}O/^{16}O_{Standard}} - 1\right] * 1000 \qquad (10)$$

Standard for oxygen isotopes was Vienna Standard Mean Ocean Water (V-SMOW). Ten samples were run in duplicates. The standard deviation of the analysis was 0,4‰. Oxygen isotope analysis was successful for all but a handful of samples, for which there was a shortage of material. Sulfur isotopes were analyzed for all but one sample.

3.2.6.2 Water isotopes

D/H and $^{18}O/^{16}O$ ratios of water were analyzed through laser adsorption spectroscopy with a Picarro L2140-*i* Liquid Water Isotope Analyzer. $\delta\,^{18}O_{H2O}$ were calculated from equation 9, and δ D from equation 11:

$$\delta D\ (‰) = \left[\frac{D/H_{Sample}}{D/H_{Standard}} - 1\right] * 1000 \qquad (11)$$

Standard for δ D and $\delta\,^{18}O$ was Vienna Standard Mean Ocean Water (V-SMOW). From our measurements, the reproducibility was calculated to be better than 0.6‰ for δ D and 0.1‰ for δ 18O.

3.2.6.3 $\delta^{13}C_{DIC}$

$^{13}C/^{12}C$ ratios of DIC were measured through a GasbenchII continuous flow preparation device coupled to a MAT253 IRMS both from Thermo Scientific and using a GC-PAL autosampler. $\delta^{13}C_{DIC}$ was calculated from equation 12:

$$\delta^{13}C\ (‰) = \left[\frac{^{13}C/^{12}C_{Sample}}{^{13}C/^{12}C_{Standard}} - 1\right] * 1000 \qquad (12)$$

Standard for $\delta^{13}C$ was Vienna Pee Dee Belemnite (VPDB). Method is well-established at SIL with a standard deviation of 0,06‰, but some samples experience a standard deviation of 0,2‰ due to low DIC concentrations. These samples are marked out in appendix 2.5.

3.2.7 Data processing

Statistical analysis was performed with JMP statistical software. The geochemical modeling code PHREEQC was used to calculate DIC concentrations and phases from alkalinity and pCO_2 as well as for calculating saturation indices and charge balances. TDS was estimated from conductivity by multiplying the value in μS by 0,7, a factor determined with the use of data from Kärkevage by Strömqvist and Rehn (1981; referenced in Darmody *et al.*, 2000b)).

4. Results

Besides the graphs and figures found in this section, compilation of all data presented in this thesis is included in tables in Appendix 2.

4.1 Meteoric Water

Rain water samples showed variation in several variables, both between the two sites and within the same site between sampling occasions. Common element atomic ratios are presented in table 2. Out of the four rain water samples, Ca concentrations of sample MM2 were about a magnitude higher when compared to the other three samples (6,98 vs 0,28-0,74 μmol/L). Rain water S and Na concentrations fell within a range between 21-24 and 7,5-11,5 μmol/L, respectively.

Sample (date)	Location	S (µmol/L)	S/Na	Ca/Na	$\delta^{34}S$ vs CDT (‰)	$\delta^{18}O_{SO4}$ vs SMOW (‰)
KM1 (1-23/7)	Kärkevagge	21,2	2,38	0,03	18,7	*n.a.*
KM2 (18/8-30/9)	Kärkevagge	21,6	1,88	0,08	15,8	*n.a.*
MM1 (8/7-16/8)	Miellajokka	22,4	2,88	0,09	11,7	-8,6
MM2 (16/8-30/9)	Miellajokka	24,0	2,29	0,67	16,1	*n.a.*

Table 2. Key characteristics of rain water samples

Rain water samples fell outside of both the global meteoric water line (GMWL) and a local meteoric water line (LMWL) constructed for the region from stream and lake water data (Jonsson *et al.*, 2009, figure 17). Deposition sulfate $\delta^{34}S$ varies between +11,7-+18,7‰. Only sample MM1 was analyzed for $\delta^{18}O_{SO4}$, displaying a signature of -8,6‰.

4.2 Solid samples

The two weathered sulfide samples, KR1-2, had $\delta^{34}S$ signatures of -4,5‰ and -1,5‰. The meadow soil sample (KSM), representing a soil depth of 5-15 cm, had a corresponding signature of +3,6, while the boulder soil sample (KSB) were heavier with an $\delta^{34}S_{SO4}$ signature of +10,3. $\delta^{18}O_{SO4}$ values for KSM and KSB were +0,7 and +5,0, respectively.

Plotting of $\delta^{33}S$ and $\Delta^{33}S$ vs $\delta^{34}S$ (figure 7) revealed that most samples fall close to the mass-dependent fraction line of $\delta^{33}S \approx 0{,}515 * \delta^{34}S$. The one exception is rock sample KR1 ($\Delta^{33}S$ = 1,68‰).

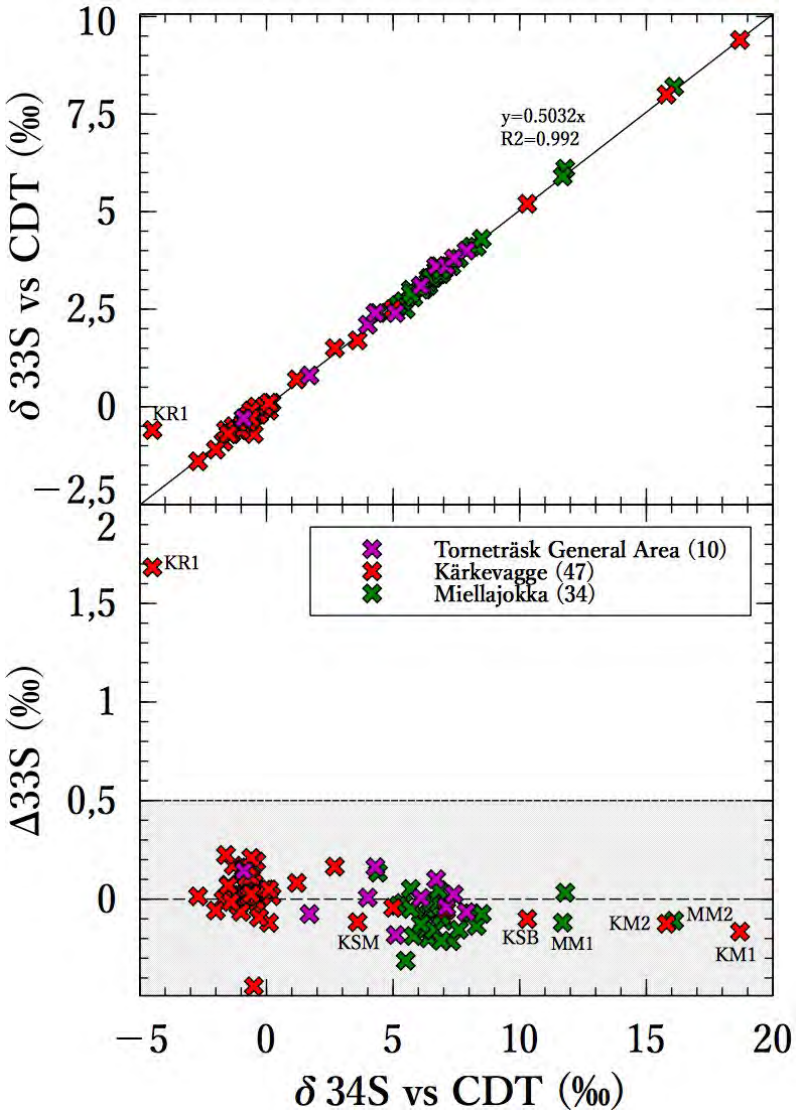

Figure 7. Top: The relationship between $\delta^{33}S$ and $\delta^{34}S$ for all samples, plotting close to the mass-dependent fractionation line of $\delta^{33}S \approx 0{,}515\ \delta^{34}S$ Bottom: $\Delta^{33}S$ vs $\delta^{34}S$. Grey area indicates the ±0,5‰ which is considered indistinguishable from mass-dependent fractionation (Domagal-Goldman et al.*, 2011).*

4.3 Stream Water

4.3.1 Water chemistry

Distributions of pCO2 concentrations along with modeled pH values are presented in figure 8 for the sample groups of main headwater sites and springs and smaller tributaries. Low discharge sites in Miellajokka displays the largest spread in pCO_2 values, as well as generally higher values when compared to the other sample groups, rivaled only by a few small sources in Kärkevagge. Kärkevagge display a larger spread in pH values than Miellajokka, but main headwater sites pH in both catchments are approximately neutral, or slightly basic in the case of Kärkevagge. Kärkevagge springs and tributaries show the biggest spread of the groups.

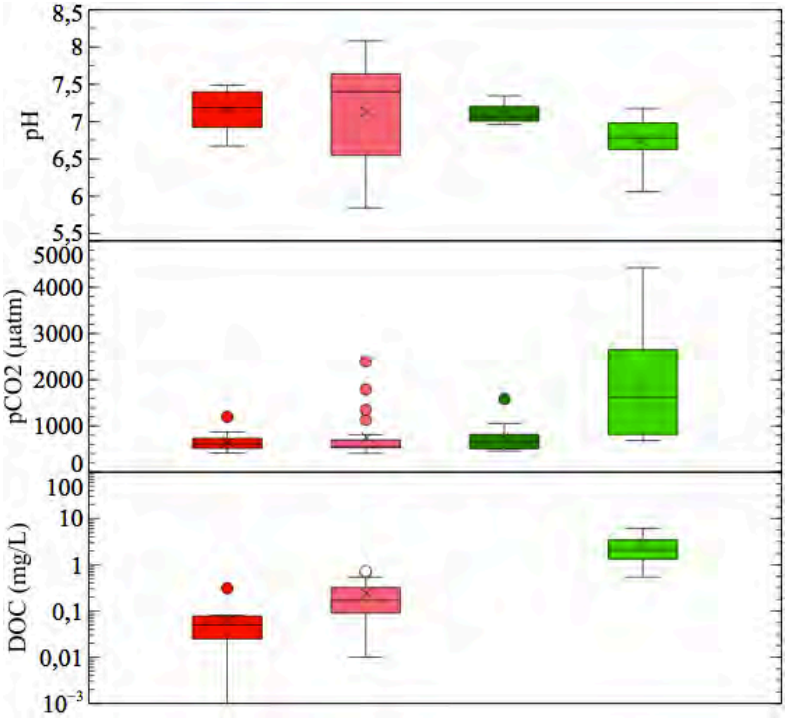

*Figure 9. Box plots over pH, pCO_2 concentration and DOC concentration distributions for groups of data. Boxes connects quartiles, and whiskers equals 1,5*Interquartile range. Crosses denotes mean. Left: Kärkevagge main headwater sites (pH, pCO_2 n=15, DOC n=14). Middle left: Kärkevagge springs and small tributaries (pCO2, pH n=22, DOC n=25). Middle right: Miellajokka main headwater (pCO2, pH n=11, DOC not available). Right: Miellajokka springs and small tributaries (n=15).*

Spatial distributions of major dissolved species Ca, S and DIC are presented together with TDS concentrations in mg/L in figures 10 and 11. The concentrations for the main headwater sites in these graphs correspond to the late summer sampling. DIC species dominates throughout Miellajokka, whereas Ca and S concentrations have a relatively larger importance in Kärkevagge when compared to Miellajokka. TDS concentrations are generally higher in Kärkevagge, reaching its highest values in small discharge sites along the central eastern valley slope. Ca is the dominant cation at all sites (see data table in Appendix 2).

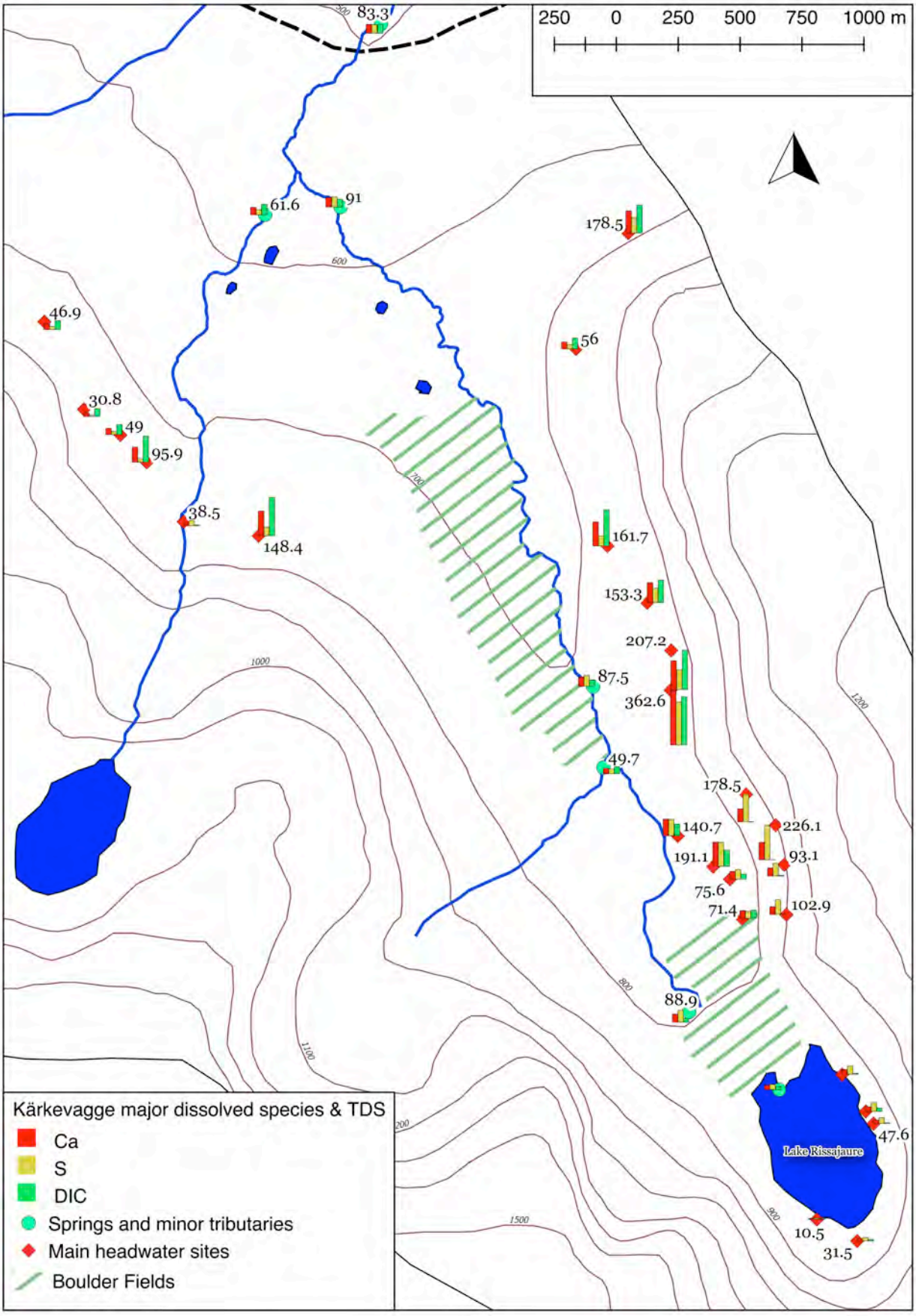

Figure 10. Major ions and elemental concentrations in Kärkevagge. Number beside sample point depicts TDS concentration in mg/L.

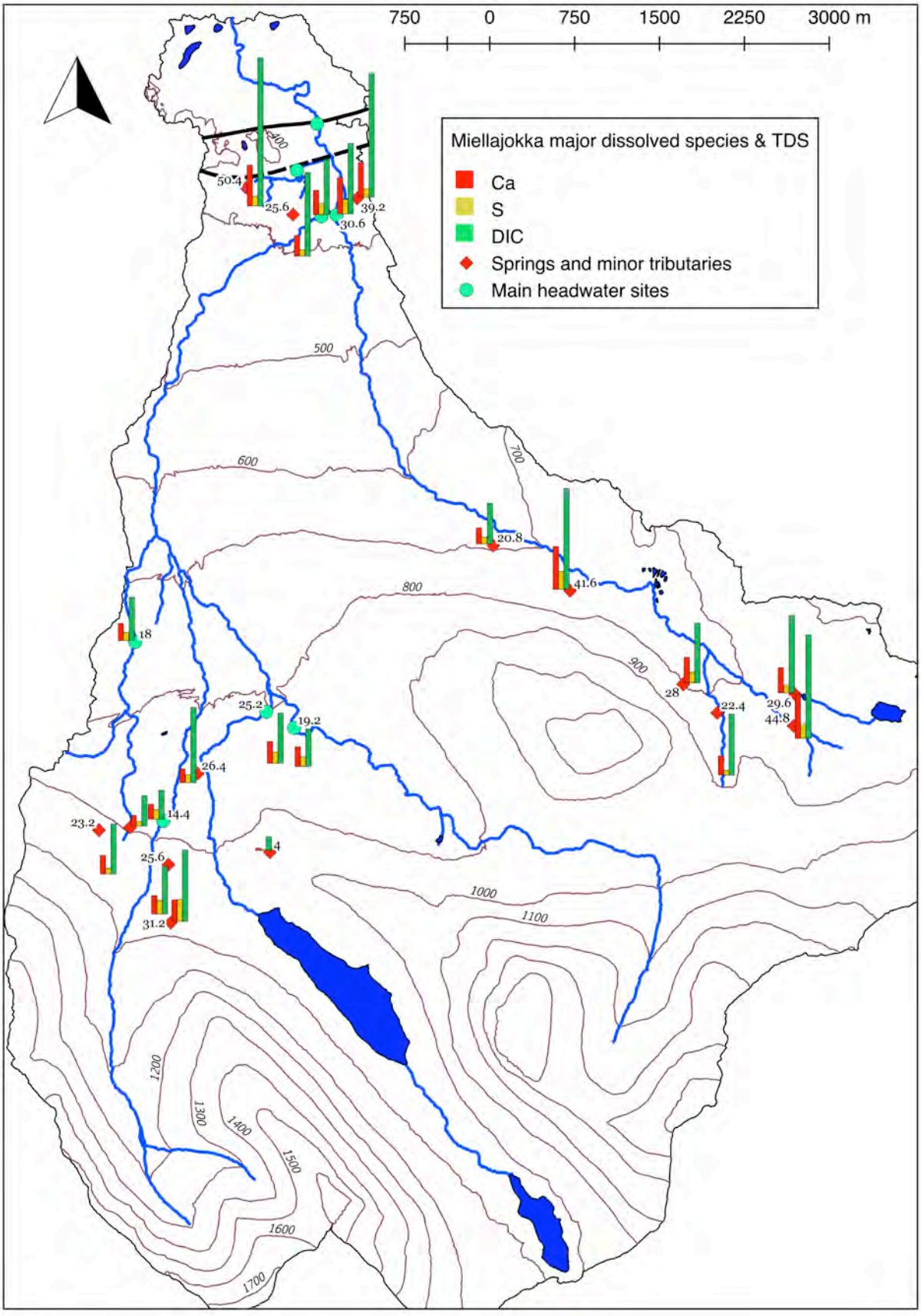

Figure 11. Major ions and elemental concentrations throughout the Miellajokka catchment area. Number beside sample point depicts TDS concentration in mg/L.

Multivariate analysis of element concentrations in both catchments revealed many good correlations in Kärkevagge but only a handful above R = 90 in Miellajokka. Relatively good correlations in Miellajokka include: Ca and Sr (R = 0,91), Al/Ni (R = 0,90), and Cu/Co (R = 0,93). For Kärkevagge, notably good correlations include Ca/Sr (R = 0,97), S/Mg (R = 0,98), Cd/Ni (R = 0,99), Cd/Zn (R = 1,00), Ce/Cu (R = 0,99), Co/Mn (R = 1,00), and Zn/Ni (R = 1,0). Trace element concentrations in Miellajokka is generally lower, and many concentrations are therefore below or close to the detection limit for this catchment. Selected element ratios are plotted in figure 12. Distribution of major rock-forming elements are presented in figure 13.

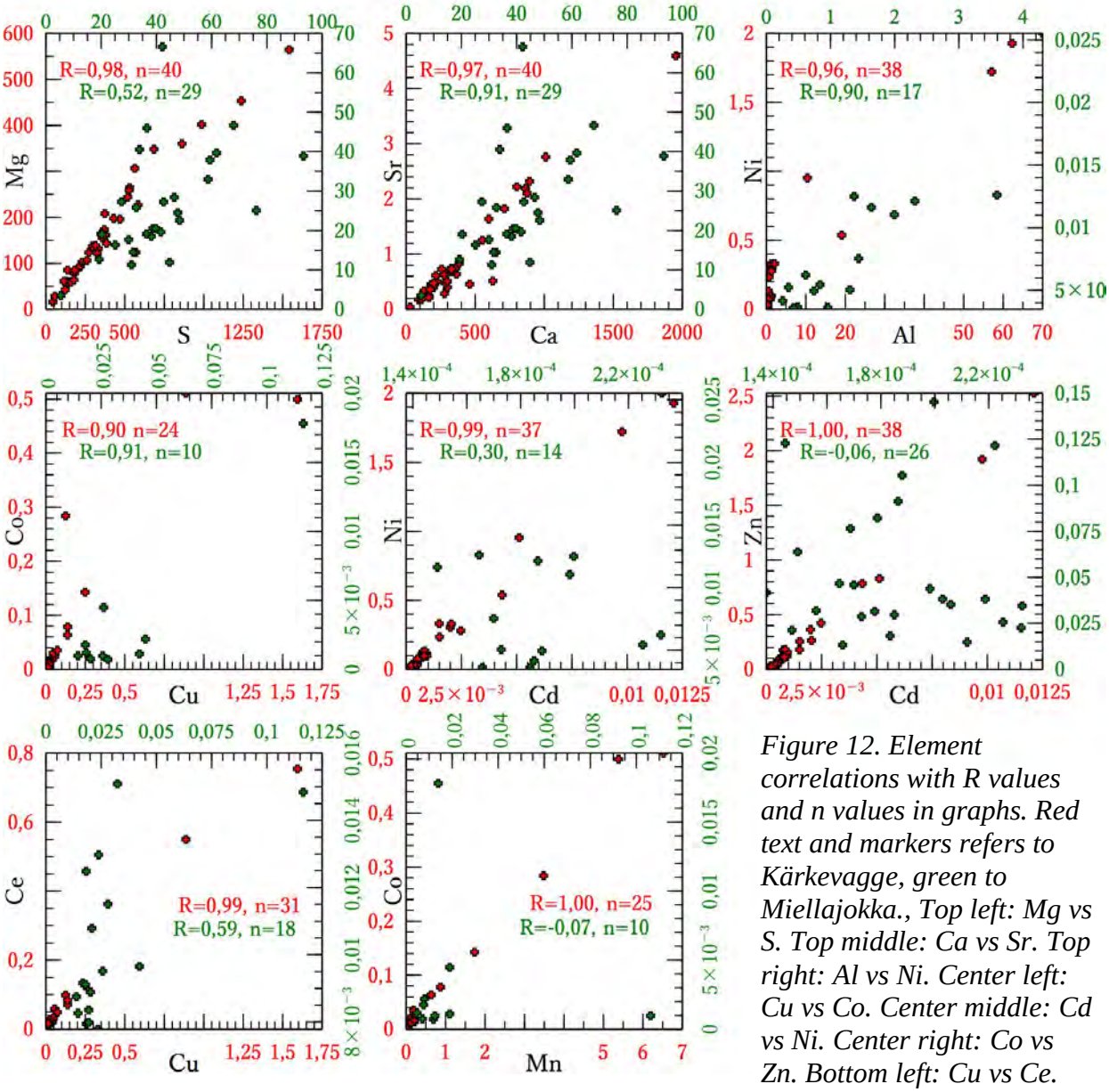

Figure 12. Element correlations with R values and n values in graphs. Red text and markers refers to Kärkevagge, green to Miellajokka., Top left: Mg vs S. Top middle: Ca vs Sr. Top right: Al vs Ni. Center left: Cu vs Co. Center middle: Cd vs Ni. Center right: Co vs Zn. Bottom left: Cu vs Ce. Bottom right: Mn vs Co.

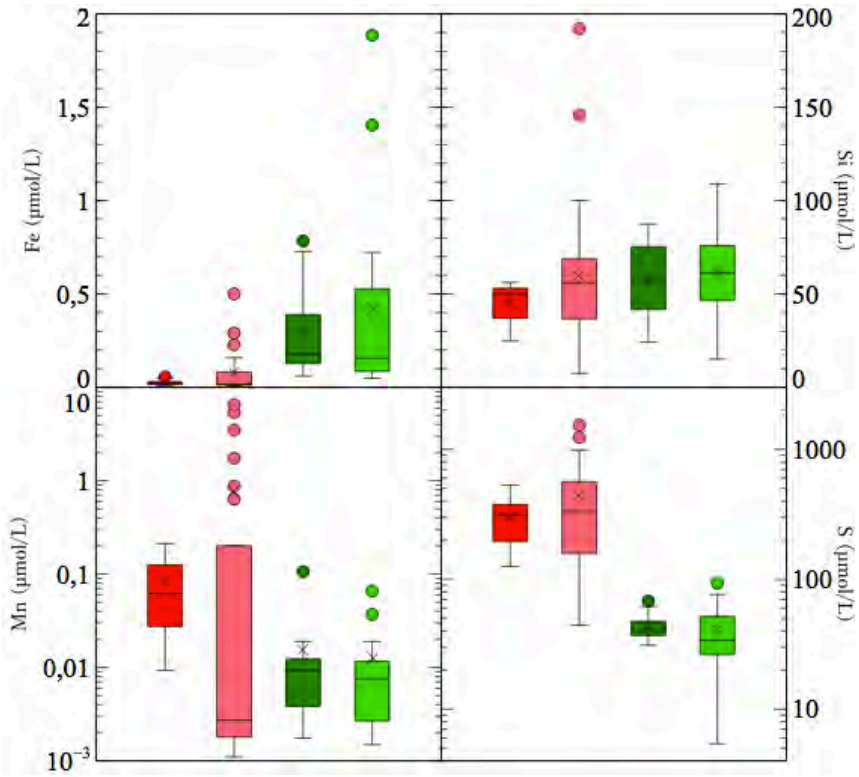

*Figure 13. Box plots over Fe (upper left), Si (upper right), Mn (lower left) and S (lower right) distributions for groups of data. Boxes connects quartiles, and whiskers equals 1,5*Interquartile range. Crosses denotes mean. Left: Kärkevagge main headwater sites (n=15). Middle left: Kärkevagge springs and small tributaries (n=25). Middle right: Miellajokka main headwater sites (Fe n=13, Si, Mn, S n=14). Right: Miellajokka springs and small tributaries (n=15).*

Water composition for stream samples within the Miellajokka versus the Kärkevagge watershed is summarized in a piper diagram (figure 14), in which rock type and weathering mechanism end members also are included (*e.g.* Spence & Telmer, 2005). In this diagram, The Kärkevagge water samples plot as a mixture between weathering of dolomite and calcite/gypsum, with a lesser contribution of granite or similar rock types. There is an overlap between Kärkevagge and Miellajokka samples, but the contribution from granitic rocks is larger within the Miellajokka watershed. Kärkevagge samples generally fall within the regime of weathering products by gypsum weathering and carbonate weathering by H_2SO_4, with a few samples more closely resembling weathering products from carbonate weathering by carbonic acid. Miellajokka samples plot within the regime of mixed weathering of carbonates and granites by carbonic and sulfuric acid, with few exceptions more strongly resembling weathering products from gypsum weathering.

Saturation indices from Kärkevagge and Miellajokka (table 3) reveals that waters within both catchments consistently are undersaturated in respect to common phases. Exceptions include the clay mineral illite, quartz and gibbsite ($Al(OH_3)$) which variates between sites or fluctuates around saturation, and iron oxides goethite ($FeO(OH)$) and hematite (Fe_2O_3)

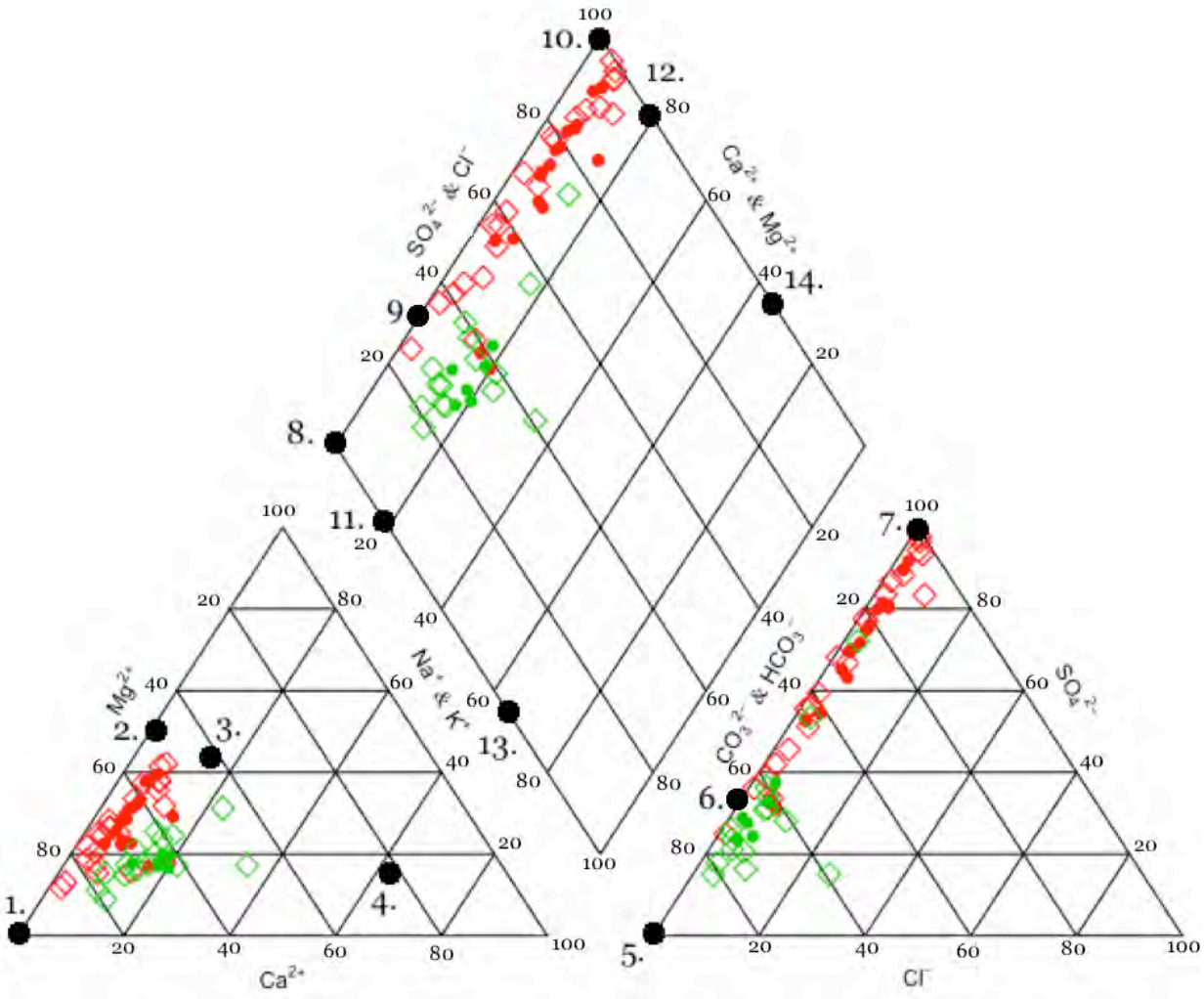

Figure 14. Piper diagram with Kärkevagge (red) and Miellajokka (green) water samples. Circles denotes main headwater sites, open squares denote springs and minor tributaries. Black dots denote end members: 1. Calcite or gypsum 2. Dolomite 3. Basalt 4. Granite 5. Silicate or carbonate weathering by H_2CO_3 6. Carbonate weathering by H_2SO_4 7. Silicate weathering by H_2SO_4 or gypsum weathering 8. Carbonate weathering by H_2CO_3 9. Carbonate weathering by H_2SO_4 10. Gypsum weathering 11. Basalt weathering by H_2CO_3 12. Basalt weathering by H_2SO_4 13. Granite weathering by H_2CO_3 14. Granite weathering by H_2SO_4. Modeled after Spence & Telmer (2005).

for which Kärkevagge is oversaturated and Miellajokka undersaturated. Charge imbalances averaged around 2,2% for 62 modeled samples. M1 data only represents the average of the early summer and autumn sampling occasions.

Group (n)	Charge balance error (%)	SI calcite	SI gibbsite	SI gypsum	SI goethite
K (15)	3,72±2,58	-2,41±0,54	1,90±0,20	-2,70±0,27	4,47±0,94
KS (22)	1,83±3,68	-2,32±1,86	1,25±0,76	-2,67±0,69	4,44±1,64
K7 (3)	2,20±2,53	-1,89±0,16	1,82±0,18	-2,56±0,14	5,28±0,26
M (10)	2,05±4,71	-2,85±0,38	-2,00±0,36	-3,89±0,22	-19,21±0,80
MS (15)	1,02±3,98	-3,31±0,86	2,30±0,31	-4,04±0,56	-21,00±1,44
M1 (2)	-1,41±2,19	-2,80±0,45	-2,37±0,25	-3,75±0,40	-19,55±0,07

Group (n)	SI CO2g	SI hematite	SI illite	SI dolomite	SI pyrite	SI quartz
K (15)	-3,21±0,12	10,86±1,88	0,42±0,51	-5,34±1,03	-93,19±4,87	-0,08±0,13
KS (22)	-3,18±0,20	10,82±3,28	-1,27±1,98	-5,18±3,52	-94,38±12,01	-0,16±0,28
K7 (3)	-3,28±0,09	12,47±0,53	0,74±0,35	-4,36±0,26	-96,94±0,13	-0,021±0,10
M (10)	-3,18±0,16	-36,48±1,64	-0,73±1,16	-6,35±0,80	-119,49±4,78	-0,01±0,23
MS (15)	-2,83±0,29	-40,09±2,89	0,89±1,05	-7,34±1,26	-112,94±5,07	0,017±0,23
M1 (2)	-2,97±0,24	-37,20±0,13	-1,71±0,33	-6,36±0,81	-115,54±2,00	0,10±0,26

Table 3: charge balances and saturation indices for groups of samples in Kärkevagge and Miellajokka. K = Kärkevagge main headwater sites KS = Kärkevagge Springs and smaller tributaries K7= mean of measurements at the Kärkejokk outflow site. M = Miellajokka main headwater sites MS = Miellajokka Springs and smaller tributaries M1 = mean of measurements at the Miellajokka outflow site. Error margin is given by one standard deviation.

4.3.2 Isotopes

A plot of $\delta^{34}S_{SO4}$ versus $\delta^{18}O_{SO4}$ values are found in figure 15. Most the Kärkevagge samples plot very close to the $\delta^{34}S_{SO4}$ values of the weathered sulfide samples KR1-2, marked by the red field in figure 15. A few samples even plot within this interval. Miellajokka sites concentrate around a $\delta^{34}S_{SO4}$ value of about +7‰.

Kärkevagge $\delta^{18}O_{SO4}$ and $\delta^{34}S_{SO4}$ values show temporal only within the range of 0,5-1‰. (figure 16). Miellajokka $\delta^{18}O_{SO4}$ and $\delta^{34}S_{SO4}$ values display a larger temporal variation. Most noticeably are the shifts in $\delta^{18}O_{SO4}$ values for sites M3 and M11, which decreases by 6-7‰ over the course of the summer months. While the $\delta^{18}O_{SO4}$ variation is larger for the Miellajokka samples, the deviation from the mean value compared to the mean $\delta^{18}O_{H2O}$ value is smaller in this catchment (table 4).

Kärkevagge $\delta^{18}O_{H2O}$ and δD signatures are generally denser than Miellajokka counterparts, and are separated from rain water samples by having generally lighter $\delta^{18}O$ or δD signatures (figure 17). Miellajokka spring sample MS2 has a significantly heavier water isotopic composition when compared to both other stream water samples and meteoric water samples.

Plotting of $\delta^{13}C_{DIC}$ values against $\ln pCO_2$ concentration (figure 18) reveals a relationship for Miellajokka sites, where high values of pCO_2 corresponds to light isotopic composition with R^2=0,803. The same relationship is not seen for Kärkevagge sites, which also show a smaller data spread with respect to both variables.

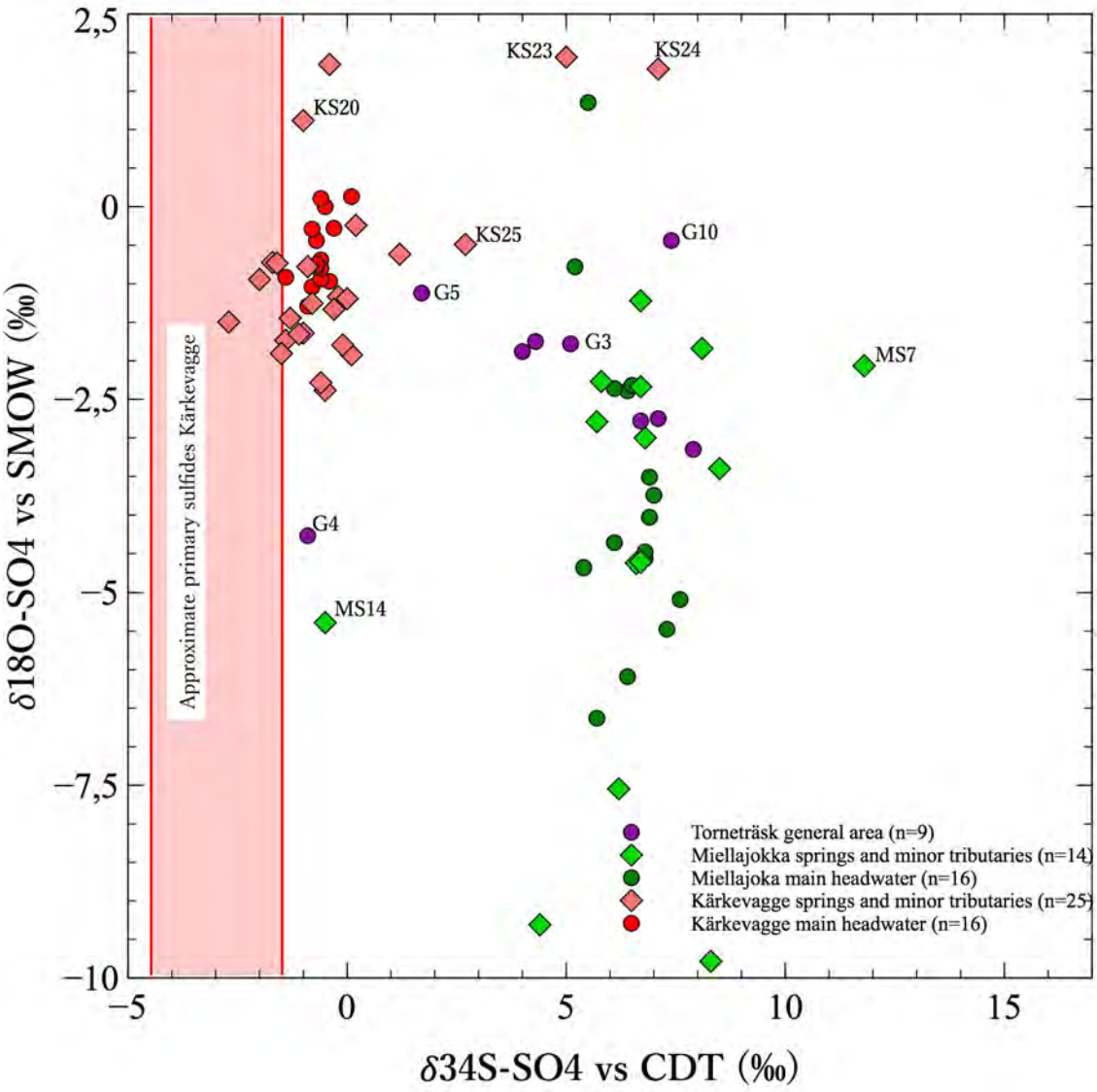

Figure 15. plotting of samples in respect to $^{34}S_{SO4}$ and $^{18}O_{SO4}$ *. Red field marks the field in between solid samples KR1-2. Rain water composition (green ring) is based on the two* $\delta^{34}S_{SO4}$ *measurements and he single* $\delta^{18}O_{SO4}$ *data point of Miellajokka rain water.*

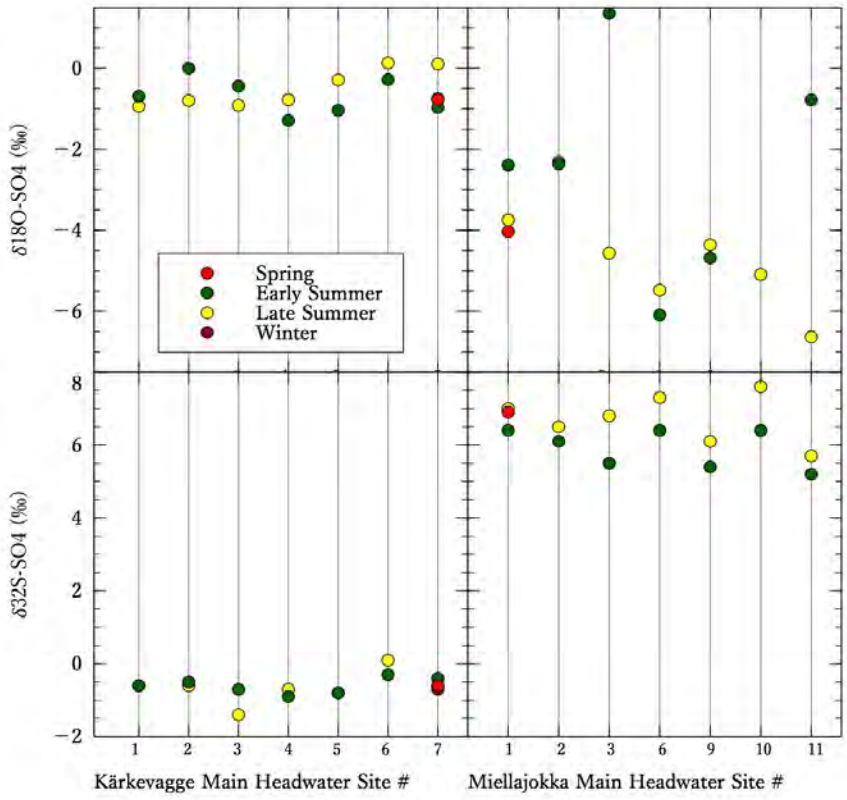

Figure 16. The temporal variation of $\delta^{34}S_{SO4}$ and $\delta^{18}O_{SO4}$ for Kärkevagge and Miellajokka mzin headwater sites.

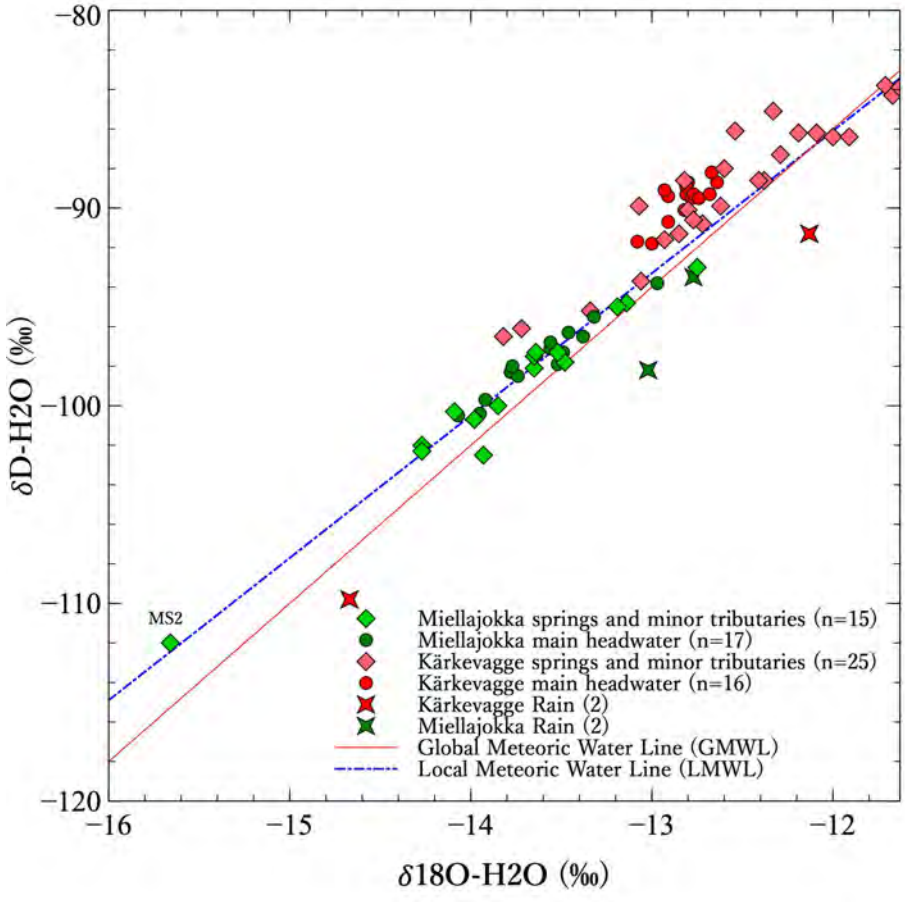

Figure 17. Water isotope plot with GMWL and LMWL (Jonsson et al., *2009) marked out.*

Catchment (N)	$\delta\ ^{18}O_{H2O}$ mean (‰)	$\delta\ ^{18}O_{SO4}$ mean (‰)	$\Delta^{18}O_{H2O-SO4}$ (‰)
Kärkevagge (40)	-12,67 ± 0,48	-0,75 ± 1,02	-11,92
Miellajokka (29)	-13,71 ± 0,52	-3,96 ± 2,47	-9,75

Table 4: key aspects of stream samples oxygen isotopes. Variation range equals one standard deviation.

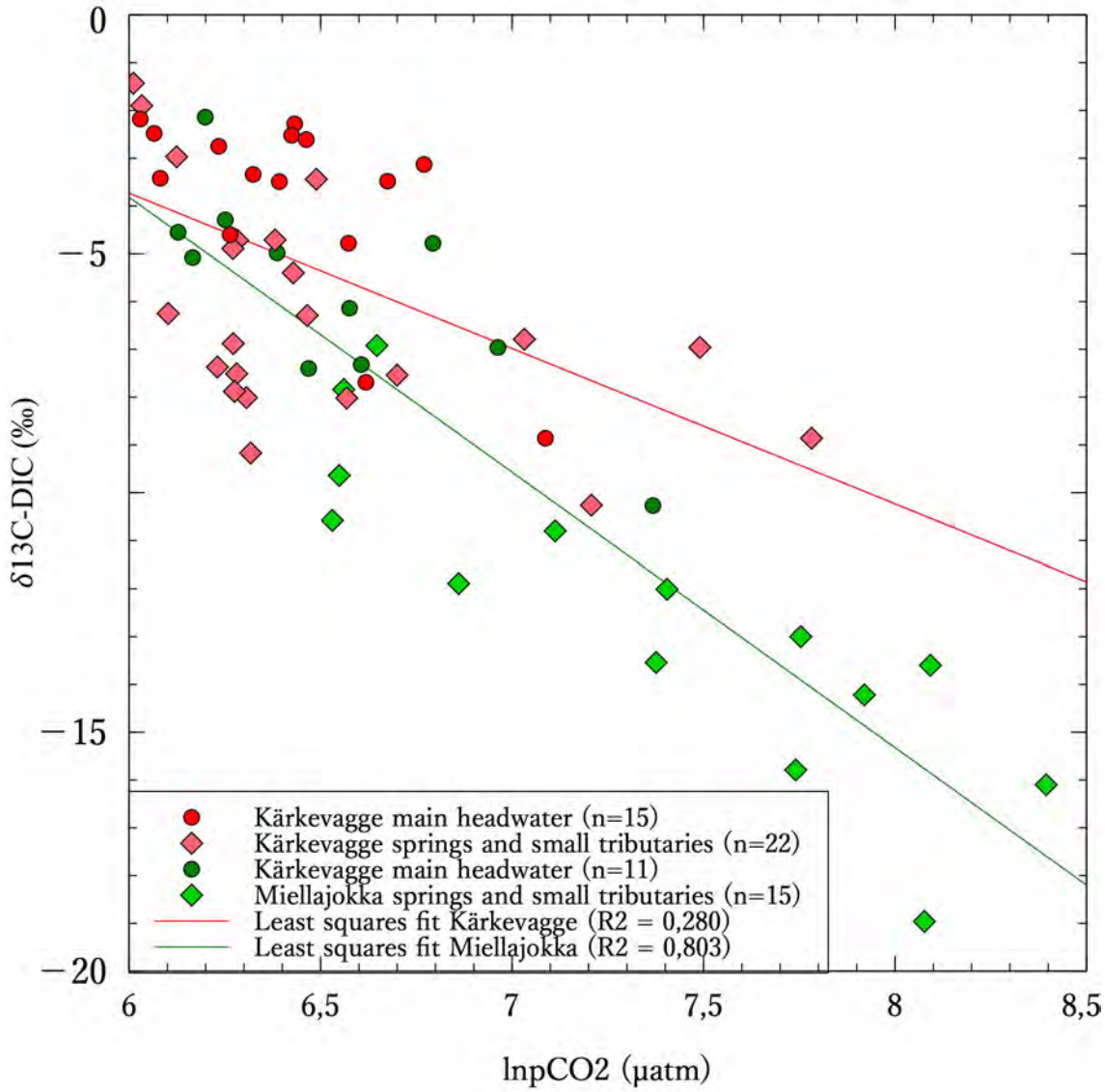

Figure 18: Plot of pCO_2 vs. $\delta^{13}C_{DIC}$. Lines determines least squares fit for all samples from the corresponding catchments.

5. Discussion

5.1 Data evaluation

5.1.1 potential error evaluation

The biggest potential errors in this work is judged to be associated with the preparation for $\delta^{34}S_{SO4}$ and $\delta^{18}O_{SO4}$ analysis, as the use of low-grade purity salt may have contaminated $\delta^{34}S_{SO4}$ and potential exchange between sulfate species and H_2O under low pH/high temperature conditions partially could contaminate $\delta^{18}O_{SO4}$ (Lloyd, 1968, Hoering & Kennedy, 1958, section 3.2.5.1). Ideally, the impact of these possible errors should have been explored further such as through monte carlo-simulations. Due to time restrictions, no such simulation was performed, and the apparent impact of these error sources are therefore instead discussed below in light of the results presented above.

Appendix 1 contains a list of the quality of salt used for column preparations and eluents for all samples and the corresponding sulfur concentrations of the low-purity salt. It is noteworthy that the salt used for most column preparations contain 2,11 mg/L S, equal to 0,422 mg S/sample. Unfortunately, $\delta^{34}S$ of the salt solutions were never measured. However, while early summer samples were collected on columns prepared with this salt, the salt used for preparations of columns for late summer main headwater samples of both sites were of high-purity grade. Comparison between $\delta^{34}S_{SO4}$ for these samples (figure 16) reveals that the variation for each sampling site is close to the error of margin. Especially so for Kärkevagge, for which $\delta^{34}S_{SO4}$ show a generally small spread (figure 15), indicating that a single sulfate source dominates and temporal variation therefore can be expected to be less. While significant contamination cannot be completely ruled out, it appears likely that the high affinity of Chloride to the chloride-form ion exchange resin used successfully rinses the column and removes sulfur simultaneously as the solution can drip through, thereby removing most the contaminating sulfur in the process. There would be no avoiding sulfur in the eluent from contaminating the sample. Fortunately, the low-purity NaCl eluent contained only 0,18 mg/L S, and was only used for a handful of samples (appendix 1). No apparent trends of deviation can be observed for these samples. However, five of the ten samples from the Torneträsk general area were eluded with low-purity salt without duplicate attempts (G1, G4-6, G8). Data interpretation of

the general Torneträsk area with respect to these five samples should therefore be done with caution.

Contamination of $\delta^{18}O_{SO4}$ values would arise from uncontrollable parameters in the lab such as uneven boiling times, water bath temperatures and beaker shapes. Two extraordinary cases, forgotten beakers and changed water bath temperatures, are noted down for affected samples in appendix 1. However, no apparent trends of deviation can be observed for the affected samples. Figure 16 displays that $\delta^{18}O_{SO4}$ stays largely constant in Kärkevagge throughout the year, as the processes of sulfate production in the sulfide-weathering dominated catchment likely does not change significantly on annual basis. Temporal $\delta^{18}O_{SO4}$ deviation in Miellajokka headwater sites are dominantly defined by the excursions of spring samples 3 and 11 towards heavier signatures. With laboratory $\delta^{18}O_{H2O}$ of ~-8‰ (Heike Siegmund, pers. Comm), this deviation is in the opposite direction compared to what would expected through exchange of oxygen between sulfate species and H_2O.

5.1.2 Rain water $\delta^{18}O_{SO4}$

The $\delta^{18}O_{SO4}$ signature of the only measured deposition value was -8,63‰. Primary anthropogenic sulfate is known to be isotopically heavy (*e.g.* Holt *et al.,* 1982), while marine sulfate has a composition of around +9.5‰ (Longinelli & Craig, 1967). Most literature examples of deposition $\delta^{18}O_{SO4}$ presents positive signatures (*e.g.* Novák *et al.,* 2007, Holt *et al.*, 1982, Jaimeson & Wadleigh, 1999*)*, and the single meteoric $\delta^{18}O_{SO4}$ data point is dissimilar to most stream water samples in the study. Additionally, the high $\delta^{34}S_{SO4}$ value of most rainwater samples combined with the proximity to the ocean suggests that a large fraction of deposition sulfate comes from sea spray, but the oxygen $\delta^{18}O_{SO4}$ values is contradictory. If the analyzed signature is correct, the origin of the sulfate remains enigmatic.

Due to the high isotopic exchange rate between oxygen in SO_2 and H_2O, any sulfate formed in the atmosphere, so-called secondary sulfates, would equilibrate with atmospheric water vapor (Holt *et al.*, 1982, Holt and Kumar, 1991). All measured $\delta^{18}O_{H2O}$ for rain water samples are negative and a dominance of secondary sulfate seems to be the most reasonable explanation for this mystery. Whatever the formation mechanism, the deposition $\delta^{18}O_{SO4}$ value is along the lowest measured in the data set, and is

therefore unlikely to be a representative end member value for deposition sulfates in any of the catchments.

5.1.3 Rain water δD & $\delta^{18}O_{H2O}$

Water isotopes for the meteoric samples fell outside of the global meteoric waterline, but were parallel, although offset, to the LMWL. This could potentially be partially due to fractionation during evaporation from the open and relatively unprotected rain collectors, which is expected to follow an evaporation line with a gentler slope in the $\delta D/\delta^{18}O$ plot in figure 17 (Jonsson *et al.*, 2009). The deviation form LMWL for all rainwater samples cannot be explained by this mechanism.

5.2 Local variations within study areas

Figure 9 shows that pCO_2 and pH of main headwater sites in Kärkevagge approximates the mean of the data from springs and minor tributaries across the valley. This trend is not observed for Miellajokka, which experiences large variations between high-discharge and small discharge sites. The elevated pCO_2 values and lower pH values for springs and minor tributaries in Miellajokka can be explained by a larger proportion of wetland sites and slow-running water in this catchment, where biologic activity can be expected to be higher. This is strengthened by higher DOC concentrations for Miellajokka springs and minor tributary sites compared to corresponding sites in Kärkevagge (figure 9 lower).

Maps of major dissolved species (figure 10 and 11) reveal significant differences and large data spreads within the two catchments. However, the temporal aspect of sampling must be considered when studying these figures, as smaller discharge sites were sampled in July with main headwater site collected in middle August. Additionally, springs and minor tributary sampling sites appears to vary greatly in terms of discharge, but no attempt has been done to quantify discharge rates. These samples were also collected from varying distance from the subaerial outlets, as the source were not always accessible. Still, several discernible patterns can be observed in the data from both catchments. In Miellajokka, DIC concentrations are strongly dominant on all sites. The relative contribution of calcium and sulfur appears to be higher along the eastern tributaries. Calcium always dominates over sulfur throughout

Miellajokka except for the two southeasternmost springs MS1 and MS3 where Ca/S are closer to one. In Kärkevagge, DIC has a generally lower importance over the water chemistry and the water chemistry is dominated by either sulfur, calcium or DIC. The western side has relatively low sulfur concentration and is most often dominated by DIC. This part of the valley has been recognized for having dolomitic marble bedrock (Kulling et al., 1964, Dixon *et al.*, 1995), explaining the smaller importance of sulfur in this area. Sulfur dominates strongly in four sites directly north of the southern boulder field (KS7-10). Four springs located directly southwest of the previously mentioned sites (KS6, KS17-19) have more evenly distributed concentrations between DIC, calcium and sulfur. Additionally, the latter sites have a higher pH when compared to the former (appendix 2,1). This could indicate that carbonate rock is being weathered in the talus, releasing more dissolved calcium and bicarbonate to the water. TDS concentrations are strongly concentrated along the central eastern valley side, an observation previously done by Campbell *et al.*, (2001). However, these authors also found that this signal disappears when normalizing towards discharge. The southern end of the catchment has the lowest TDS concentrations, likely reflecting pure meltwater entering lake Rissajaure from the mountains above.

Plotting $\delta\,^{34}S_{SO4}$ and $\delta\,^{18}O_{SO4}$ for Kärkevagge and Miellajokka (figure 15) reveals outliers in all directions. For $\delta\,^{34}S_{SO4}$, MS7 and MS14 have uncommonly high and low isotopic signatures, respectively. MS14, a spring from the western part of Miellajokka, is similar to the lithospheric end member and may represent a local sulfide exposure. Kärkevagge outliers mainly include samples from the western valley side, known for dolomitic bedrock and thus a smaller sulfidic influence.

For the entire dataset, one single sample, solid sample KR1, deviates from the mass-dependent fractionation line by more than 0,5‰, and is therefore interpreted as a true signal of MIF and an archaic sample age outside of measuring error and/or small natural fractionation variations (figure 7, Domagal-Goldman *et al.*, 2011). This find would therefore indicate the presence of a geological window in or in the vicinity of Kärkevagge, where archaic rocks crop out. The bedrock of the walls and floor of Kärkevagge only dates to the Neoproterozoic era (Thelander 2009). However, since the sample was taken from a free-lying boulder in the valley, the exact location of the window cannot be determined, and may in fact have been transported a long distance before ending up on the sampling location. A more common-spread occurrence of archaic rocks in the valley would leave a mark in the isotopic

signature of more than one sample, especially since sulfide influence appear to be central to the geochemistry of the valley.

Water isotope composition of sample MS2 deviates from all other measured samples (figure 17). This could possibly be due to the sampled seep draining a snowpatch (figure 3), as melt-water from the mid-summer snow patch already have been selectively enriched in lighter isotopes, leading to a successive enrichment in heavier isotopes of both snow and melt water over the course of the summer (Taylor *et al.*, 2001). Sample MS2 was not successfully analyzed for sulfate isotopes.

5.3 Comparison between study areas

Compared to Miellajokka, Kärkevagge shows a larger variation in pH, sulfur concentration, calcium concentration, and DIC (figure 9, 10 and 13). A possible explanation for these phenomena is that chemical processes is responsible for shifts in these parameters, an explanation backed by the apparent rise in pH and Calcium+DIC concentrations relative to sulfur when traveling downstream (figure 10, appendix 2.1). Additionally, trace element correlations are more abundant and generally stronger throughout Kärkevagge than Miellajokka (figure 12). This could indicate that trace element concentrations in Kärkevagge is dominated by a single source, whereas the mixed results for Miellajokka reflects that this catchment is affected by many competing sources. The lower trace element concentrations in Miellajokka, often on the brink of the detection limit, could however at least partially explain this difference between the catchments.

Figure 15 reveals that the homogeneity of Kärkevagge holds true also for $\delta\,^{34}S_{SO4}$ and $\delta\,^{18}O_{SO4}$. Apart from outliers mainly found along the northwestern valley side, Kärkevagge concentrates around slightly negative $\delta\,^{34}S_{SO4}$ and $\delta\,^{18}O_{SO4}$ values. Miellajokka, however, displays a large data spread in terms of $\delta\,^{18}O_{SO4}$. As seen in figure 16, $\delta\,^{18}O_{SO4}$ also varies temporally over the course of the season, most evident by the $\delta\,^{18}O_{SO4}$ shift towards positive values for sites M3 and M11. Additionally, the mean $\delta\,^{18}O_{SO4}$ value deviates more from $\delta\,^{18}O_{H2O}$ ($\Delta^{18}O_{H2O\text{-}SO4}$ (‰), table 4). This could indicate that there is a different in formation processes when considering the whole dataset. $\delta\,^{34}S_{SO4}$ also displays some temporal shift in Miellajokka headwaters, whereas Kärkevagge remains much more stable over the course of the season both in terms of $\delta\,^{34}S_{SO4}$ and $\delta\,^{18}O_{SO4}$. This indicates that while SO_4^{2-} in Kärkevagge is dominated by a single source and process of formation, Miellajokka experience changes in sulfate

formation processes on temporal and spatial scales, possibly also together with a source shift over the course of the summer season.

The similarity between $\delta^{34}S_{SO4}$ of the Kärkevagge water samples and the $\delta^{34}S$ of rock samples KR1 and KR2 indicates that lithospheric sulfide is the dominating source of stream water sulfate. Soil samples resemble mixtures between rock samples and rain water samples of different proportions. The isotopic evidence indicates that the large importance of gypsum in Kärkevagge signaled by the piper plot is faulty, as gypsum in known for positive $\delta^{34}S$ values often in the range of +10-30‰ (*e.g.* Thode 1991, and refernces therein, Claypool *et al.*, 1980). As sulfide weathering produces sulfuric acid, this acid would typically be neutralized by the consecutive weathering of carbonate or silicate rock. Figure 13 displays that Si concentrations in Kärkevagge is comparable to Miellajokka in terms of magnitude and variation. Therefore, weathering of carbonate rocks with sulfuric acid (equation 5) is suggested to explain many of the phenomena observed in Kärkevagge. High calcium concentrations, Large pH shifts throughout the valley and a larger relative importance of calcium and DIC below the thalus, the overall higher pH in Kärkevagge compared to Miellajokka, and the good correlation between sulfur and magnesium (figure 12) are all congruent with this explanation. The occurrence of marble bedrock also validates this hypothesis, as does the occurrence of efflorescent white coatings on the valley walls, which have been shown to contain gypsum, an expected secondary mineral in gypsum-undersaturated waters containing products of equation 5 (Malmsten & Bodström (2002), Darmody *et al.*, 2001, 2002, Dixon *et al.*, 2002). This explanation is in line with the numerous previous geochemical studies undertaken in Kärkevagge (*e.g.* Malmsten & Bodström, 2002, Darmody *et al.*, 2002, Thorn *et al.*, 2001, Allen *et al.*, 2001), who also have underlined the importance of glaciation for the exposure of the sulfide-bearing black shales for the large-scale sulfide weathering occurring in the valley (*e.g.* Thorn, 2001). As hematite (Fe_2O_3) is formed as a secondary mineral during pyrite weathering (equation 4), it may appear puzzling that iron concentrations are lower in Kärkevagge than throughout Miellajokka. This could possibly be explained by the immobilization of iron in soils and sediments, as well as on weathering rinds and coatings observed in the valley (Dixon *et al.*, 1995, 2002). Additionally, hematite is oversaturated throughout the valley as would be expected when produced as a large-scale byproduct. Manganese, an element bearing similarities with and often found together with iron, are found in higher quantities in Kärkevagge when compared to Miellajokka (figure 13). High chemical weathering rates have been calculated for Kärkevagge at several occasions

(Rapp, 1960, Darmody *et al.*, 2000b, Campbell *et al.*, 2002). Despite this well studied phenomenon, several mineral phases remain undersaturated in Kärkevagge (table 3).

In contrast to Kärkevagge, Miellajokka appears not to be dominated by a single weathering pathway. The piper plot (figure 14) indicates that Miellajokka could represent a mixture between carbonate weathering by H_2CO_3, carbonate weathering by H_2SO_4, granite weathering by H_2CO_3, granite weathering by H_2SO_4 and gypsum weathering. With relatively low $\delta^{34}S_{SO4}$ signatures, gypsum appears unlikely also in Miellajokka (figure 15). The four remaining mixing members are likely taking place in Miellajokka to various extent. The contribution of different sources to the Miellajokka water chemistry could likely explain the lower number of good correlations between trace elements for this catchment.

5.3 Sulfide weathering in the Torneträsk region

5.3.1 Relative importance of carbonate and silicate rock weathering

Gaillardet *et al* (1999) compiled Ca/Na and HCO_3/Na ratios for rivers draining single lithologies of carbonate and silicates, and identified a plausible range for the chemical end member of evaporites based on 60 major rivers partly draining evaporite formations. The carbonate end member was defined by Ca/Na ratios of 50 and HCO_3/Na ratios of 12, whereas the silicate end member were approximated to Ca/Na ratios of 0,35± 0,15, and HCO_3/Na ratios of 2±1. The evaporite end member, while more uncertain, were pinned down to a range of HCO/Na ratios between approximately 0,15-0,35, and Ca/Na ratios between 0,13-0,29. The main indication of evaporites present in the basin would however be a deviation from the silicate-carbonate mixing line towards lower HCO_3 concentrations. The end members as defined by Gaillardet *et al* (1999) are marked out in figure 1, together with the data from this study. HCO_3^- data were lacking for rain water samples, but Ca/Na ratios of rain water generally plotted well below 0 (table 2). With all stream water samples Ca/Na ratios >1, it appears that deposition have little control over general stream water chemistry. As discussed in the previous section, sulfur isotope data are not consistent with a strong gypsum influence. Instead, the lower HCO/Na ratios for all sites in general, but Kärkevagge sites in particular, could be

explained by the larger proportion of sulfuric acid-based weathering, lowering the expected production of bicarbonate during weathering (compare equations 4 & 6). The majority of the samples in figure 19 which has the lowest HCO_3/Na and highest Ca/Na ratios are derived from around lake Rissajaure in the southern end of Kärkevagge. A good explanation is lacking for what makes these samples deviate so strongly in this direction. Early summer main headwater sites K1 and K2, also from the lake Rissajaure area in southern Kärkevagge, experienced much lower HCO_3/Na and Ca/Na ratios when compared to later in the season, possibly due to higher

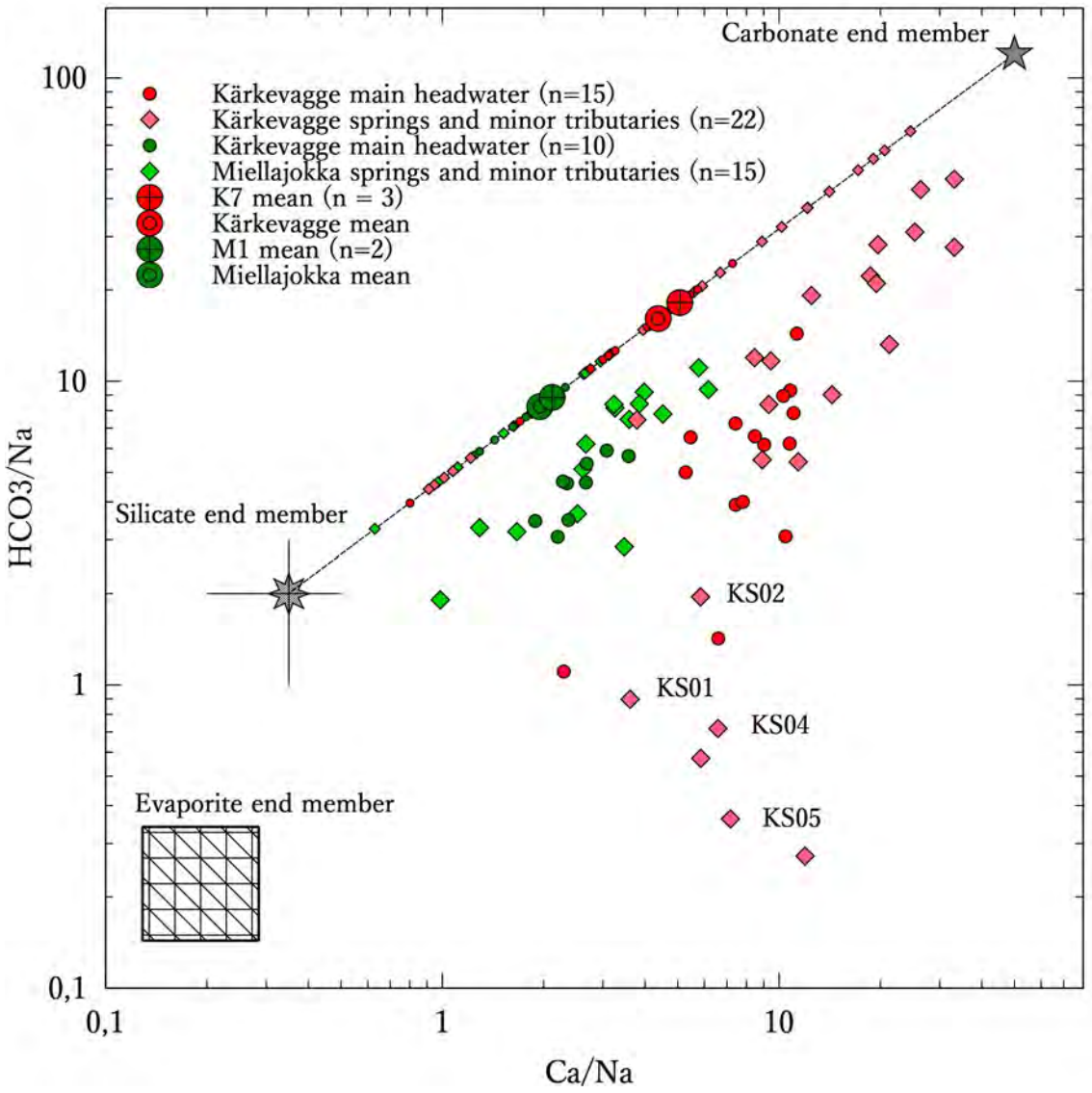

Figure 19. Log-log relationship between Ca/Na and HCO3/Na for all sample groups, together with rock type end members as defined by Gaillardet et al., 1999. Samples (large symbols) were projected onto the theoretical mixing line (small symbols) according to the method in appendix 3.

carbonate weathering rates changing water chemistry over the course of the summer, or a change in groundwater level during the same period causing a drastic change in water chemistry.

With the assumption that the evaporite end member is insignificant and that the deviation from the carbonate/silicate end member mixing line is explained by other factors, the mixing between carbonate and silicate weathering differs between Kärkevagge and Miellajokka. All samples were projected on to the linear mixing line assuming a perpendicular angle between the mixing line and the actual point location, calculated using linear algebra. The method is summarized in appendix 4).

Assuming the two-component mixing between silicate and carbonate weathering and using mean for the outflow sites as representable bulk values for the whole catchments, silicate weathering in Miellajokka is responsible for about 63,7% of rock weathering products, compared to 46,1% in Kärkevagge. Carbonate weathering is responsible for 53,9% and 36,3% of weathering products in Kärkevagge and Miellajokka, respectively. This mixing is in line with the general trends of the piper diagram in figure 12, although the silicate weathering fraction is more pronounced in the mixing line of figure 19.

5.3.2 δ34S end members

Sulfate in natural environments is potentially a mix of many sources and sinks. Before constructing mixing models, these must first be evaluated. As discussed above, consistently low $\delta\,^{34}S_{SO4}$ signatures effectively rule out gypsum as an important end member for the whole study area. Bacterially mediated anaerobic sulfate reduction could potentially take place in this catchment, and thereby cause strong fractionation on the remaining dissolved sulfate. This process is however unlikely on catchment scales since intense anaerobic bacterial activity is unreasonable in water with higher discharge. Additionally, immobilization of light sulfur by this process would lead to lower sulfide concentrations of higher values, and is unlikely to have a large-scale importance due to the generally low sulfide values in the catchments. Despite this, local occurrences of SR cannot be excluded.

Figure 19 displays $\delta^{34}S_{SO4}$ as a function of Cl/SO_4 ratios. Chloride is a conservative ion and it is likely that the SO_4/Cl ratio is representative to the relative contribution of precipitation to the sample (*e.g.* Spence & Telmer, 2005). Unfortunately, Cl were never measured in the rain water samples. Rain water Cl/SO_4 ratios were therefore estimated after data from the central Atlantic (Echo ocean station, Cl/SO4 = 4,17 (Kroopnick, 1977) and a long-term average of four measurement stations in Sweden (Aneboda, Gårdssjön, Kindla & Gammtratten, SITES) with combined mean value of Cl/SO_4 for the period 1999-2015 of about 1,03. The true value for Miellajokka precipitation can be assumed to lie in between these values, with a small proximity to the ocean and a likely small anthropogenic influence due to the northern latitude. In figure 19, Miellajokka sample MS7 stands out as a potential

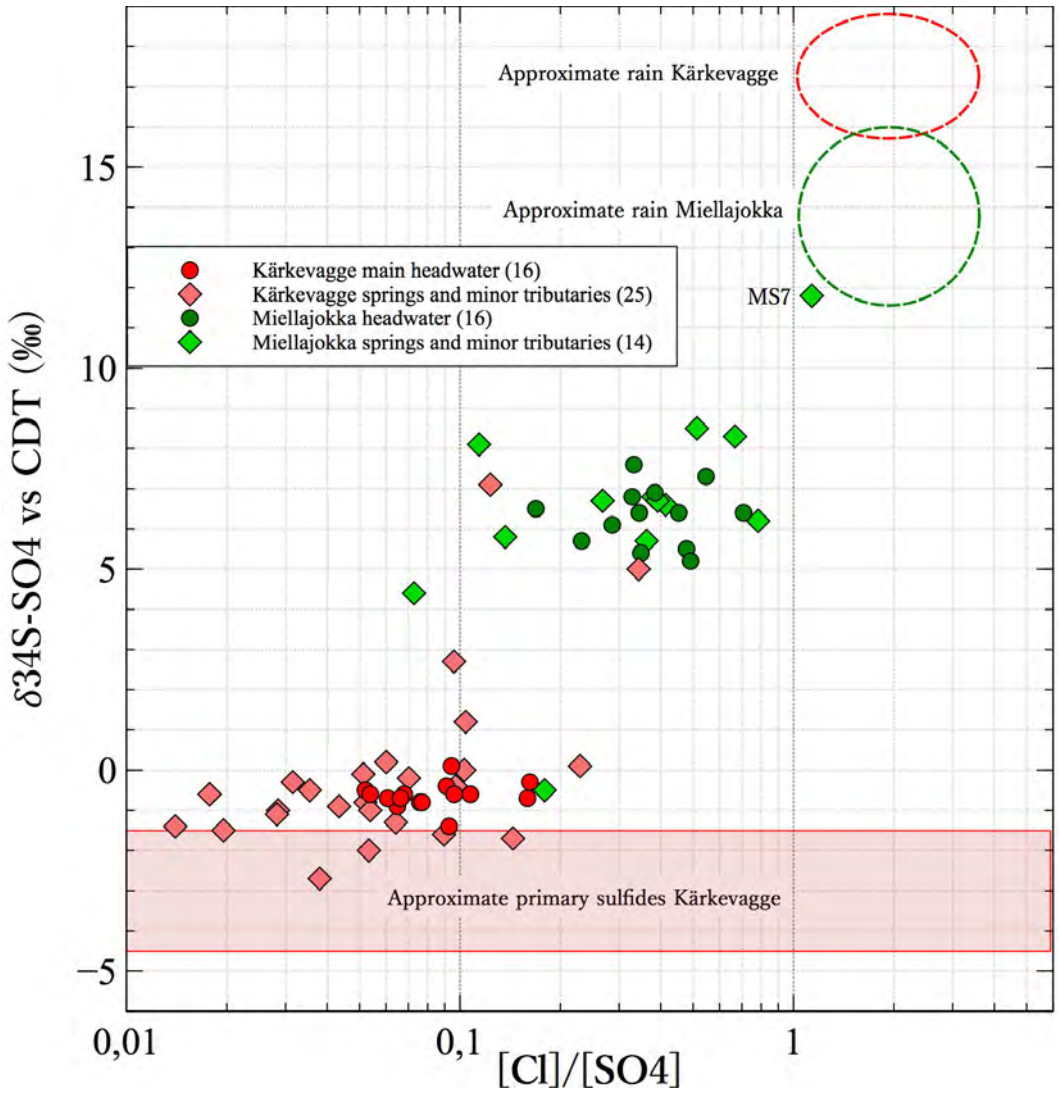

Figure 20. $\delta^{34}S_{SO4}$ plotted against SO_4/Cl ratios. Rain end members are marked out based on the approximate SO_4/Cl ratios of rain based on data from Swedish measurement data (SITES) and Kroopnick (1977)

site where intense SR takes place. This signal is identical with large deposition fraction, but SR is a likely contender since the sampled spring originates in a wetland. Even so, the low discharge of MS7 and lack of evidence of influence of SR for the remaining samples, the potential influence of SR to the general sample pool is thought to be negligible.

The Keeling and Miller Tans mixing models for two end members were utilized to determine a theoretical end member for both watersheds. In a Keeling plot, δ values are plotted against $SO4^{-1}$, and the intercept determines an end member as concentration approximates infinity. In a Miller Tans plot, the product of δ and concentration are plotted as a function of concentration, and the slope determines one of the background end members. Simple linear regression yielded similar end members for both watersheds, but the R^2 value for the Miellajokka Keeling plot was very low. Also, linear regression is known to produce systematic errors because it does not account for errors in x. Instead, the orthogonal method reduced major axis was utilized, as this method considers the relative variation of changes in both x and y (Miller & Tans (2003), Pataki *et al.*, (2003) and references therein). Variations of the keeling plots were tested, in which $\delta^{34}S_{SO4}$ is plotted against Cl/SO_4 and DOC/SO_4 ratios in search of the best factor for normalization. Cl/SO_4 resulted in the best reduced major axis fit with correlations of 0,55 for Miellajokka and 0,54 for Kärkevagge, indicating that normalization of rain water influence better explains the variation in $\delta^{34}S_{SO4.}$ All Keeling plots gives an end member for Kärkevagge between -2-2.5‰ and Miellajokka at around +2,5‰. Keeling plots are available in appendix 4.

The Miller-Tans model for Kärkevagge yielded the best correlation of 0,85 (figure 20). Here, the background end member for Kärkevagge is $\delta^{34}S$ -2,09‰ and the end member for Miellajokka is +11,02‰. Lower and upper confidence levels for the background isotope composition at α=0.05 in Kärkevagge is -2,63 and -1,73, respectively. For Miellajokka, these levels are 6,97 and 26,40, respectively. The background end-member as defined by the Miller Tans mixing model is unlikely to represent only one source, but more likely a mixture of sources (Miller and Tans, 2003). The value achieved for Miellajokka closest resembles deposition, but is on the lighter end of the spectrum when compared to meteoric $\delta^{34}S$ values from this study (11,7-18,7‰). On the other hand, the end member for Kärkevagge can be interpreted as a true sulfide $\delta^{34}S$ end member. Not only does it fall in between the $\delta^{34}S_{Sulfides}$ values of the two solid samples from the valley, but several samples also fall within this field (figure ##). This would indicate that solid sample KR2 is slightly heavier than the theoretical end member for the bulk

of Kärkevagge. The deviating $\delta^{34}S$ value of sample KR1 also undermines the likelihood of this sample representing an important sulfide source in the valley (figure 7), and could very well have a slightly lighter isotopic composition than most sulfides in the valley, as indicated by the mixing models. Kärkevagge samples are strongly concentrated around a similarly low $\delta^{34}S$ value, with relatively small variation (figure 15). Sample KS12 is isotopically lighter than the suggested sulfide end member suggested, but this could be explained by a local excursion in the sulfide $\delta^{34}S$ value. The good correlation between keeling plots and the Miller-Tans mixing model, as well as the narrow confidence interval for the Kärkevagge Miller-tans model, strengthens the validity of the sulfidic end member in Kärkevagge.

In conclusion, it is assumed that $\delta^{34}S_{Sulfide}$ = -2,1‰. The variation in $\delta^{34}S_{SO4}$ signature between the four measured rain water samples leads to some uncertainty associated with assigning a value for the deposition end member. It will therefore be assumed in the following mass balance calculations that this end member is equal to the mean of the four meteoric water samples, corresponding to $\delta^{34}S_{meteoric}$ = +15,6‰, with a standard deviation of 1,44‰.

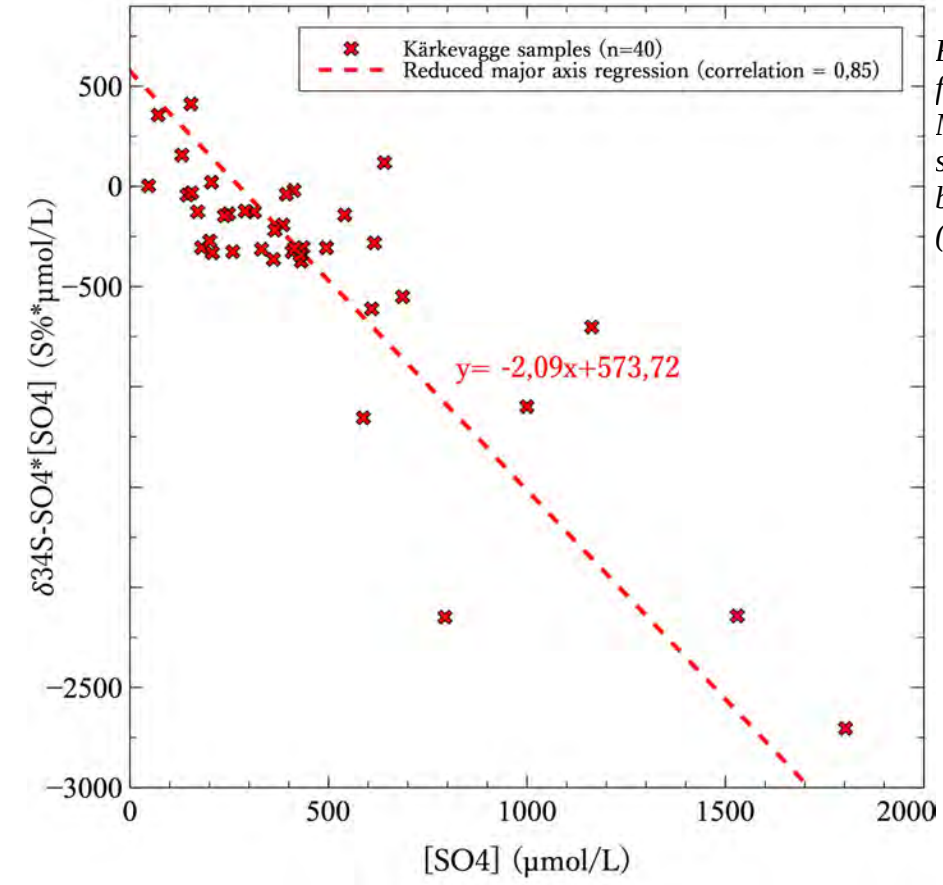

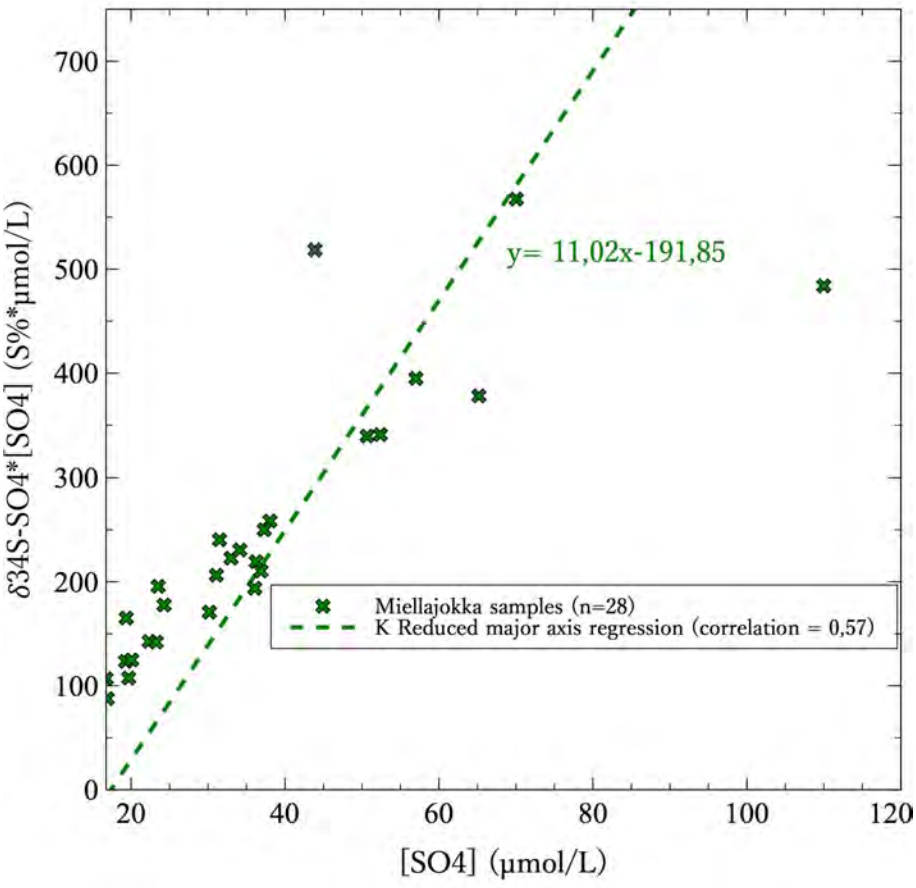

Figure 21. Miller Tans plots for Kärkevagge (top) and Miellajokka (bottom). The slope determines the background isotope value (Miller & Tans, 2002).

5.3.3 Mass balances

A generic mass balance model for the observed isotopic composition of a water (δ_{Rw}) can be constructed according to the following formula (equation 13):

$$\delta_{Rw} = f_A * \delta_A + f_B * \delta_B + \cdots f_i * \delta_i \qquad (13)$$

Where A, B$\cdots$ i are the various contributing components of unique proportions and delta values, so that:

$$f_A + f_B + \cdots f_i = 1 \qquad (14)$$

Based on the discussion in the previous section, it will now be assumed that the observed $\delta^{34}S$ values in Kärkevagge and Miellajokka represents a two-component mixing between the meteoric and sulfide source.

For the two-component mixing model, equation 13 can be simplified as equation 15:

$$\delta_{Rw} = f_{sulfide} * \delta^{34}S_{sulfide} + (1 - f_{sulfide}) * \delta^{34}S_{deposition} \qquad (15)$$

Solving the equation with the end members determined in section 5.2.1 for Kärkevagge and Miellajokka sites yields theoretical proportions of the two end members summarized in table 5.

The mean and standard deviation in Kärkevagge is affected by the outliers on the northwestern valley side draining the dolomitic bedrock. Similarly, a lower standard deviation is achieved by removing the outliers MS7 and MS14 from the Miellajokka dataset. K7 and M1 correspond well to the average contributions of lithospheric and deposition sulfates for the whole catchments, and are regarded as good representative sites as these sites represents the outflow of both headwaters. The higher standard deviation observed for Miellajokka could be the effect of changes in the relative contribution of sulfur throughout the catchment. It could possibly also reflect on fluctuations in $\delta^{34}S_{deposition}$, as similar fluctuations will not have the same effect in Kärkevagge where the sulfidic end members are strongly dominant. In Miellajokka, where half of the stream sulfate is derived from deposition, fluctuations in $\delta^{34}S_{deposition}$ on the scale already observed for the rain water samples collected in this study has the potential to shift the $\delta^{34}S_{SO4}$ signatures a few permil in either direction.

Group (N)	Mean $f_{(sulfide)}$	Mean $f_{(deposition)}$	s
Kärkevagge (41)	0,90	0,10	0,10
Kärkevagge w/o outliers (38)	0,92	0,08	0,04
K7 (4)	0,92	0,08	0,01
Miellajokka (31)	0,52	0,48	0,11
Miellajokka w/o outliers (29)	0,52	0,48	0,05
M1 (4)	0,50	0,50	0,02
Torneträsk general region (10)	0,60	0,40	0,16
G3 (1)	0,59	0,40	

Table 5. Mass balance results for groups of samples, with M1 and K7 interpreted as the bulk of the whole catchment.

The estimated sulfide fraction of stream water SO_4 is 92% and 50% for Kärkevagge and Miellajokka, respectively. If the end members hold through on a larger scale, the sulfide fraction for the general Torneträsk area is 60% The validity of this estimation is strengthened by a similar fraction calculated for site G3, collected from Laxforsen at the outflow of Torneträsk (figure 1). When plotting $\delta^{34}S_{SO4}$ vs $\delta^{18}O_{SO4,}$ (figure 15), sample G3 plots approximately in the middle of the complete data set. Samples G4 and G5, which have lower $\delta^{34}S_{SO4}$ signatures, are collected from streams geographically close to Kärkevagge, and could likely reflect an influence of the same black sulfide-bearing schist which crop out in Kärkevagge. As higher sulfur concentrations also likely equal a larger lithospheric component, it is not impossible that most catchments around Torneträsk resemble Miellajokka in terms of $\delta^{34}S_{SO4}$ and sulfate end member mixing proportions, whereas relatively small geographic areas with significant sulfide sources have a large influence over headwater $\delta^{34}S_{SO4}$ signatures.

It is worth pointing out, that if the assessment that SR and primary gypsum are negligible in the studied catchments is faulty, this would drive $\delta^{34}S_{SO4}$ towards higher values, thereby underestimating the sulfide contribution and not the opposite way.

5.3.4 Flux estimations

With the relative contributions of sulfide weathering to sulfate in solution known, a straight-forward method for quantifying the importance of this process within a catchment is to multiply the contribution factor with the sulfate concentration and discharge data. For this study, no discharge measures were made, and a scarcity of temporal measurements for the catchment outlets complicates the calculations further. A rough estimation was performed through an alternative method.

Giesler *et al.,* (2014) performed daily stream flows for Miellajokka for the months May-September of 2008, and assumed small variation and a low stream flow in the discharge for the winter months. This distribution is typical for streams in the region (SMHI, Campbell *et al.*, 2002). For these months, SMHI discharge data from the nearby Abiskojokken stream was used and scaled after the Miellajokka watershed size. Precipitation in Abisko for the period 1 may 2008-30 April 2009 was measured by SMHI to 266 mm. Total runoff for Miellajokka for the corresponding period was calculated to 394 mm (Giesler *et al.*, 2014), giving a precipitation/total runoff ratio of approximately 0,67. Assuming that this ratio stays constant, total runoff was calculated for the year 2016 for both Kärkevagge and Miellajokka, based on the 743,5 mm and 363,4 mm total rain collected at measuring stations Katterjokk representative of Kärkevagge and Abisko representative of Miellajokka, respectively (SMHI, 2017). Estimations of total runoff for the year 2016 thus equals $29{,}2*10^6$ m^3 for Kärkevagge and $27{,}9*10^6$ m^3 for Miellajokka. These estimations are relatively similar of previous values $23{,}8*10^6$ m^3 calculated for Kärkevagge by Campbell *et al.*, (2002) for an 82-day period for the summer of 2001, and $20{,}3*10^6$ m^3 calculated for Miellajokka for the season 2008-2009 by Giesler *et al* (2014). Comparison of precipitation data shows that precipitation was higher in the present study than during the previously mentioned seasons (SMHI, 2017).

Continuous measurements for a whole year October 2015-september 2016 at site M1 reveal that sulfate concentrations is at the highest point in April before the spring flood, during which concentrations is about four times the minimum value acquired in June. During the summer months, late june-early august, sulfate concentrations varies less, about ±20% total variation from the mean 21/6-15/8 (Reiner Giesler, pers. Comm.). Since the summer discharge dominates the total annual runoff, it will be assumed that the early July SO_4^{2-} concentrations for M1 and K7 are representative for the whole year in both Kärkevagge and Miellajokka. ICP data is available for both these occasions and it can be assumed that all S

exists as SO_4^{2-} in these waters. With a concentration of 0,272 and 0,039 mmol/L S at Kärkevagge and Miellajokka respectively, and the relative sulfide contribution for sites M1 and K7 given of $7{,}3*10^6$ and $3{,}9*10^5$ is derived from annual sulfide weathering from Miellajokka and Kärkevagge, respectively.

The prior estimations are based on several assumptions. To account for the assumptions, estimations were also made using a second method. Sulfur concentration in the rain water samples all fall within the range of ~21-24 μmol/L. Based on the total annual precipitation collected at measuring stations at Katterjokk and Abisko, and the relative contributions of SO_4^{2-} from precipitation and weathering in the catchments (table 5), this equals 4,8-5,4*10^6 and 3,9-4,5*10^5 mol/yr for Kärkevagge and Miellajokka respectively. This estimation is however also based on a number of assumptions: 1) The measured $\delta^{34}S_{SO4}$ value represents a two-way mixing model between the lithospheric sulfide component and meteoric water 2) The span of $\delta^{34}S_{SO4}$ and S concentrations for the four meteoric water samples are representative for whole-year deposition in the region 3) the measured amounts of precipitation at Katterjokk and Abisko measuring stations are representative for the Miellajokka and Kärkevagge watersheds 4) there exists no selectivity or bias on which SO_4 of which origin escapes the watersheds, so that homogenous mixing between sources occur throughout the watershed 5) as for the estimation produced above, the measuring sites K7 and M1 are assumed to be representative for the catchment as a whole. Assumption 1) is justified through the previous section, and assumptions 4) and 5) are strengthened by the similarity between the catchments and the catchment outlets (table 5). Finally, the relatively similar results achieved by two different methods is a good indication that the assumptions behind the estimations are roughly correct.

Earlier model estimates of sulfide weathering rates by François & Walker (1992) and Berner & Berner (1996) have estimated global sulfide weathering to produce 0,48-0,65*10^{12} mol/yr. The sulfide weathering estimates by Calmels *et al.*, (2007) for the Mackenzie River resulted in rates of 20-27% of these older global model estimates. With a drainage area of 1,8*10^6 km^2, this equals 12-16 times these global average rates. Das *et al.*, (2012) calculated rates about 400 times the old global averages for the wet and warm region of Taiwan, in which strong mechanical erosion were thought to be a supporting cause for the continuous exposure and weathering of sulfide minerals. With catchment areas of 26,3 km^2 for Kärkevagge and 51,5 km^2 for Miellajokka (SMHI 2017, Giesler *et al.*, 2013) sulfide weathering rates are estimated to

be 30,4-62,9 times higher in Kärkevagge and 1,3-2,4 times higher in Miellajokka when compared to the global average estimated by François & Walker (1992) and Berner & Berner (1996). According to these calculations, the working hypothesis therefore stands, even though sulfide weathering rates in Miellajokka are close to the old global estimates. However, due to the low annual temperatures and deposition rates in Miellajokka, weathering rates can be expected to be relatively low in this catchment, whereas also relatively low sulfide weathering rates can become significant. While Miellajokka is judged to be more representative of the Scandinavian mountain chain in terms of lithology and, presumably, sulfide weathering, this does not necessarily mean that Kärkevagge is unique in the broader region. Not only is the sulfide component strong in neighboring streams analyzed in this study, but the occurrence of other significant sulfide sources within the Caledonian nappes mean that geochemical regimes alike Kärkevagge may exist in more places throughout the mountain chain (Thelander 2009, Bergman *et al.*, 2012).

5.3.5 Relative importance of sulfuric acid weathering

In accordance with conceptual equations 5 and 6 in the introduction, every mole of sulfate derived from sulfide weathering is accompanied by two moles of $CaCO_3$ or one mole of $CaSiO_4$. The fractions of weathering mediated by sulfuric acid contra carbonic acid has not been determined, since the relative contribution of these pathways to carbonate and silicate weathering remains unknown. For a simple calculation example, Ca concentrations was assumed to be fully derived from rock weathering. This is deemed likely, since Ca/Na of stream water at all instances were much larger than the Ca/Na ratios of deposition (neglecting the outlier MM2, table 2). Using the fraction of sulfide weathering-derived sulfate at the outflow of Kärkevagge and Miellajokka calculated in section 5.3.3, concentrations of sulfide-derived sulfate ($SO_{4sulfide}$) were calculated for both sites. The mean concentration of $SO_{4sulfide}$ for three samples taken at site K7 from early summer to late autumn derived equaled 335 μmol/L. The corresponding value, calculated for the mean of the early summer and late autumn site at site M1 in Miellajokka, equal 20 μmol/L. The mean calcium concentrations for the same samples taken at sites K7 and M1 were 332 and 118 μmol/L, respectively (appendix 2.1). Thus, the ratio $SO_{4sulfide}$/Ca thus equals 1,01 in Kärkevagge, and 0,16 in Miellajokka.

In practice, the proportion of weathering reactions are not known, and Ca is not the only important cation in calcium nor carbonate rocks. The above calculation therefore only serves

to illustrate that weathering by sulfuric acid is a strong, possibly even dominant, pathway in Kärkevagge. This pathway also appears to be significant in Miellajokka, although to a smaller extent. Plotting $\delta^{13}C_{DIC}$ vs lnpCO_2 concentration (figure 18) provides some extra information about sulfuric acid weathering, which is discussed below.

The possible contributors to DIC in natural waters have different but distinct end members. The carbonate end member of the area has earlier been estimated to a value of +2‰, whereas soil CO_2, derived from respiration of soil organic material, has been assigned a value of -28‰ (Giesler *et al.*, 2013). Isotopic signatures are thereafter affected by fractionation factors of the carbonate system (Zhang *et al.*, 1994). Stream water DIC values and pCO_2 concentrations are also overprinted by degassing of CO_2, photosynthesis and respiration (Waldron *et al.*, 2007, and references therein). Nevertheless, carbonate weathering by sulfuric acid can be expected to maintain a heavy δ^{13}C-DIC signature, since carbonate in this process is fully derived from the carbonate rock end member (equation 5 in introduction). In Kärkevagge, $\delta^{13}C_{DIC}$ signatures are relatively high. Additionally, no convincing correlation exists between ln$pCO2$ and δ^{13}C-DIC. This could be explained by a strong influence of carbonate weathering by sulfuric acid in Kärkevagge, sustaining heavy isotopic compositions for DIC throughout the valley. This trend is not observed for the Miellajokka sites, for which an increase in lnpCO_2 correlates with lighter $\delta^{13}C_{DIC}$, a trend most apparent for springs and minor tributaries within the Miellajokka catchment. In Miellajokka, there is a stronger relationship between lnpCO_2 concentrations and a lighter isotopic composition. This relationship is especially defined for low-discharge sites, and could be due to a larger fraction of DIC derived from respiration of light organic matter in these sites, which generally are characterized by high DOC concentrations (figure 9 lower).

The high $SO_{4sulfide}$/Ca ratio, poor lnpCO_2/$\delta^{13}C_{DIC}$ correlation and heavy $\delta^{13}C_{DIC}$ signatures all point towards a strong contribution of carbon derived from sulfuric acid weathering in Kärkevagge, possibly even indicating that chemical weathering in Kärkevagge cannot be considered a sink for CO_2. This study is unable to calculate accurate CO_2 consumption or evasion rates, but significant sulfide weathering rates in Miellajokka also indicate that CO_2 consumption in the catchment may be an ineffective process. These results could potentially contain the key to a problem presented by Giesler *et al.*, (2013). As shown by these authors, streams in the Torneträsk region experienced higher δ^{13}C-DIC values than expected when compared to a mixing model. The large portion of sulfide-derived sulfates in both catchments in the present study point towards sulfuric acid-mediated weathering playing

an important part in both catchments. The larger proportion of DIC derived from the heavier carbonate end member does therefore provide a potential explanation for the heavy δ^{13}C-DIC values observed by Giesler *et al.*, (2013).

6. Conclusions

This multi-parameter study of Kärkevagge and Miellajokka establishes an improved image of the weathering mechanisms in the two catchments, and enables for the extrapolation over a larger geographic area. The spatial and temporal trends observed in Kärkevagge is coherent with prior studies in the valley, identifying sulfide weathering and carbonate weathering by sulfuric acid as dominant geochemical processes with a concentration along the eastern valley side but with a lesser importance in the southern and western valley ends, partially associated with bedrock differences. Indications of a geological window to older, also strongly sulfidic, bedrock near Kärkevagge is also found. Miellajokka is less dominated by sulfide weathering, but this process is still significant, as indicated by the chemical composition of the stream water and sulfate isotope composition. The catchment also contains small local sulfide sources. $\delta\,^{18}O_{SO4}$ signatures indicate that sulfide formation processes may vary spatially and temporally in Miellajokka, possibly also indicating shifts sources of sulfate. Silicate weathering contra carbonate weathering are calculated to be of about the same importance in Miellajokka, while carbonate weathering rates are approximately double that of silicate weathering in Kärkevagge. The weathering of primary gypsum deposits within both catchments are deemed unlikely, and bacterial sulfate reduction probably only occur at minor rates with little implication on $\delta\,^{34}S_{SO4}$ signatures for bulk catchments.

Mass balance calculations and primitive flux estimations reveal that sulfide weathering rates in Kärkevagge are 30-60 times higher than global averages calculated by François & Walker (1992) and Berner & Berner (1996). Sulfide weathering in Miellajokka is slightly elevated in comparison to these estimations. While the relative contribution of sulfuric acid to weathering is hard to quantify, $\delta\,^{13}C_{DIC}$ and pCO_2 data indicate that weathering mediated by sulfuric acid could have a large relative importance in Kärkevagge. This has implications for the assumed control on weathering over atmospheric carbon content, since this weathering pathway leads to carbon flows through dissolution of carbonate rocks not associated with a drawdown of atmospheric CO_2. While Kärkevagge probably is unrepresentative in a regional and global context due to the large and glacially exposed sulfide mineralization in the valley walls, auxiliary sulfur isotope data from the larger Torneträsk region matches a mixture between the Kärkevagge and Miellajokka watersheds. Significant sulfide outcrops may also exist elsewhere in the Caledonian nappes. It can thereby

be implied that sulfide weathering and associated weathering with sulfuric acid remain significant processes throughout the larger geographical region. It cannot be excluded that this conclusion extends across the larger Caledonides bedrock units of the Scandinavian mountain chain, although more data is necessary to test this hypothesis.

This study coherent to a series of modern studies utilizing stable isotope geochemistry to reevaluate the importance of sulfide weathering worldwide (*e.g.* Calmels *et al.,* 2007, Li et al., 2008, Das et al., 2012). The current study corroborates the conclusion from prior studies of an underestimation of total global sulfide weathering rates. In a context of low temperature and deposition rates, even the sulfide weathering rates for Miellajokka could be of large relative importance, as saturation indices point towards generally low weathering rates. This further accentuates the need for more data to construct a new global estimation for sulfide weathering rates. A reevaluation of the importance of sulfide weathering can potentially have important consequences for the established view of the coupling between weathering rates and consumption of atmospheric CO_2, and may thereby lead to a reassessment of what we know about climate controls over geologic time scales.

Acknowledgements

This study has been made possible by data from the Swedish Infrastructure for Ecosystem Science (SITES), in this case at Aneboda, Gårdssjön, Kindla & Gammtratten.

The help from supervisor Carl-Magnus Mörth and co-supervisor Reiner Giesler have been crucial for this work, by helping to answer questions and through guidance along the way. Reiner helped with DOC analysis and Magnus also contributed vastly with knowledge and help for the programming language R and by helping with the ICP analysis, data treatment, and geochemical modeling. Heike Siegmund deserves a big mention due to her endurance with isotope analysis despite troubles with the instruments, and for the good company she provided in the labs. In the field and in the lab, Gerard Rocher and Albin Bjärhall were both good company and helping hands. Gerard also helped answering questions and by providing information whenever needed. Erik Smedberg were of good advice for finding data sources for map constructions and Gudrun Brattström helped with statistical and algebraic queries. Niels West helped with photo editing.

References

Allen, C. E. (2001). Weathering regimes and pedogenic variability on large boulders in Kärkevagge, Northern Scandinavia. *PhD Dissertation*.

Allen, C. E. (2002). The influence of schistocity on soil weathering on large boulder tops, Kärkevagge, Sweden. *Catena, 49*, pp. 157-169.

Allen, C. E., Darmody, R. G., Thorn, C. E., Dixon, J. C., & Schlyter, P. (2001). Clay mineralogy, chemical weathering and landscape evolution in Arctic-Alpine Sweden. *Geoderma, 99*, pp. 277-294.

Andersson, P., Torssander, P., & Ingri, J. (1992). Sulphur isotope ratios in sulphate and oxygen isotopes in water from a small watershed in Central Sweden. *Hydrobiologia, 235/236*, pp. 205-217.

Baublys, K., Golding, S., Young, E., & Kamber, B. (2004, 10 21). Simultaneous determination of δ33SV-CDT and δ34SV-CDT using masses 48, 49 and 50 on a continuous flow isotope ratio mass spectrometer. *Rapid Communications in Mass Spectrometry*, pp. 2765-2769.

Bergman, S., Stephens, M., Andersson, J., Kathol, B., & Bergman, T. (2012). Bedrock map of Sweden, scale 1:1 million. *K423*.

Berner, E. K., & Berner, R. A. (1987). *The Global Water Cycle: Geochemistry and Environment.* Prentice-Hall.

Berner, K. E., & Berner, R. A. (1996). *Global Environment: Water, air and geochemical cycles.* Upper Saddle River, New Jersey: Prentice Hall.

Berner, R. A., Lasaga, A. C., & Garrels, R. M. (1983). The carbonate-silicate geochemical cycle and its effect on atmospheric carbon dioxide over the past 100 million years. *American Journal of Science, 283*, pp. 641-683.

Berner, Z. A., Stüben, D., Leosson, M. A., & Klinge, H. (2002). S- and O-isotopic character of dissolved sulphate in the cover rock aquifers of a Zechstein salt dome. *Applied Geochemistry 17, 17*, pp. 1515-1528.

Beylich, A. A., Molau, U., Luthbom, K., & Gintz, D. (2005). Rates of Chemical and Mechanical Fluvial Denudation in an Arctic Oceanic Periglacial Environment, Latnjavagge Drainage Basin, Northernmost Swedish Lapland. *Arctic, Antarctic, and Alpine Research, 37*(1), pp. 75-87.

Brüchert, V. (2004). Physiological and ecological aspects of sulfur isotope fractionation during bacterial sulfate reduction. *Geological Society of America, Special Paper 379*, pp. 1-16.

Callaghan, T. V., Bergolm, F., Christensen, T. R., Jonasson, C. K., & Johansson, M. (2010). A new climate era in the sub-Arctic: Accelerating climate changes and multiple impacts. *Geophysical Research Letters, 37*, pp. 1-6.

Callaghan, T. V., Jonasson, C., Thierfelder, T., Yang, Z., Hedenås, H., Johansson, M., . . . Sloan, V. L. (2013). Ecosystem change and stability over multiple decades in the Swedish subarctic: complex processes and multiple drivers. *Philosophical Transactions of the Royal Society of London, 368*, p. 20120488.

Campbell, S. W., Dixon, J. C., Darmody, R. G., & Thorn, C. E. (2001). Spatial variation of early season surface water chemistry in Kärkevagge, Swedish Lapland. *Geografiska Annaler, 83A*, pp. 169-178.

Campbell, S. W., Dixon, J. C., Thorn, C. E., & Darmody, R. G. (2002). Chemical denudation rates in Kärkevagge, Swedish Lapland. *Geografiska Annaler, 84A*, pp. 179-185.

Claypool, G. E., Holser, W. T., Sakai, H., & Zak, I. (1980). The age curves of sulfur and oxygen isotopes in marine sulfate and their mutual interpretation. *Chemical Geology, 28*, pp. 199-260.

Darmody, R. G., Allen, C. E., Thorn, C. E., & Dixon, J. C. (2001). The poisonous rocks of Kärkevagge. *Geomorphology, 41*, pp. 53-62.

Darmody, R. G., Allen, C. E., Thorn, C. E., & Dixon, J. C. (2001). The posionous rocks of Kärkevagge. *Geomorphology, 41*, pp. 53-62.

Darmody, R. G., Campbell, S. W., Dixon, J. .., & Thorn, C. E. (2002). Enigmatic efflorescence in Kärkevagge, Swedish Lapland: The key to chemical weathering? *Geografiska Annaler, 84A*, pp. 187-192.

Darmody, R. G., Thorn, C. E., & Allen, C. E. (2005). Chemical weathering and boulder mantles, Kärkevagge, Swedish Lapland. *Geomorphology, 67*, pp. 159-170.

Darmody, R. G., Thorn, C. E., & Allen, C. E. (2005). Chemical weathering and boulder mantles, Kärkevagge, Swedish Lapland. *Geomorphology, 67*, pp. 157-170.

Darmody, R. G., Thorn, C. E., & Dixon, J. C. (2008). Differential rock weathering in the 'Valley of the Boulders', Kärkevagge, Swedish Lapland. *Geografiska Annaler, 90 A*, pp. 201-209.

Darmody, R. G., Thorn, C. E., & Dixon, J. C. (2008). Differntial rock weathering in the 'Valley of the Boulders', Kärkevagge, Swedish Lapland. *Geografiska Annaler, 90A*, pp. 201-209.

Darmody, R. G., Thorn, C. E., Dixon, J. C., & Schlyter, P. (2000). Soils and Landscapes of Ka¨rkevagge, Swedish Lapland. *Soil Sci. Soc. Am. J., 64*, pp. 1455-1466.

Darmody, R. G., Thorn, C. E., Harder, R. L., Schlyter, J. P., & Dixon, J. C. (2000). Weathering implications of water chemistry in an arctic–alpine environment, northern Sweden. *Geomorphology, 34*, pp. 89-100.

Das, A., Chung, C.-H., & You, C.-F. (2012). Disproportionately high rates of sulfide oxidation from mountainous river basins of Taiwan orogeny: Sulfur isotope evidence. *Geophysical Research Letters, 39*, pp. 1-6.

de Laeter, J. R., Böhlke, J. K., P. De Bièvre, P., Hidaka, H., Peiser, H. S., Rosman, K. J., & Taylor, P. D. (2003). Atomic weights of the elements. Review 2000 (IUPAC Technical Report). *Pure and Applied Chemistry, 75*, pp. 683-800.

Deer, W. A., Howie, R. A., & Zussman, J. (1992). *An Introduction to the Rock-forming Minerals.* Harlow : Longman.

Dixon, J. C., Campbell, S. W., Thorn, C. E., & Darmody, R. G. (2006). Incipient weathering rind development on introduced machine-polished granite discs in an Arctic alpine environment, northern Scandinavia. *Earth surface Processes and Landforms, 31*, pp. 111-121.

Dixon, J. C., Darmody, R. G., Schlyter, P., & Thorn, C. E. (1995). Preliminary investigation of geochemical process responses to potential environmental change in Kärkevagge, Northern Scandinavia. *Geografiska Annaler, 77A*, pp. 259-267.

Dixon, J. C., Darmody, R. G., Schlyter, P., & Thorn, C. E. (n.d.). Preliminary investigation of geochemical process responses to potential environmental change in Kärkevagge, Northern Scandinavia. *Geografiska Annaler, 77A*, pp. 259-267.

Dixon, J. C., Thorn, C. E., Darmody, R. G., & Campbell, S. W. (2002). Weathering rinds and rock coatings from an Arctic alpine environment, northern Scandinavia. *Gelogical Society of America Bulletin, 114*(2), pp. 226-238.

Dixon, J. C., Thorn, C. E., Darmody, R. G., & Schlyter, P. (2001). Weathering rates of fine pebbles at the soil surface in Kärkevagge, Swedish Lapland. *Catena 45, 45*, pp. 273-286.

Dogramaci, S. S., Herczeg, A. L., Schiff, S. L., & Bone, Y. (2001). Controls on d34S and d18O of dissolved sulfate in aquifers of the Murray Basin, Australia and their use as indicators of flow processes. *Applied Geochemistry, 16*, pp. 475-488.

Dold, B., & Spangenberg, J. E. (2005). Sulfur Speciation and Stable Isotope Trends of Water-Soluble Sulfates in Mine Tailings Profiles. *Environmental Science & Technology, 39*, pp. 5650-5656.

Dold, B., Diaby, N., & Spangenberg, J. E. (2011). Remediation of a Marine Shore Tailings Deposit and the Importance of Water - Rock Interaction on Element cycling in the Coastal Aquifer. *Environmental Science & Technology, 45*, pp. 4876-4883.

Domagal-Goldman, S. D., Poirier, B., & Wing, B. (2013). *Summary report from workshop in "Mass-Independent Fractionation of Sulfur Isotopes: Carriers and Sources".*

François, L. M., & Walker, J. C. (1992). Modelling the Phanerozoic carbon cycle and climate: constraints from the 87Sr/86Sr isotopic ratio of seawater. *American Journal of Science, 292*, pp. 81-135.

Gaillardet, J., Dupré, B., Louvat, P., & Allègre, C. J. (1999). Global silicate weathering and CO consumption rates deduced 2 from the chemistry of large rivers. *Chemical Geology, 159*, pp. 3-30.

Garrels, R. M., & Mackenzie, F. T. (1971). *Evolution of Sedimentary Rocks.* New York: W. W. Norton & Company. Inc.

Garrels, R. M., Perry, E. A., & 303-336., E. A. (1974). Cycling of carbon, sulfur, and oxygen through geologic time. *The sea*, pp. 303-336.

Gibson, J. J., Edwards, T. W., & Bursey, G. G. (1993). Estimating Evaporation Using Stable Isotopes: Quantitative Results and Sensitivity Analysis for Two Catchments in Northern Canada. *Nordic Hydrology, 24*, pp. 79-94.

Giesler, R., Lyon, S. W., Mörth, C.-M., Karlsson, J., Karlsson, E. M., Jantze, E. J., . . . Humborg, C. (2014). Catchment-scale dissolved carbon concentrations and export estimates across six subarctic streams in northern Sweden. *Biogeosciences, 11*, pp. 1-13.

Giesler, R., Mörth, C.-M., Karlsson, J., Lundin, E. J., Lyon, S. W., & Humborg, C. (2013). Spatiotemporal variations of pCO2 and d13C-DIC in subarctic streams in northern Sweden. *Global Biogeochemical Cycles, 27*, pp. 1-11.

Hoering, Thomas C., & Kennedy, Joseph W. (1956). The Exchange of Oxygen between Sulfuric Acid and Water. *Journal of the American Chemical Society, 79*, pp. 56-60.

Holland, H. D. (1978). *The chemistry of the atmosphere and oceans.* New York: Wiley.

Holt, B. D., & Kumar, R. (1991). Oxygen Isotope Fractionation for Understanding the Sulphur Cycle. In H. R. Krouse, & V. A. Grinenko, *Stable Isotopes in the Assessment of Natural and Anthropogenic Sulfur in the Environment* (pp. 27-41). John Wiley & Sons Ltd.

Holt, B. D., Kumar, R., & T, C. P. (1982). *Primary Sulfates in Atmospheric Sulfates: Estimation by Oxygen Isotope Ratio Measures* (Vol. 217). Science.

Ingri, J., Torssander, P., Andersson, P. S., Mörth, C.-M., & Kusakabe, M. (1997). Hydrogeochemistry of sulfur isotopes in the Kalix River catchment, northern Sweden. *Applied Geochemistry, 12*, pp. 483-496.

Jamieson, R. e., & Wadleigh, M. A. (1999). A Study of the Oxygen Isotopic Composition of Precipitation Sulphate in Eastern Newfoundland. *Water, Air and Soil Pollution, 110*, pp. 405-420.

Johnson, M. S., Billett, M. F., Dinsmore, K. J., Wallin, M., Dyson, K. E., & Jassal, R. S. (2009). Direct and continuous measurement of dissolved carbon dioxide in freshwater aquatic systems - method and applications. *Ecohydrology*.

Jonsson, C. E., Leng, M. J., Rosqvist, G., Seibert, J., & Arrowsmith, C. (2009). Stable oxygen and hydrogen in sub-Arctic lake waters from northern Sweden. *Journal of Hydrology, 376*, pp. 143-151.

Kaplan, I. R., & Rittenberg, S. C. (1964). Microbiological Fractionation of Sulfur Isotopes. *J. Gen. Microbiol., 34*, pp. 195-212.

Kroopnick, P. (1977). The SO4 : Cl Ratio in Oceanic Rainwater. *Pacific Science, 31*, pp. 91-106.

Kroopnick, P., & Craig, H. (1972). Atmospheric Oxygen: Isotopic Composition and Solubility Fractionation. *Science, 175*, pp. 54-55.

Kulling, O. (1964). *Översikt över norra Norrbottensfjällens kaledonidberggrund.* Stockholm: Sveriges Geologiska Undersökning, SGU.

Kusakabe, M., & Robinson, B. W. (1977). Oxygen and sulfur isotope equilibria in the BaSO,--HSOh-I&O system from 110 to 350°C and applications. *Geochimica et Cosmoehimica Acta, 41*, pp. 1033-1040.

Li, S.-L., Calmels, D., Han, G., Gaillardet, J., & Liu, C.-Q. (2008). Sulfuric acid as an agent of carbonate weathering constrained by d13C-DIC: Examples from Southwest China. *Earth and Planetary Science Letters, 270*, pp. 189-199.

Lloyd, R. M. (1967). Oxygen Isotope Behaviour in the Sulfate-Water System. *Journal of Geophysical Research, 73*, pp. 6099-6110.

Longinelli, A., & Craig, H. (1967). Oxygen-18 Variations in Sulfate Ions in Sea Water and Saline Lakes. *Science, 156*, pp. 56-59.

Lyons, J. R. (2007). Mass-independent fractionation of sulfur isotopes by isotope-selective photodissociation of SO2. *Gephysical Research Letters, 34*(22), pp. 1-5.

Malmsten, I., & Boström, K. (2002). The Hydrogeochemsitry of the Kärkevagge Valley, Lapland, Sweden. *Geografiska Annaler, 84 A (3-4)*, pp. 245-259.

Miller, J. B., & Tans, P. P. (2003). Calculating isotopic fractionation from atmospheric measurements at various scales. *Tellus, 55B*, pp. 207-214.

Novák, M., Mitchell, M. J., Jačkova, I., Buzek, F., Schweigstillová, J., Erbanová, L., . . . Fottová, D. (2007). Processes Affecting Oxygen Isotope Ratios of Atmospheric and Ecosystem Sulfate in Two Contrasting Forest Catchments in Central Europe. *Environmental Science and Technology, 41*, pp. 703-709.

Owen, T., Cess, R. D., & Ramanathan, V. (1979). Enhanced C02 greenhouse to compensate for reduced solar luminosity on early Earth,. *Nature, 277*, pp. 640-641.

Pataki, D. E., Ehleringer, J. R., Flanagan, L. B., Yakir, D., Bowling, D. R., Still, C. J., . . . Berry, J. A. (2003). The application and interpretation of Keeling plots in terrestrial carbon cycle research. *Global Biogeochemical Cycles, 17*, p. 1022.

Pavlov, A. A., & Kasting, J. F. (2004). Mass-Independent Fractionation of Sulfur Isotopes in Archean Sediments: Strong Evidence for an Anoxic Archean Atmosphere. *Astrobiology, 2*(1), pp. 27-41.

Rapp, A. (1960). Recent Development of Mountain Slopes in Kärkevagge and Surroundings, Northern Scandinavia. *Geografiska Annaler, 42*, pp. 65-200.

Rees, C. E. (1991). Hydrosphere. In H. R. Krouse, & V. Grinenko, *Stable Isotopes int he Assessment of Natural and Anthropogenic Sulfur in the Environment* (pp. 177-265). John Wiley & Sons.

Rees, C. E., Jenkins, W. J., & Monster, J. (1978). The sulphur isotopic composition of ocean water sulphate. *Geochimica et Cosmochimica Acta, 42*, pp. 377-381.

Sagan, C., & Mullen, G. (1972). Earth and Mars: Evolution of Atmospheres and Surface Temperatures . *Science, 177*, pp. 52-56.

Spence, J., & Telmer, K. (2005). The role of sulfur in chemical weathering and atmospheric CO2 fluxes: Evidence from major ions, 13CDIC, and 34SSO4 in rivers of the Canadian Cordillera. *Geochimica et Cosmochimica Acta, 69*, pp. 5441-5458.

Strömqvist, L., & Rehn, J. (1981). Rainfall measurements: runoff and sediment transport in Kärkevagge, Swedish Lappland. *Japanese Geomorphological Union Transactions, 2*, pp. 211-222.

Swedish Meteorological and Hydrological Institute, SMHI. (2017, 03 15). *SMHI öppna data.* Retrieved 03 15, 2017, from smhi.se: http://opendata-download-metobs.smhi.se/explore/#

Taipale, S. J., & Sonninen, E. (2009). The influence of preservation method and time on the δ13C value of dissolved inorganic carbon in water samples. *Rapid Communications in Mass Spectrometry, 16*, pp. 2507-2510.

Taylor, S., Feng, X., Kirchner, J. W., Osterhuber, R., Klause, B., & Renshaw, C. E. (2001). Isotopic evolution of a seasonal snowpack and its melt. *Water Resources Research, 37*, pp. 759-769.

Thelander, T. (2009). *Beskrivning till berggrundskartan Kaledoniderna i norra Sverige.* Sveriges Geologiska Undersökning.

Thode, H. G. (1991). Sulphur Isotopes in Nature and the Environment: An Overview. In H. R. Krouse, & V. A. Grinenko, *Stable Isotopes int he Assessment of Natural and Anthropogenic Sulphur in the Environment.* John Wiley and Sons.

Thorn, C. E., Darmody, R. G., Dixon, J. C., & Schlyter, P. (2001). The geochemical weathering regime of Kärkevagge, arctic-alpine Sweden. *Geomorphology, 41*, pp. 37-52.

Thorn, C. E., Darmody, R. G., Dixon, J. C., & Schlyter, P. (2002). Weathering reates of buried machine-polished rock disks, Kärkevagge, Swedish Lapland. *Earth Surface Processes and Landforms, 27*, pp. 831-845.

Thorn, C. E., Dixon, J. C., Darmody, R. G., & Allen, C. E. (2006). A 10-year record of the weathering rates of surficial pebbles in Kärkevagge, Swedish Lapland. *Catena, 65*(272-278).

Thorn, C. E., Schlyter, J. P., Darmody, R. G., & Dixon, J. C. (1999). Statistical relationships between daily and monthly air and shallow-ground temperatures in Kärkevagge, Swedish Lapland. *Permafrost and Periglacial Processes, 10*, pp. 317-330.

Urey, H. C. (1952). *The Planets: Their Origin and Development.* New Haven, Conn.: Yale University Press.

Waldron, S., Scott, M., & Soulsby, C. (2007). Stable Isotope Analysis Reveals Lower-Order River Dissolved Inorganic Carbon Pools Are Highly Dynamic. *Environmental science and Technology, 41*, pp. 6156-6162.

Walker, J. C., Hays, P. B., & Kasting, J. F. (1981). A negative feedback mechanism for the long-term stabilization of Earth's surface temperature. *Journal of Geophysical Research, 86*, pp. 9776-9782.

Zhang, J., Quay, P.D., & Wilbur, D.O. (1994). Carbon isotope fractionation during gas-water exchange and dissolution of CO_2. *Geochimica et Cosmochimica Acta, 59*, pp. 107-114.

Appendix

Appendix 1: potential contamination and other potential errors during sulfur isotope preparation

Below follows a list of sulfur concentrations measured for NaCl used for the sulfur isotope analysis preparation steps. H.P. = High purity salt, concentration of S not measured on ICP.

Sample ID	Date	Column preparation [S] in 0,5M NaCl (mg/L)	Eluation [S] in 0,5M NaCl (mg/L)
K7[1]	2016-06-22	2,11	0,18
K1	2016-07-09	2,11	H.P
K2	2016-07-09	2,11	H.P
K3[2]	2016-07-09	2,11	H.P
K4[2]	2016-07-09	2,11	H.P
K5	2016-07-09	2,11	H.P
K6	2016-07-09	2,11	H.P
K7	2016-07-09	2,11	H.P
K1	2016-08-18	H.P	H.P
K2	2016-08-18	H.P	H.P
K3	2016-08-18	H.P	H.P
K4	2016-08-18	H.P	H.P
K5	2016-08-18	H.P	H.P
K6	2016-08-18	H.P	H.P
K7	2016-08-18	H.P	H.P
K7	2016-10-25	H.P	H.P
KS01	2016-07-22	2,11	H.P
KS02	2016-07-22	2,11	H.P
KS03	2016-07-22	2,11	H.P
KS04	2016-07-22	2,11	H.P
KS05	2016-07-22	2,11	H.P
KS06[2]	2016-07-23	2,11	H.P
KS07	2016-07-23	2,11	H.P
KS08[2]	2016-07-23	2,11	H.P
KS09	2016-07-23	2,11	H.P
KS10[2]	2016-07-23	2,11	H.P
KS11	2016-07-23	2,11	H.P
KS12	2016-07-23	2,11	H.P
KS13	2016-07-24	2,11	H.P
KS14	2016-07-24	2,11	H.P
KS15	2016-07-24	2,11	H.P
KS16	2016-07-24	2,11	H.P
KS17	2016-07-24	2,11	H.P

KS18	2016-07-24	2,11	H.P
KS19	2016-07-24	2,11	H.P
KS20	2016-07-26	2,11	0,18
KS21	2016-07-26	2,11	H.P
KS22	2016-07-26	2,11	H.P
KS23	2016-07-26	H.P	H.P
KS24	2016-07-26	H.P	H.P
KS25	2016-07-26	H.P	H.P
M1	2016-05-23	2,11	H.P
M16	2016-06-23	2,11	H.P
M1	2016-07-06	2,11	0,18
M2	2016-07-06	2,11	H.P
M3	2016-07-06	2,11	H.P
M6	2016-07-08	2,11	H.P
M9	2016-07-08	2,11	H.P
M10	2016-07-08	2,11	H.P
M11	2016-07-08	2,11	H.P
M1	2016-08-17	H.P	H.P
M2	2016-08-17	H.P	H.P
M3	2016-08-17	H.P	H.P
M6	2016-08-16	H.P	H.P
M9	2016-08-16	H.P	H.P
M10	2016-08-16	H.P	H.P
M11	2016-08-16	H.P	H.P
M01	2016-10-26	H.P	H.P
MS01	2016-07-12	2,11	H.P
MS02	2016-07-12	2,11	H.P
MS03	2016-07-12	2,11	H.P
MS04	2016-07-12	2,11	H.P
MS05	2016-07-14	2,11	H.P
MS06	2016-07-14	2,11	H.P
MS07[1]	2016-07-13	2,11	0,18
MS08	2016-07-13	2,11	H.P
MS09	2016-07-13	2,11	H.P
MS10	2016-07-15	2,11	H.P
MS11	2016-07-15	2,11	H.P
MS12	2016-07-15	2,11	H.P
MS13	2016-07-15	2,11	60% 0,181 40% H.P
MS14	2016-07-15	2,11	H.P
MS15	2016-07-15	2,11	H.P
G1	2016-05-23	2,11	0,18
G2	2016-05-24	2,11	H.P

G3	2016-05-24	2,11	H.P
G4	2016-06-22	2,11	0,18
G5[1]	2016-06-27	2,11	0,18
G6[1]	2016-06-20	2,11	0,18
G7	2016-06-21	2,11	H.P
G8[1]	2016-06-28	2,11	0,18
G9		2,11	H.P
G10	2016-07-01	2,11	H.P
MM1	2016-07-08-2016-08-16	H.P	H.P
MM2	2016-08-16 - 2016-09-30	H.P	H.P
KM1	2016-06-30-2016-07-23	H.P	H.P
KM2	2016-08-18 - 2016-09-30	H.P	H.P
KSM	2016-08-18	H.P	H.P
KSB	2016-08-18	H.P	H.P

1) Waterbath were set to 110°C 2) BaCl were added approximately 8 minutes after position on bath

Appendix 2: Data tables

2.1 Main water characteristics

Conductivity$_{field}$ & T$_{field}$ depicts in-situ conductivity and temperature measurements. Conductivity$_{lab}$ & T$_{lab}$ represents measurements in laboratory.

Sample ID	Date	pH$_{field}$	pH$_{lab}$	Conductivity$_{field}$ (μS/cm)	Conductivity$_{lab}$ (μS/cm)	T$_{field}$ (° C)	T$_{lab}$ (° C)	pCO2 (μatm)
K7	2016-06-22	n.a.	n.a.	n.a.	n.a.	n.a.	n.a.	n.a.
K1	2016-07-09	n.a.	6,88	76	85,5	3,55	19,6	557,73
K2	2016-07-09	n.a.	6,56	157	170,8	2,39	20,1	792,32
K3	2016-07-09	n.a.	7,1	78	70,4	5,59	20,3	748,65
K4	2016-07-09	n.a.	6,97	123	136	4,45	20,1	525,24
K5	2016-07-09	n.a.	7,21	125	138,6	5,15	20	437,67
K6	2016-07-09	n.a.	7,33	62	70	5,88	20,1	415,39
K7	2016-07-09	n.a.	7,54	101	112,3	5,81	20,4	430,66
K1	2016-08-18	n.a.	7,14	71	69,3	8,25	19,1	621,64
K2	2016-08-18	n.a.	6,82	127	129,3	4,88	18,5	871,43
K3	2016-08-18	n.a.	7,21	71	72	9,5	18,3	1196,32
K4	2016-08-18	n.a.	7,09	125	126,5	7,26	18,1	715,37
K5	2016-08-18	n.a.	7,38	130	123,3	7,91	17,9	597,24
K6	2016-08-18	n.a.	7,39	88	87,9	9,62	18,1	616,68
K7	2016-08-18	n.a.	7,4	119	114,7	8,74	18,8	640,71
K7	2016-10-25	n.a.	7,32	162	134,7	1,6	17,6	509,78
KS01	2016-07-22	n.a.	5,74	15	15,38	10,12	20,2	534,18
KS02	2016-07-22	n.a.	6,43	45	46,8	9,42	19,1	590,61
KS03	2016-07-22	n.a.	4,71	100	112,8	12,65	19,1	554,10
KS04	2016-07-22	n.a.	5,95	68	77,6	13,58	18,1	529,49
KS05	2016-07-22	n.a.	5,84	85	97,9	14,08	17,6	548,10
KS06	2016-07-23	n.a.	7,19	102	116	4,95	18,5	657,71
KS07	2016-07-23	n.a.	5,38	147	169,5	13,27	18,5	n.a..
KS08	2016-07-23	n.a.	5,82	133	151,2	14,06	16,9	531,27
KS09	2016-07-23	n.a.	4,64	323	354	16,14	17,7	n.a..
KS10	2016-07-23	n.a.	4,76	255	291	16,33	18,2	474,68
KS11	2016-07-23	n.a.	7,71	518	593	11,1	18,3	1132,47
KS12	2016-07-23	n.a.	7,48	296	351	7,63	18,4	2397,14
KS13	2016-07-24	n.a.	7,8	255	289	1,69	22,4	535,51
KS14	2016-07-24	n.a.	7,07	80	93,7	7,94	22,5	1348,99
KS15	2016-07-24	n.a.	8,06	231	259	7,45	22,5	507,98
KS16	2016-07-24	n.a.	7,91	219	252	13,83	22,5	619,38
KS17	2016-07-24	n.a.	7,25	201	228	3,64	22,4	712,20

KS18	2016-07-24	n.a.	7,5	273	318	7,06	22,4	642,14
KS19	2016-07-24	n.a.	n.a.	108	127,2	7,06	22,5	812,29
KS20	2016-07-26	n.a.	7,73	212	238	4,89	21,9	1790,56
KS21	2016-07-26	n.a.	6,01	55	66	10,4	21,7	446,78
KS22	2016-07-26	n.a.	7,71	70	80,1	11,88	21,9	416,96
KS23	2016-07-26	n.a.	7,58	44	51,5	8,45	22,1	528,99
KS24	2016-07-26	n.a.	7,6	67	79,3	14,57	21,7	407,96
KS25	2016-07-26	n.a.	8,19	137	151,2	13,42	21,8	456,70
M1	2017-05-23	n.a.	n.a.	n.a.	n.a.	n.a.	n.a.	n.a.
M16	2017-06-23	n.a.	n.a.	n.a.	n.a.	n.a.	n.a.	n.a.
M1	2017-07-06	7,13	6,91	n.a.	27,8	7,6	16,1	717,43
M2	2017-07-06	7,12	7,09	n.a.	28,5	n,d,	19,8	476,21
M3	2017-07-06	7,2	6,96	n.a.	26	n,d,	19,6	518,61
M6	2017-07-08	7,86	6,93	20	23,5	5,67	17,8	n.a.
M9	2017-07-08	7,84	7,15	31	35,1	7,27	17,7	n.a.
M10	2017-07-08	7,47	6,95	18	20	5,42	17,5	n.a.
M11	2017-07-08	7,5	6,85	14	16,48	3,8	17,3	n.a.
M1	2016-08-17	n.a.	n.a.	40	n.a.	10,52	n.a.	1056,75
M2	2016-08-17	n.a.	7,44	48	49,9	9,96	17,1	891,95
M3	2016-08-17	n.a.	7,48	35	34,8	10,7	17,6	492,23
M6	2016-08-16	n.a.	7,2	25	29,6	5,64	20	739,72
M9	2016-08-16	n.a.	7,43	32	36,8	8,74	20	593,69
M10	2016-08-16	n.a.	7,25	30	36,1	6	19,8	644,66
M11	2016-08-16	n.a.	7,11	22	25,1	4,61	19,3	458,46
M01	2016-10-26	n.a.	7,13	36	57,2	1,77	17,9	1584,14
MS01	2017-07-12	n.a.	6,78	32	39,2	9,33	20,7	1597,50
MS02	2017-07-12	n.a.	6,17	5	6,15	7,64	19,7	685,89
MS03	2017-07-12	n.a.	6,1	39	46,5	2,72	19,7	3218,79
MS04	2017-07-12	n.a.	6,37	33	36,3	11,6	20,1	3269,41
MS05	2017-07-14	n.a.	6,7	18	19,9	5,43	17,5	659,70
MS06	2017-07-14	n.a.	7,01	29	31,8	4,28	17,4	698,42
MS07	2017-07-13	n.a.	6,74	63	72,1	11,8	20,4	4423,51
MS08	2017-07-13	n.a.	6,89	32	37,8	8,06	20,1	2331,23
MS09	2017-07-13	n.a.	6,81	49	57,4	3,8	20,2	2751,44
MS10	2017-07-15	n.a.	7,12	37	41,5	8,16	19,5	1643,56
MS11	2017-07-15	n.a.	7,52	56	64,3	7,67	19,3	1227,37
MS12	2017-07-15	n.a.	7,39	28	33,2	6,03	19,4	770,44
MS13	2017-07-15	n.a.	7,32	35	40,8	2,43	19,3	953,85
MS14	2017-07-15	n.a.	6,97	52	59,5	4,15	19,4	2300,14
MS15	2017-07-15	n.a.	7,13	26	28,2	9,38	19,6	706,61

2.2 Main elements (ICP-OES)

Samples were analyzed for main elements in two turns, thus generating two sets of detection limits and errors. Color of data font corresponds to the color of correct DL.

Sample ID	Date	Ca (µmol/L)	Mg (µmol/L)	Na (µmol/L)	K (µmol/L)	S (µmol/L)	Si (µmol/L)
		DL = 0,0025, error ±4,42%	DL = 0,1752, error ±4,14%	DL = 0,0718, error ±0,22%	DL = 0,0400, error ±0,75%	DL = 1,1098	DL = 0,7439, error±3,08 %
		DL = 0,0039, error ±4,53%	DL = 0,0560, error ±6,96%	DL = 0,0503, error ±1,50%	DL = 0,0321, error ±1,17%	DL = 0,4924	DL = 0,3842, error ±4,28%
K7	2016-06-22	n.a	n.a	n.a	n.a	n.a	n.a
K1	2016-07-09	197,91	102,84	86,24	17,16	229,91	33,84
K2	2016-07-09	364,90	264,69	55,28	31,99	531,02	56,20
K3	2016-07-09	180,49	60,94	34,17	19,22	152,40	40,17
K4	2016-07-09	317,43	173,20	42,70	25,49	370,40	50,78
K5	2016-07-09	327,77	164,45	36,30	25,54	349,02	50,07
K6	2016-07-09	181,50	61,67	33,24	10,42	125,26	24,76
K7	2016-07-09	282,09	123,68	33,29	20,17	272,04	42,39
K1	2016-08-18	173,15	90,94	22,18	13,86	207,34	31,41
K2	2016-08-18	298,17	197,71	28,53	26,46	429,35	51,98
K3	2016-08-18	199,71	64,17	26,91	21,96	178,09	45,38
K4	2016-08-18	331,62	161,55	30,84	25,46	379,28	54,11
K5	2016-08-18	358,76	161,90	32,49	26,78	372,81	55,83
K6	2016-08-18	274,57	85,22	24,32	13,89	182,91	33,60
K7	2016-08-18	330,20	138,96	30,60	23,14	312,92	49,81
K7	2016-10-25	384,39	143,56	37,37	26,25	383,68	55,47
KS01	2016-07-22	29,10	16,38	8,06	4,06	44,18	7,50
KS02	2016-07-22	89,81	57,43	15,37	12,17	137,28	25,87
KS03	2016-07-22	166,82	132,19	18,72	20,77	331,52	67,37
KS04	2016-07-22	133,84	93,27	20,33	18,25	218,06	59,32
KS05	2016-07-22	166,15	137,58	23,17	22,45	294,83	61,87
KS06	2016-07-23	289,22	106,46	31,03	24,18	259,95	52,66
KS07	2016-07-23	277,72	258,93	30,15	26,61	527,38	100,14
KS08	2016-07-23	299,53	196,22	25,08	27,75	468,93	72,30
KS09	2016-07-23	627,92	453,39	42,41	48,35	1237,61	192,13
KS10	2016-07-23	459,85	401,88	38,02	42,50	986,77	145,62
KS11	2016-07-23	1953,43	564,49	58,93	54,03	1540,33	70,45
KS12	2016-07-23	1010,75	348,27	39,96	32,90	684,59	53,26
KS13	2016-07-24	801,55	306,26	42,94	48,17	563,37	61,99
KS14	2016-07-24	257,76	58,82	27,27	13,84	157,71	38,83
KS15	2016-07-24	864,54	208,44	43,98	39,25	373,33	68,94
KS16	2016-07-24	711,76	244,25	36,58	36,90	518,56	56,03

KS17	2016-07-24	598,66	227,11	41,66	30,44	583,99	63,53
KS18	2016-07-24	875,35	360,19	41,16	38,03	862,25	83,20
KS19	2016-07-24	283,91	155,94	24,91	24,48	356,90	54,46
KS20	2016-07-26	893,47	121,80	26,95	19,27	324,61	36,63
KS21	2016-07-26	111,44	77,63	19,03	12,37	180,55	38,18
KS22	2016-07-26	225,82	61,36	18,10	8,31	114,80	20,53
KS23	2016-07-26	129,89	28,87	34,34	14,99	57,62	20,99
KS24	2016-07-26	215,76	42,89	25,52	15,35	122,26	15,77
KS25	2016-07-26	552,21	85,32	20,98	11,24	138,02	24,83
M1	2017-05-23	n.a	n.a	n.a	n.a	n.a	n.a
M16	2017-06-23	n.a	n.a	n.a	n.a	n.a	n.a
M1	2017-07-06	73,89	20,47	31,50	11,75	38,75	46,30
M2	2017-07-06	80,13	20,49	30,02	8,60	39,80	55,06
M3	2017-07-06	64,51	18,49	28,29	12,63	38,14	40,19
M6	2017-07-08	53,49	14,45	35,12	6,44	32,56	58,95
M9	2017-07-08	87,36	22,59	29,27	21,64	48,37	24,18
M10	2017-07-08	45,05	14,50	28,38	8,42	31,68	48,06
M11	2017-07-08	37,37	11,32	21,23	4,12	31,00	34,65
M1	2016-08-17	n.a	n.a	n.a	n.a	n.a	n.a
M2	2016-08-17	155,38	39,67	43,46	13,49	61,76	87,41
M3	2016-08-17	103,44	28,43	38,55	18,10	46,50	63,75
M6	2016-08-16	73,13	19,14	38,76	7,75	36,42	79,17
M9	2016-08-16	92,28	24,54	29,99	21,44	47,72	36,50
M10	2016-08-16	84,71	27,27	38,48	12,77	42,61	86,71
M11	2016-08-16	62,63	19,63	26,43	8,35	41,62	61,53
M01	2016-10-26	163,40	46,69	45,20	19,42	67,95	84,70
MS01	2017-07-12	78,56	32,97	31,20	14,38	58,70	34,81
MS02	2017-07-12	9,87	3,53	10,01	4,23	5,42	15,06
MS03	2017-07-12	92,89	38,93	26,78	13,66	93,25	71,35
MS04	2017-07-12	59,28	40,55	45,95	14,09	33,89	37,01
MS05	2017-07-14	45,26	12,66	27,19	4,37	19,30	67,17
MS06	2017-07-14	79,62	16,36	22,19	5,68	25,11	61,20
MS07	2017-07-13	172,04	66,59	64,47	21,86	42,17	108,79
MS08	2017-07-13	87,43	27,29	26,85	16,59	27,42	50,84
MS09	2017-07-13	146,42	45,99	36,84	13,33	36,58	88,65
MS10	2017-07-15	105,06	25,84	27,32	8,09	32,72	42,16
MS11	2017-07-15	188,76	37,88	32,69	11,39	59,40	90,49
MS12	2017-07-15	80,98	19,05	25,04	8,56	20,33	55,45
MS13	2017-07-15	106,10	11,97	23,49	9,00	44,79	60,79
MS14	2017-07-15	179,98	25,12	29,21	13,57	76,17	80,49
MS15	2017-07-15	67,87	17,69	25,95	6,68	29,96	65,55
KM1	2016-06-30-2016-07-23	0,28	0,33	8,94	1,06	21,24	1,36
KM2	2016-08-18 - 2016-09-30	0,93	1,17	11,48	1,54	21,63	1,48
MM1	2016-07-08-2016-08-16	0,74	0,42	7,79	1,89	22,47	1,75

MM2	2016-08-16 - 2016-09-30	6,98	1,73	10,49	3,55	24,03	1,96

2.3 Main anions (IC)

n.d. = not detected.

Sample ID	Date	Cl (µmol/L) LOQ = 0,71 µmol/L	NO3 (µmol/L)	SO4 (µmol/L) LOQ = 0,26 µmol/L
K7	2017-06-22	n.a.	n.d.	n.a.
K1	2017-07-09	26,67	n.d.	248,29
K2	2017-07-09	32,04	6,32	615,68
K3	2017-07-09	27,13	4,82	170,32
K4	2017-07-09	27,98	6,54	431,26
K5	2017-07-09	30,94	6,44	408,46
K6	2017-07-09	23,36	n.d.	144,16
K7	2017-07-09	28,50	5,55	312,90
K1	2016-08-18	22,84	n.d.	237,77
K2	2016-08-18	26,63	4,45	494,84
K3	2016-08-18	18,63	n.d.	200,78
K4	2016-08-18	26,45	5,15	435,68
K5	2016-08-18	32,96	4,36	428,35
K6	2016-08-18	19,35	n.d.	205,21
K7	2016-08-18	24,84	n.d.	365,00
K7	2016-10-25	27,48	5,33	414,16
KS01	2016-07-22	10,68	n.d.	46,64
KS02	2016-07-22	10,90	5,22	155,18
KS03	2016-07-22	13,65	n.d.	385,19
KS04	2016-07-22	16,62	4,35	258,87
KS05	2016-07-22	14,38	n.d.	331,41
KS06	2016-07-23	28,14	6,28	290,07
KS07	2016-07-23	17,34	n.d.	608,76
KS08	2016-07-23	17,05	n.d.	540,83
KS09	2016-07-23	21,43	n.d.	1529,88
KS10	2016-07-23	20,65	n.d.	1163,30
KS11	2016-07-23	35,22	n.d.	1802,68
KS12	2016-07-23	30,11	n.d.	793,38
KS13	2016-07-24	38,52	14,15	640,95
KS14	2016-07-24	26,01	4,58	180,38
KS15	2016-07-24	42,54	7,04	412,99
KS16	2016-07-24	31,34	n.d.	587,77
KS17	2016-07-24	35,76	6,70	686,66
KS18	2016-07-24	28,25	n.d.	999,77
KS19	2016-07-24	20,20	n.d.	393,67
KS20	2016-07-26	19,44	n.d.	361,21

KS21	2016-07-26	18,58	n.d.	207,46
KS22	2016-07-26	13,58	n.d.	130,52
KS23	2016-07-26	24,38	n.d.	71,00
KS24	2016-07-26	16,73	n.d.	135,62
KS25	2016-07-26	14,71	n.d.	153,33
M1	2017-05-23	0.84	0.15	2.18
M16	2017-06-23	n.a.	n.a.	n.a.
M1	2017-07-06	7,71	n.d.	22,36
M2	2017-07-06	0,00	n.d.	23,28
M3	2017-07-06	9,42	n.d.	19,70
M6	2017-07-08	13,66	n.d.	19,29
M9	2017-07-08	12,58	n.d.	36,07
M10	2017-07-08	7,59	n.d.	16,77
M11	2017-07-08	8,31	n.d.	16,90
M1	2016-08-17	n.a.	n.d.	n.a.
M2	2016-08-17	8,84	n.d.	52,38
M3	2016-08-17	11,21	n.d.	34,14
M6	2016-08-16	13,28	n.d.	24,29
M9	2016-08-16	10,37	n.d.	36,24
M10	2016-08-16	10,46	n.d.	31,50
M11	2016-08-16	6,99	6,60	30,18
M01	2016-10-26	21,90	7,78	57,01
MS01	2017-07-12	7,99	n.d.	70,05
MS02	2017-07-12	8,39	n.d.	<LOQ
MS03	2017-07-12	8,01	4,96	109,99
MS04	2017-07-12	13,38	n.d.	36,89
MS05	2017-07-14	15,73	n.d.	20,09
MS06	2017-07-14	15,70	4,94	23,53
MS07	2017-07-13	49,79	6,36	43,90
MS08	2017-07-13	12,85	n.d.	31,08
MS09	2017-07-13	14,46	9,63	38,04
MS10	2017-07-15	9,99	n.d.	37,31
MS11	2017-07-15	8,91	n.d.	65,19
MS12	2017-07-15	9,95	4,33	19,38
MS13	2017-07-15	13,56	6,04	50,66
MS14	2017-07-15	14,76	n.d.	82,31
MS15	2017-07-15	12,92	n.d.	33,00

2.4 Trace elements (ICP-OES)

Samples were analyzed for trace elements in two turns, thus generating two sets of detection limits and errors. Color of data font corresponds to the color of correct DL.

Sample ID	Date	Al (µmol/L)	Cd (µmol/L)	Ce (µmol/L)	Co (µmol/L)	Cu (µmol/L)
		DL=4,07 E-03, error ±12,80 %	DL = 1,17E-02, error ±2,52%	DL = 1,70E-03	DL = 1,70E-03, error ±1,48%	DL = 3,25E-03, error ±17,88 %
		DL=4,77 E-03, error ±1,08%	DL = 1,26E-04, error ±4,07%	DL = 6,69E-03	DL = 7,19E-04, error ±6,59%	DL = 1,03E-02, error ±1,29%
K7	2017-06-22	n.a.	n.a	n.a	n.a	n.a
K1	2017-07-09	0,34	9,30E-04	1,71E-02	1,36E-02	2,01E-02
K2	2017-07-09	0,71	1,51E-03	5,87E-02	2,30E-02	5,60E-02
K3	2017-07-09	0,27	4,00E-04	1,40E-02	6,99E-03	1,53E-02
K4	2017-07-09	0,52	7,60E-04	1,45E-02	1,09E-02	1,95E-02
K5	2017-07-09	0,56	7,00E-04	1,73E-02	8,17E-03	1,85E-02
K6	2017-07-09	1,26	9,40E-04	2,06E-02	1,76E-02	3,28E-02
K7	2017-07-09	0,83	7,20E-04	1,66E-02	9,80E-03	1,89E-02
K1	2016-08-18	0,46	7,60E-04	1,83E-02	1,58E-02	1,91E-02
K2	2016-08-18	0,49	8,40E-04	2,79E-02	6,08E-03	2,38E-02
K3	2016-08-18	0,26	2,40E-04	1,28E-02	<DL	1,19E-02
K4	2016-08-18	0,23	5,80E-04	1,47E-02	2,66E-03	1,37E-02
K5	2016-08-18	0,34	5,80E-04	1,39E-02	2,34E-03	1,32E-02
K6	2016-08-18	1,04	8,30E-04	1,95E-02	9,91E-03	2,21E-02
K7	2016-08-18	0,51	5,10E-04	1,63E-02	3,55E-03	1,47E-02
K7	2016-10-25	0,30	4,80E-04	1,24E-02	1,26E-03	<DL
KS01	2016-07-22	1,00	5,50E-04	2,00E-02	1,92E-02	4,11E-02
KS02	2016-07-22	0,35	7,30E-04	1,65E-02	9,77E-03	2,00E-02
KS03	2016-07-22	19,11	4,34E-03	1,26E-01	1,43E-01	2,49E-01
KS04	2016-07-22	1,42	2,00E-03	7,09E-02	7,82E-02	1,38E-01
KS05	2016-07-22	1,21	2,04E-03	3,15E-02	2,98E-02	4,73E-02
KS06	2016-07-23	0,34	2,00E-04	<DL	<DL	1,07E-02
KS07	2016-07-23	10,41	5,12E-03	9,89E-02	2,84E-01	1,25E-01
KS08	2016-07-23	2,08	1,50E-03	4,96E-02	3,51E-02	7,24E-02
KS09	2016-07-23	62,27	1,21E-02	7,54E-01	5,00E-01	1,59E+00
KS10	2016-07-23	57,09	9,76E-03	5,49E-01	5,11E-01	8,87E-01

KS11	2016-07-23	0,34	4,10E-04	<DL	1,85E-03	2,11E-02
KS12	2016-07-23	0,08	2,40E-04	<DL	<DL	1,36E-02
KS13	2016-07-24	0,08	2,60E-04	1,35E-02	<DL	1,20E-02
KS14	2016-07-24	0,38	2,40E-04	1,38E-02	<DL	1,65E-02
KS15	2016-07-24	0,27	4,00E-04	1,18E-02	<DL	1,17E-02
KS16	2016-07-24	0,07	2,20E-04	1,19E-02	<DL	1,45E-02
KS17	2016-07-24	0,14	5,10E-04	<DL	<DL	1,15E-02
KS18	2016-07-24	0,10	2,50E-04	1,19E-02	<DL	1,18E-02
KS19	2016-07-24	0,05	3,10E-04	<DL	<DL	<DL
KS20	2016-07-26	0,06	1,70E-04	1,24E-02	<DL	1,65E-02
KS21	2016-07-26	1,36	2,48E-03	8,40E-02	6,36E-02	1,37E-01
KS22	2016-07-26	0,22	1,60E-04	<DL	<DL	<DL
KS23	2016-07-26	0,06	<DL	<DL	<DL	<DL
KS24	2016-07-26	0,18	<DL	<DL	<DL	1,17E-02
KS25	2016-07-26	0,09	1,60E-04	1,21E-02	<DL	1,16E-02
M1	2017-05-23	n.a.	n.a.	n.a.	n.a.	n.a.
M16	2017-06-23	n.a.	n.a.	n.a.	n.a.	n.a.
M1	2017-07-06	1,64	1,50E-04	9,66E-03	1,11E-03	4,23E-02
M2	2017-07-06	2,31	1,90E-04	1,15E-02	7,20E-04	2,81E-02
M3	2017-07-06	1,37	2,00E-04	9,51E-03	9,80E-04	2,57E-02
M6	2017-07-08	1,47	1,70E-04	8,89E-03	<DL	2,01E-02
M9	2017-07-08	1,56	1,80E-04	7,94E-03	1,18E-03	1,83E-02
M10	2017-07-08	1,26	1,40E-04	8,89E-03	7,50E-04	2,02E-02
M11	2017-07-08	0,52	2,20E-04	7,79E-03	<DL	2,35E-02
M1	2016-08-17	n.a.	n.a.	n.a.	n.a.	n.a.
M2	2016-08-17	0,74	2,20E-04	8,36E-03	<DL	1,94E-02
M3	2016-08-17	0,60	1,80E-04	1,08E-02	<DL	2,08E-02
M6	2016-08-16	0,93	1,40E-04	9,15E-03	<DL	1,67E-02
M9	2016-08-16	0,57	2,10E-04	7,99E-03	<DL	1,93E-02
M10	2016-08-16	0,64	2,00E-04	8,75E-03	<DL	1,38E-02
M11	2016-08-16	0,32	1,60E-04	9,11E-03	<DL	1,80E-02
M01	2016-10-26	0,39	1,50E-04	8,26E-03	**9,80E-04**	1,45E-02
MS01	2017-07-12	2,00	2,00E-04	<DL	2,19E-03	4,50E-02
MS02	2017-07-12	1,30	1,70E-04	<DL	1,77E-03	1,79E-02
MS03	2017-07-12	4,31	2,30E-04	1,48E-02	1,78E-02	1,16E-01
MS04	2017-07-12	3,59	1,60E-04	<DL	4,48E-03	2,62E-02
MS05	2017-07-14	0,96	1,70E-04	<DL	<DL	2,15E-02
MS06	2017-07-14	1,23	2,10E-04	1,30E-02	<DL	2,39E-02
MS07	2017-07-13	0,35	<DL	1,25E-02	<DL	1,82E-02
MS08	2017-07-13	0,49	<DL	<DL	<DL	2,10E-02
MS09	2017-07-13	0,41	<DL	<DL	<DL	2,09E-02
MS10	2017-07-15	0,74	1,90E-04	<DL	<DL	2,09E-02

MS11	2017-07-15	0,61	2,30E-04	<DL	<DL	2,30E-02
MS12	2017-07-15	0,42	1,80E-04	<DL	<DL	1,81E-02
MS13	2017-07-15	0,25	1,90E-04	<DL	<DL	1,32E-02
MS14	2017-07-15	0,84	2,30E-04	1,51E-02	<DL	3,24E-02
MS15	2017-07-15	1,44	1,70E-04	<DL	<DL	3,10E-02
KM1	2016-06-30-2016-07-23	0,09	3,20E-04	8,16E-03	9,10E-04	<DL
KM2	2016-08-18 - 2016-09-30	0,07	2,70E-04	8,54E-03	1,06E-03	<DL
MM1	2016-07-08-2016-08-16	0,10	2,40E-04	7,63E-03	<DL	<DL
MM2	2016-08-16 - 2016-09-30	0,08	3,10E-04	8,00E-03	7,20E-04	<DL

Sample ID	Date	Fe (µmol/L)	Mn (µmol/L)	Ni (µmol/L)	Sr (µmol/L)	Zn (µmol/L)
		DL = 1,81E-03, error ±4,84%	DL = 1,05E-03, error ±0,91%	DL = 2,75E-03, error ±1,76%	DL = 2,31E-03 = error ±3,16%	DL = 2,37E-03, error 1,11%
		DL = 1,59E-03, error ±4,29%	DL = 9,07E-04, error ±1,30%	DL = 1,38E-03, error ±1,08%	DL = 1,32E-03, error ±0,02%	DL = 1,50E-02, error ±5,88%
K7	2017-06-22	n.a	n.a	n.a	n.a	n.a
K1	2017-07-09	2,63E-02	2,12E-01	1,11E-01	3,96E-01	1,18E-01
K2	2017-07-09	1,39E-02	2,08E-01	2,35E-01	6,40E-01	2,54E-01
K3	2017-07-09	1,59E-02	4,39E-02	5,30E-02	4,49E-01	4,22E-02
K4	2017-07-09	5,51E-02	8,02E-02	1,25E-01	6,84E-01	1,75E-01
K5	2017-07-09	3,18E-02	6,16E-02	1,06E-01	7,49E-01	1,20E-01
K6	2017-07-09	1,22E-02	1,62E-01	9,75E-02	4,40E-01	1,56E-01
K7	2017-07-09	2,46E-02	8,81E-02	9,80E-02	6,41E-01	1,17E-01
K1	2016-08-18	1,10E-02	1,96E-01	1,08E-01	3,58E-01	1,17E-01
K2	2016-08-18	1,83E-02	5,40E-02	1,34E-01	5,11E-01	1,82E-01
K3	2016-08-18	2,34E-02	9,30E-03	2,61E-02	4,74E-01	2,54E-02
K4	2016-08-18	4,93E-02	2,10E-02	7,75E-02	6,91E-01	7,05E-02
K5	2016-08-18	2,74E-02	2,24E-02	7,23E-02	7,46E-01	7,03E-02
K6	2016-08-18	1,17E-02	8,60E-02	9,78E-02	6,25E-01	1,12E-01
K7	2016-08-18	4,97E-02	3,26E-02	7,42E-02	7,29E-01	7,33E-02
K7	2016-10-25	1,82E-02	1,27E-02	3,24E-02	8,33E-01	4,75E-02
KS01	2016-07-22	1,10E-01	8,69E-02	7,32E-02	4,39E-02	7,97E-02
KS02	2016-07-22	4,67E-02	5,04E-02	8,77E-02	1,79E-01	9,25E-02
KS03	2016-07-22	1,48E-01	1,73E+00	5,38E-01	2,42E-01	7,85E-01
KS04	2016-07-22	2,29E-01	8,72E-01	3,03E-01	2,62E-01	3,63E-01
KS05	2016-07-22	2,37E-02	2,01E-01	3,29E-01	2,14E-01	2,62E-01
KS06	2016-07-23	1,06E-02	2,42E-03	8,91E-03	6,55E-01	3,19E-02
KS07	2016-07-23	1,59E-01	3,48E+00	9,52E-01	2,85E-01	8,30E-01
KS08	2016-07-23	6,51E-02	1,92E-01	3,32E-01	4,01E-01	1,79E-01
KS09	2016-07-23	5,01E-01	5,38E+00	1,93E+00	5,16E-01	2,53E+00
KS10	2016-07-23	2,90E-01	6,52E+00	1,72E+00	4,56E-01	1,92E+00
KS11	2016-07-23	1,42E-02	1,17E-02	1,76E-02	4,60E+00	3,23E-02
KS12	2016-07-23	1,02E-02	2,72E-03	7,96E-03	2,76E+00	2,48E-02
KS13	2016-07-24	7,06E-02	1,65E-03	1,33E-02	2,22E+00	2,75E-02
KS14	2016-07-24	9,64E-03	1,80E-03	1,91E-02	7,31E-01	2,37E-02
KS15	2016-07-24	1,59E-02	2,64E-03	2,23E-02	2,19E+00	5,49E-02
KS16	2016-07-24	1,47E-02	2,03E-03	1,14E-02	1,82E+00	1,59E-02
KS17	2016-07-24	1,23E-02	1,70E-03	3,70E-02	1,64E+00	4,25E-02
KS18	2016-07-24	1,60E-02	1,17E-03	1,41E-02	2,10E+00	2,23E-02

KS19	2016-07-24	9,75E-03	1,83E-03	3,56E-02	4,76E-01	2,16E-02
KS20	2016-07-26	1,29E-02	1,10E-03	5,60E-03	2,32E+00	1,08E-02
KS21	2016-07-26	8,24E-02	6,35E-01	2,80E-01	1,81E-01	4,23E-01
KS22	2016-07-26	9,65E-03	2,85E-03	7,64E-03	5,06E-01	1,29E-02
KS23	2016-07-26	5,22E-02	1,83E-03	<DL	3,34E-01	9,94E-03
KS24	2016-07-26	1,78E-02	1,15E-03	3,18E-03	6,16E-01	2,62E-02
KS25	2016-07-26	9,02E-03	1,11E-03	<DL	1,25E+00	1,11E-02
M1	2017-05-23	n.a.	n.a.	n.a.	n.a.	n.a.
M16	2017-06-23	n.a.	n.a.	n.a.	n.a.	n.a.
M1	2017-07-06	6,23E-01	1,90E-02	1,16E-02	<DL	6,37E-02
M2	2017-07-06	7,84E-01	1,19E-02	1,21E-02	<DL	9,13E-02
M3	2017-07-06	<DL	1,25E-02	1,25E-02	<DL	1,45E-01
M6	2017-07-08	2,31E-01	3,18E-03	<DL	8,41E-02	7,65E-02
M9	2017-07-08	1,78E-01	4,71E-03	<DL	1,46E-01	8,22E-02
M10	2017-07-08	2,78E-01	7,08E-03	<DL	7,35E-02	1,23E-01
M11	2017-07-08	6,05E-02	1,75E-03	<DL	3,93E-02	1,22E-01
M1	2016-08-17	<DL	<DL	<DL	<DL	<DL
M2	2016-08-17	1,12E-01	3,55E-03	<DL	<DL	3,81E-02
M3	2016-08-17	1,37E-01	1,42E-02	<DL	<DL	3,15E-02
M6	2016-08-16	1,27E-01	2,26E-03	<DL	1,07E-01	4,16E-02
M9	2016-08-16	3,90E-01	7,60E-03	<DL	1,50E-01	3,52E-02
M10	2016-08-16	1,70E-01	1,09E-02	<DL	1,32E-01	3,81E-02
M11	2016-08-16	6,15E-02	1,13E-02	<DL	6,41E-02	3,19E-02
M01	2016-10-26	7,28E-01	1,06E-01	<DL	2,58E-01	2,13E-02
MS01	2017-07-12	5,46E-01	8,03E-03	1,10E-02	1,23E-01	4,38E-02
MS02	2017-07-12	2,05E-01	7,56E-03	5,05E-03	2,24E-02	2,87E-02
MS03	2017-07-12	7,22E-01	1,40E-02	2,55E-02	1,55E-01	3,44E-02
MS04	2017-07-12	1,89E+00	1,89E-02	1,26E-02	1,23E-01	4,67E-02
MS05	2017-07-14	9,26E-02	2,57E-03	3,63E-03	6,49E-02	1,32E-02
MS06	2017-07-14	1,32E-01	2,25E-03	<DL	7,64E-02	1,48E-02
MS07	2017-07-13	1,40E+00	6,57E-02	5,24E-03	4,24E-01	1,02E-02
MS08	2017-07-13	6,16E-02	3,57E-03	3,67E-03	1,34E-01	1,28E-02
MS09	2017-07-13	7,82E-02	9,45E-03	3,48E-03	2,30E-01	1,75E-02
MS10	2017-07-15	2,41E-01	9,05E-03	4,95E-03	2,02E-01	1,05E-01
MS11	2017-07-15	5,10E-01	3,69E-02	6,23E-03	2,29E-01	2,25E-02
MS12	2017-07-15	6,57E-02	1,49E-03	3,60E-03	1,20E-01	1,82E-02
MS13	2017-07-15	4,87E-02	4,31E-03	4,16E-03	1,61E-01	2,96E-02
MS14	2017-07-15	1,56E-01	2,78E-03	5,44E-03	3,27E-01	2,56E-02
MS15	2017-07-15	1,54E-01	2,01E-03	7,54E-03	6,77E-02	4,58E-02
MM1	2016-07-08-2016-08-16	3,36E-02	5,86E-03	<DL	8,50E-04	8,89E-02
MM2	2016-08-16 - 2016-09-30	2,35E-02	3,19E-02	<DL	3,94E-03	8,35E-01

KM1	2016-06-30-2016-07-23	1,21E-02	4,64E-03	<DL	7,40E-04	9,19E-02
KM2	2016-08-18 - 2016-09-30	1,66E-02	7,43E-03	<DL	1,87E-03	1,93E-01

2.5 Isotope data

$\delta^{13}C_{DIC}$ values marked with * experienced a standard deviation of 0,2‰ instead of 0,06‰ due to low sample concentrations

Sample ID	Date	δ D vs V-SMOW (‰)	δ 18O vs V-SMOW (‰)	δ 13C vs PDB, ‰	δ 34S vs V-CDT (‰)	δ 33S vs V-CDT (‰)	δ 18O in SO4 vs V-SMOW (‰)
K7	2017-06-22	n.a	n.a	n.a	-0,63	-0,30	-0,77
K1	2017-07-09	-88,66	-12,80	-3,34	-0,55	-0,20	-0,69
K2	2017-07-09	-89,28	-12,81	-3,48	-0,46	-0,16	0,00
K3	2017-07-09	-89,35	-12,91	-7,69	-0,75	-0,38	-0,44
K4	2017-07-09	-89,46	-12,78	-4,60	-0,87	-0,42	-1,29
K5	2017-07-09	-88,69	-12,64	-3,42	-0,80	-0,30	-1,04
K6	2017-07-09	-89,05	-12,93	-2,18	-0,30	-0,20	-0,28
K7	2017-07-09	-88,88	-12,81	-2,48	-0,41	-0,22	-0,97
K1	2016-08-18	-91,81	-13,00	-2,28	-0,62	-0,21	-0,94
K2	2016-08-18	-91,69	-13,08	-3,13	-0,62	-0,29	-0,80
K3	2016-08-18	-89,31	-12,77	-8,86	-1,36	-0,71	-0,92
K4	2016-08-18	-90,74	-12,91	-4,78	-0,70	-0,20	-0,78
K5	2016-08-18	-90,13	-12,82	-3,49	-0,80	-0,40	-0,29
K6	2016-08-18	-88,18	-12,67	-2,52	0,10	0,10	0,13
K7	2016-08-18	-89,51	-12,74	-2,61	-0,60	-0,10	0,11
K7	2016-10-25	-89,30	-12,68	-2,75	-0,75	-0,37	-0,75
KS01	2016-07-22	-96,54	-13,82	-7,51*	0,06	-0,09	-1,92
KS02	2016-07-22	-96,12	-13,72	-4,71*	-0,21	-0,09	-1,17
KS03	2016-07-22	-95,17	-13,34	-9,17*	-0,50	-0,70	-2,38
KS04	2016-07-22	-93,71	-13,06	-6,88*	-1,26	-0,48	-1,45
KS05	2016-07-22	-90,85	-12,72	-8,01*	-0,95	-0,33	-0,78
KS06	2016-07-23	-89,89	-12,62	-3,44	-0,42	-0,03	1,85
KS07	2016-07-23	-88,63	-12,38	-8,88	-1,01	-0,52	-1,64
KS08	2016-07-23	-91,33	-12,85	-7,88*	-0,26	-0,23	-1,33
KS09	2016-07-23	-86,43	-12,00	n.a.	-1,40	-0,70	-1,73
KS10	2016-07-23	-86,40	-11,91	n.a.	-0,60	-0,27	-2,28
KS11	2016-07-23	-83,80	-11,71	-6,79	-1,50	-0,70	-1,91
KS12	2016-07-23	-84,32	-11,67	-8,86	-2,71	-1,38	-1,50
KS13	2016-07-24	-86,16	-12,19	-4,72	0,19	0,11	-0,24
KS14	2016-07-24	-90,07	-12,80	-10,26	-1,70	-0,88	-0,72
KS15	2016-07-24	-86,17	-12,09	-7,37	-0,05	0,02	-1,19
KS16	2016-07-24	-83,95	-11,63	-5,40	-1,97	-1,07	-0,94
KS17	2016-07-24	-88,60	-12,41	-8,02	-0,80	-0,30	-1,25

KS18	2016-07-24	-87,31	-12,29	-6,29	-1,10	-0,60	-1,65
KS19	2016-07-24	-91,58	-12,93	-7,54	-0,10	0,00	-1,79
KS20	2016-07-26	-90,57	-12,77	-6,96	-1,01	-0,58	1,12
KS21	2016-07-26	-88,65	-12,82	-6,25*	-1,60	-0,60	-0,73
KS22	2016-07-26	-89,87	-13,07	-1,90	1,20	0,70	-0,62
KS23	2016-07-26	-85,14	-12,33	-4,89	5,03	2,54	1,94
KS24	2016-07-26	-86,14	-12,54	-1,43	7,10	3,60	1,79
KS25	2016-07-26	-88,02	-12,60	-2,97	2,69	1,55	-0,49
M1	2017-05-23	-102,00	-14.24	-5.16	6,89	3,46	-4,03
M16	2017-06-23	n.a.	n.a.	n.a.	6,85	3,57	-4,48
M1	2017-07-06	-98,3	-13,78	-6,14	6,38	3,09	-2,39
M2	2017-07-06	-95,5	-13,32	-5,08	6,10	3,07	-2,36
M3	2017-07-06	-97,9	-13,52	-4,29	5,45	2,50	1,35
M6	2017-07-08	-100,4	-13,95	-6,81	6,40	3,22	-6,09
M9	2017-07-08	-99,7	-13,92	-4,07	5,37	2,75	-4,68
M10	2017-07-08	-98,5	-13,74	-6,53	6,37	3,25	n.a.
M11	2017-07-08	-100,5	-14,07	-3,68	5,18	2,63	-0,78
M1	2016-08-17	n.a.	n.a.	-6,96	6,97	3,48	-3,74
M2	2016-08-17	-93,8	-12,97	-4,78	6,51	3,34	-2,32
M3	2016-08-17	-96,5	-13,38	-2,14	6,75	3,45	-4,56
M6	2016-08-16	-98,0	-13,77	-7,32	7,31	3,55	-5,48
M9	2016-08-16	-97,1	-13,56	-4,98	6,05	2,99	-4,36
M10	2016-08-16	-96,3	-13,46	-7,40	7,63	3,77	-5,09
M11	2016-08-16	-96,8	-13,56	-4,55	5,66	2,86	-6,63
M01	2016-10-26	-97,3	-13,49	-10,27	6,93	3,45	-3,51
MS01	2017-07-12	-94,83	-13,14	-13,54	8,10	4,10	-1,84
MS02	2017-07-12	-112,04	-15,66	-10,58*	n.a.	n.a.	n.a.
MS03	2017-07-12	-97,77	-13,48	-18,96	4,40	2,40	-9,31
MS04	2017-07-12	-98,08	-13,65	-13,6	5,70	2,99	-2,79
MS05	2017-07-14	-100,30	-14,09	n.a.	6,22	3,04	-7,55
MS06	2017-07-14	-102,05	-14,27	-9,64	8,31	4,14	-9,78
MS07	2017-07-13	-102,52	-13,93	-16,10	11,81	6,12	-2,06
MS08	2017-07-13	-99,95	-13,85	-13,00	6,64	3,26	-4,62
MS09	2017-07-13	-100,66	-13,98	-14,22	6,79	3,45	-3,00
MS10	2017-07-15	-93,03	-12,75	-12,01	6,70	3,40	-1,22
MS11	2017-07-15	-94,97	-13,19	-10,80	5,80	2,80	-2,27
MS12	2017-07-15	-97,51	-13,65	-6,92	8,52	4,31	-3,40
MS13	2017-07-15	-97,33	-13,64	-11,89	6,70	3,40	-2,34
MS14	2017-07-15	-97,33	-13,52	-15,79	-0,50	-0,20	-5,39
MS15	2017-07-15	-102,26	-14,27	-7,84	6,75	3,46	-4,61
G1	2017-05-23	-98,4	-13,76	-4,45	4,34	2,40	-1,75
G2	2017-05-24	-108,1	-14,4	-8,64	7,93	4,02	-3,15

G3	2017-05-24	-104,7	-14,31	-5,96	5,08	2,44	-1,78
G4	2017-06-22	n.a.	n.a.	n.a.	-0,92	-0,33	-4,27
G5	2017-06-27	n.a.	n.a.	n.a.	1,70	0,80	-1,12
G6	2017-06-20	n.a.	n.a.	n.a.	4,01	2,07	-1,88
G7	2017-06-21	n.a.	n.a.	n.a.	6,06	3,13	n.a.
G8	2017-06-28	n.a.	n.a.	n.a.	6,75	3,57	-2,78
G9		n.a.	n.a.	n.a.	7,06	3,60	-2,75
G10	2016-07-01	n.a.	n.a.	n.a.	7,42	3,84	-0,44
KM1	2016-06-30- 2016-07-23	-109,8	-14,67	n.a.	18,66	9,4	n.a.
KM2	2016-08-18 - 2016-09-30	-91,3	-12,13	n.a.	15,75	8,0	n.a.
MM1	2016-07-08- 2016-08-16	-93,5	-12,77	n.a.	11,71	5,9	-8,63
MM2	2016-08-16 - 2016-09-30	-98,2	-13,02	n.a.	16,15	8,2	n.a.
KR1	2016-08-18	n.a.	n.a.	n.a.	-4,49	-0,6	n.a.
KR2	2016-08-18	n.a.	n.a.	n.a.	-1,49	-0,7	n.a.
KSM	2016-08-18	n.a.	n.a.	n.a.	3,61	1,7	0,66
KSB	2016-08-18	n.a.	n.a.	n.a.	10,32	5,2	5,00

2.6 DIC, alkalinity and DOC

Sample ID	Date	CO2 µmol/Kg	HCO3 µmol/kg	CO3 µmol/kg	DIC µmol/Kg	Alkalinity (meq/L)	DOC (mg/L)
K7	2017-06-22	n.a.	n.a.	n.a.	n.a.		
K1	2017-07-09	37,80	95,50	2,35E-02	133,56	0,10	0,08
K2	2017-07-09	56,20	78,70	1,10E-02	135,29	0,08	0,02
K3	2017-07-09	47,10	170,79	6,08E-02	218,25	0,17	0,04
K4	2017-07-09	34,40	167,22	8,10E-02	202,37	0,17	0,31
K5	2017-07-09	28,00	224,24	1,80E-01	253,26	0,23	0,08
K6	2017-07-09	25,80	217,37	1,79E-01	243,84	0,22	0,07
K7	2017-07-09	26,90	218,64	1,78E-01	246,40	0,22	0,04
K1	2016-08-18	35,50	88,70	2,21E-02	124,41	0,09	0,00
K2	2016-08-18	56,20	87,80	1,37E-02	144,39	0,09	0,00
K3	2016-08-18	65,40	195,49	5,89E-02	261,42	0,20	0,01
K4	2016-08-18	42,30	191,96	8,85E-02	235,13	0,19	0,04
K5	2016-08-18	34,50	254,64	1,92E-01	290,45	0,26	0,07
K6	2016-08-18	33,60	348,68	3,68E-01	383,77	0,35	0,08
K7	2016-08-18	36,00	285,32	2,31E-01	322,66	0,29	0,06
K7	2016-10-25	37,30	334,13	2,95E-01	372,98	0,34	n.a.
KS01	2016-07-22	28,60	7,23	1,78E-04	35,80	0,01	0,09
KS02	2016-07-22	32,40	30,00	2,76E-03	62,40	0,03	0,02
KS03	2016-07-22	27,20	103,21	4,07E-02	130,79	-0,06	0,17
KS04	2016-07-22	25,30	14,60	8,75E-04	39,90	0,02	0,16
KS05	2016-07-22	25,70	8,38	2,86E-04	34,10	0,01	0,16
KS06	2016-07-23	42,30	259,99	1,59E-01	303,29	0,26	0,11
KS07	2016-07-23	n.a.	n.a.	n.a.	n.a.	-0,01	0,54
KS08	2016-07-23	25,00	6,84	2,00E-04	31,80	0,01	0,32
KS09	2016-07-23	n.a.	n.a.	n.a.	n.a.	n.a.	0,68
KS10	2016-07-23	n.a.	n.a.	n.a.	n.a.	n.a.	0,73
KS11	2016-07-23	58,50	1631,23	5,16E+00	1727,73	1,68	0,51
KS12	2016-07-23	139,86	1235,18	1,16E+00	1388,45	1,25	0,32
KS13	2016-07-24	39,00	954,01	2,37E+00	1003,63	0,97	0,21
KS14	2016-07-24	77,90	317,61	1,30E-01	396,48	0,32	0,19
KS15	2016-07-24	29,80	1241,71	5,42E+00	1290,33	1,27	0,28
KS16	2016-07-24	29,30	769,43	2,21E+00	808,29	0,78	0,40
KS17	2016-07-24	48,10	376,19	2,99E-01	426,84	0,38	0,08
KS18	2016-07-24	38,20	544,02	8,19E-01	588,20	0,55	0,13
KS19	2016-07-24	48,40	134,83	3,80E-02	183,74	0,14	0,06
KS20	2016-07-26	115,45	1253,76	1,40E+00	1379,79	1,27	0,36
KS21	2016-07-26	23,70	10,90	5,05E-04	34,60	0,01	0,07
KS22	2016-07-26	21,00	346,56	5,85E-01	369,20	0,35	0,02

KS23	2016-07-26	30,00	255,98	2,15E-01	286,58	0,26	0,01
KS24	2016-07-26	18,90	305,34	5,15E-01	325,57	0,31	0,17
KS25	2016-07-26	21,90	899,18	3,93E+00	931,99	0,92	0,17
M1	2017-05-23	n.a.	n.a.	n.a.	n.a.	0.1562	n.a.
M16	2017-06-23	n.a.	n.a.	n.a.	n.a.		n.a.
M1	2017-07-06	41,90	144,83	4,85E-02	186,94	0,15	n.a.
M2	2017-07-06	16,20	138,80	1,31E-01	155,31	0,15	n.a.
M3	2017-07-06	17,60	132,33	1,09E-01	150,22	0,14	n.a.
M6	2017-07-08	n.a.	n.a.	n.a.	n.a.	0,13	n.a.
M9	2017-07-08	n.a.	n.a.	n.a.	n.a.	0,19	n.a.
M10	2017-07-08	n.a.	n.a.	n.a.	n.a.	0,11	n.a.
M11	2017-07-08	n.a.	n.a.	n.a.	n.a.	0,08	n.a.
M1	2016-08-17	55,80	227,57	9,06E-02	283,48	0,23	n.a.
M2	2016-08-17	48,00	246,09	1,26E-01	294,67	0,25	n.a.
M3	2016-08-17	25,80	205,77	1,63E-01	232,04	0,21	n.a.
M6	2016-08-16	46,40	134,39	3,73E-02	180,95	0,14	n.a.
M9	2016-08-16	33,30	176,69	9,19E-02	210,31	0,18	n.a.
M10	2016-08-16	39,90	117,60	3,33E-02	157,67	0,12	n.a.
M11	2016-08-16	29,90	92,10	2,70E-02	122,08	0,09	n.a.
M01	2016-10-26	115,11	355,41	1,05E-01	471,18	0,36	n.a.
MS01	2017-07-12	87,90	113,72	1,45E-02	201,74	0,12	4,98
MS02	2017-07-12	40,00	19,10	8,62E-04	59,10	0,02	1,33
MS03	2017-07-12	225,44	76,10	2,44E-03	301,57	0,08	4,10
MS04	2017-07-12	166,51	150,77	1,36E-02	317,44	0,16	6,13
MS05	2017-07-14	41,70	86,70	1,71E-02	128,53	0,09	1,20
MS06	2017-07-14	46,10	166,08	5,69E-02	212,37	0,17	1,19
MS07	2017-07-13	223,76	400,13	7,29E-02	624,84	0,40	4,60
MS08	2017-07-13	134,08	219,11	3,50E-02	353,45	0,22	1,80
MS09	2017-07-13	184,92	339,25	5,99E-02	524,74	0,34	2,53
MS10	2017-07-15	94,20	230,48	5,52E-02	324,99	0,23	2,44
MS11	2017-07-15	71,60	362,50	1,82E-01	434,95	0,37	2,07
MS12	2017-07-15	47,70	209,84	8,88E-02	257,77	0,21	1,32
MS13	2017-07-15	67,60	182,81	4,67E-02	250,58	0,18	0,54
MS14	2017-07-15	152,56	273,72	4,74E-02	426,75	0,28	1,53
MS15	2017-07-15	38,80	133,43	4,49E-02	172,39	0,14	2,79

Appendix 3: linear algebra projection method

The real x and y coordinates were converted to logarithms X and Y according to X=log(x). The mixing line between the end members was treated as a linear function for X and Y on the form $Y=a*X+b$, connecting points $(X_{silicate,}\ Y_{silicate})$ to $(X_{carbonate,}\ Y_{carbonate})$. The formula for the mixing line was found by solving for *a* and *b* in accordance with equations 1-2:

$$a = (Y_{carbonate} - Y_{silicate})/ (X_{carbonate} - X_{silicate}) \quad (1)$$

$$b = Y_{carbonate} - a*X_{carbonate} \quad (2)$$

Sample points $(X_{n,}\ Y_n)$ were projected onto the line as $(Xp_n,\ Yp_n)$ according to two conditions: 1) that the vector connecting point X_n and point Xp_n is shifted 90° compared to the mixing line, *i.e.* that 2) that the projected point $(Xp_n,\ Xp_y)$ is found on the mixing line. This gives two new equations for the relationship between $(X_{n,}\ Y_n)$ and $(Xp_n,\ Xp_y)$ (equations 3-4):

$$(X_{n,}\ Y_n) + a(Xp_n,\ Yp_n) = 0 \quad (3)$$

$$Yp_n = a\ Xp_n + b \quad (4)$$

These equations were then solved individually for every sample by replacing any of the two variables with the expression of the other.

Appendix 4: Keeling plots

Keeling plots are presented below. End members are defined by Y-axis intersect for trend lines. Plots normalized for DOC and Cl are also included.

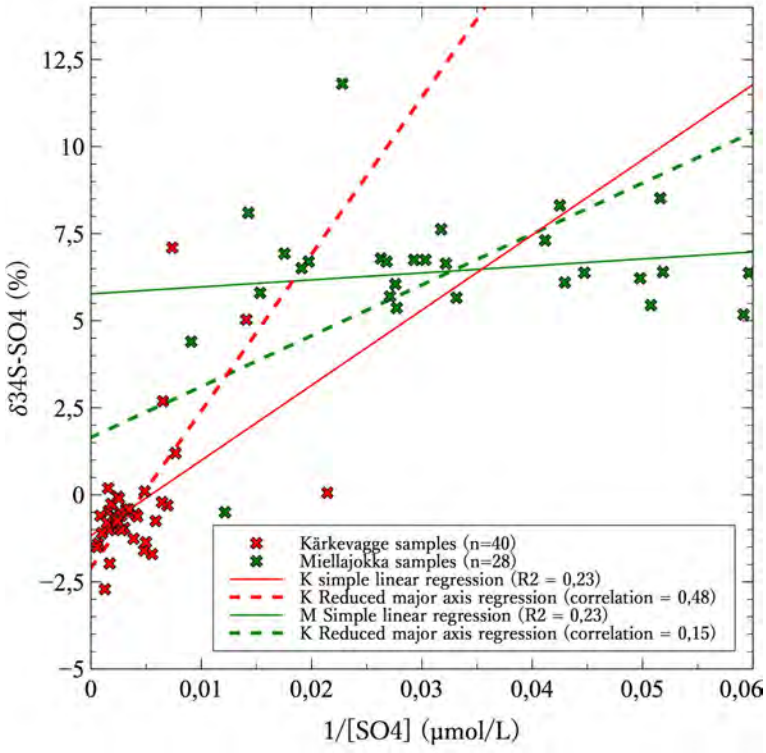

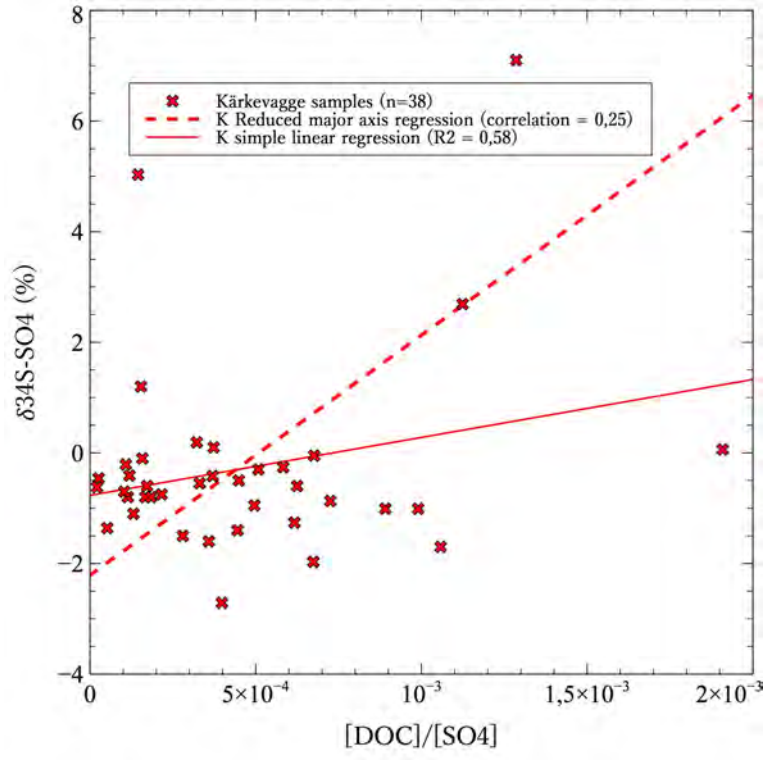

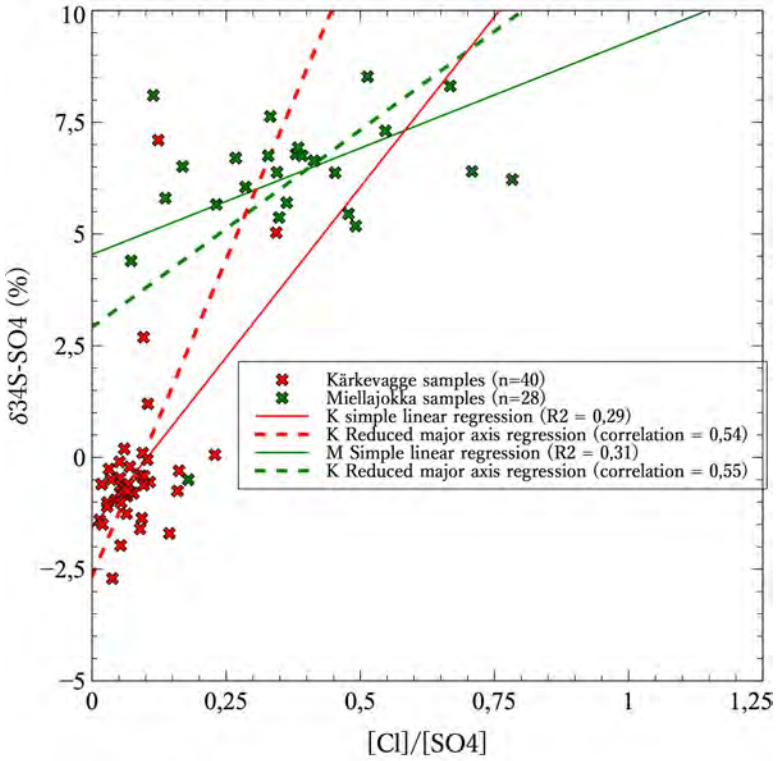
10
7,5
5
2,5
0
−2,5
−5
0
0,25
0,5
0,75
1
1,25
δ34S-SO4 (%)
[Cl]/[SO4]
Kärkevagge samples (n=40)
Miellajokka samples (n=28)
K simple linear regression (R2 = 0,29)
K Reduced major axis regression (correlation = 0,54)
M Simple linear regression (R2 = 0,31)
K Reduced major axis regression (correlation = 0,55)